Scalar Fields and Alternatives in Cosmology and Black Holes

A thesis

submitted in partial fulfilment

of the requirements for the Degree

of

Doctor of Philosophy in Physics

in the

University of Canterbury

by

Ben Maitland Leith

University of Canterbury

2007

Disclaimer

The work described in this thesis was carried out under the supervision of Dr D.L. Wiltshire in the Department of Astronomy and Physics, University of Canterbury. Chapters three–five are comprised of original work except where explicit reference is made to the work of others. Chapter three is based on work done in collaboration with Alex Nielsen and submitted to Phys. Rev. D. [arxiv:0709.2541]. Part of chapter four is based on work done in collaboration with Ishwaree Neupane, published in JCAP **0705**, 019 (2007), further work was done individually and will appear in a forthcoming paper. Chapter five is based on work done in collaboration with Benedict Carter, Cindy Ng, Alex Nielsen and David Wiltshire in arxiv:astro-ph/0504192, and a further paper, with Cindy Ng and David Wiltshire submitted to Astrophys. J. [arxiv:0709.2535]. No part of this thesis has been submitted for any degree, diploma or other qualification at any other University.

Acknowledgements

I would like to thank my supervisor, David Wiltshire, for his support and guidance, and Ishwaree Neupane, Alex Nielsen, Benedict Carter and Cindy Ng for their fruitful collaborations. I would also like to thank my family and friends for their constant support.

Contents

Abstract

Extensions to general relativity are often considered as possibilities in the quest for a quantum theory of gravity on one hand, or to resolve anomalies within cosmology on the other. Scalar fields, found in many areas of physics, are frequently studied in this context. This is partly due to their manifestation in the effective four dimensional theory of a number of underlying fundamental theories, most notably string theory. This thesis is concerned with the effects of scalar fields on cosmological and black hole solutions. By comparison, an analysis of an inhomogeneous cosmological model which requires no extensions to general relativity is also undertaken.

In chapter three, examples of numerical solutions to black hole solutions, which have previously been shown to be linearly stable, are found. The model includes at least two scalar fields, non-minimally coupled to electromagnetism and hence possesses non-trivial contingent primary hair. We show that the extremal solutions have finite temperature for an arbitrary coupling constant.

Chapter four investigates the effects of higher order curvature corrections and scalar fields on the late-time cosmological evolution. We find solutions which mimic many of the phenomenological features seen in the post-inflation Universe. The effects due to non-minimal scalar couplings to matter are also shown to be negligible in this context. Such solutions can be shown to be stable under homogeneous perturbations. Some restrictions on the value of the slope of the scalar coupling to the Gauss-Bonnet term are found to be necessary to avoid late-time superluminal behaviour and dominant energy condition violation.

A number of observational tests are carried out in chapter five on a new approach to averaging the inhomogeneous Universe. In this "Fractal Bubble model" cosmic acceleration is realised as an apparent effect, due to quasilocal gravitational energy gradients. We show that a good fit can be found to three separate observations, the type Ia supernovae, the baryon acoustic oscillation scale and the angular scale of the sound horizon at last scattering. The best fit to the supernovae data is $\chi^2 \backsimeq 0.9$ per degree of freedom, with a Hubble parameter at the present epoch of $H_0 = 61.7^{+1.4}_{-1.3}$ km sec^{-1} Mpc^{-1} , and a present epoch volume void fraction of 0.76 ± 0.05.

Overview

The thesis is structured as follows. Chapters 1 and 2 contain introductory material, while chapters 3, 4 and 5 present original investigations which form the major work of this thesis.

- In chapter 1 we outline the applications of general relativity relevant to this thesis. A quick review of the homogeneous cosmological models is given. The current concordance model, the Λ Cold Dark Matter model, is also considered along with some of the observational evidence and concordance parameters. Various inhomogeneous cosmological models are covered to give a perspective of the previous work done in this area. Particular emphasis is put on the Fractal Bubble model for which a number of observation tests are carried out in chapter 5. A number of current cosmological observations are discussed, the type Ia supernovae data, the cosmic microwave background and the baryon acoustic oscillation scale. The last section of the chapter covers two well-known black hole solutions, the Schwarzschild solutions and the Reissner-Nordström solution, which are relevant to the work in chapter 3.

- Chapter 2 is dedicated to extensions to general relativity. It covers the Kaluza-Klein compactification scheme, which gives a simplified version of compactification from higher dimensions, and the resulting manifestation of scalar fields in the effective theory. A number of potentially physical scalar field candidates are outlined and a basic description given of the mechanisms that create them. A summary of previous work incorporating scalar fields into cosmological and black hole solutions is given. We also consider higher-order curvature terms, particularly the Gauss-Bonnet term which is central to the work in chapter 4.

- Chapter 3 presents and discusses results found for multi-scalar black hole solutions coupled to electromagnetism. These show interesting properties with regard to the extremal solutions.

- Chapter 4 presents a number of results regarding the cosmological implications of including leading order curvature corrections and scalar fields. A number of different scenarios are examined, giving possible late-time evolutions.

- In chapter 5 the concordance of the fractal bubble model to the type Ia supernovae data is presented. Two other observations, the baryon acoustic oscillation scale and angular scale of the sound horizon in the CMB are also compared to the model.

Throughout this thesis, the 4-dimensional Newton constant is given by G. We use natural units in which the constants c, k, $\hbar$ and μ_0 do not appear, or equivalently may be considered to have a numerical value of unity. There is one exception to this, in the data analysis $c = 2.998 \times 10^8$ ms^{-1}. One may transform between our natural units and rationalised practical (SI) units by making the following transformations for the five SI base dimensions:

$$\begin{aligned}
\text{Length: } & x = x_{\text{SI}} \\
\text{Time: } & t = ct_{\text{SI}} \\
\text{Mass: } & m = \frac{c}{\hbar} m_{\text{SI}} \\
\text{Temperature: } & T = \frac{k}{\hbar c} T_{\text{SI}} \\
\text{Current: } & i = \left(\frac{\mu_0}{\hbar c}\right)^{1/2} i_{\text{SI}}.
\end{aligned}$$

Chapter 1

Introduction to General Relativity

1.1 Homogeneous Cosmology and the Current Concordance Model

Many assumptions must be made in order to have any chance of modelling the universe due to the extremely complex nature of the structure observed. For many years the major assumption in most cosmological models has been that the universe is spatially homogeneous and isotropic or equivalently the universe can be foliated by spacelike hypersurfaces that are maximally symmetric in the three spatial dimensions intrinsic to the surface[1]. The level of assumption here is obviously huge as many observations point to a highly inhomogeneous universe on scales of less than 100–300 Mpc, with regions of very low density, where space is empty give or take some radiation and the odd particle, through to extremely high density areas such as planets, stars and even black holes.

There is, however, some basis to such a claim. The most well-known piece of evidence is the observation of the cosmic microwave background (CMB). This radiation, which permeates the whole universe, is a remnant of last scattering indicating a highly homogeneous universe at this epoch. The temperature profile is incredibly smooth, only varying in the order of 10^{-3}, or 10^{-5} if our local motion with respect

[1]We are considering 4-dimensional spacetime at this point with a 3+1 split generally being possible, ie. it is globally hyperbolic.

to the cosmic rest frame is subtracted. There is evidence that the Universe is still isotropic and homogeneous on large scales today but only in an average sense. Galaxy clustering statistics suggest that the distribution of matter is homogeneous if we sample on scales greater than about 200Mpc [1, 2]. Observations of the diffuse x-ray and γ-ray backgrounds also support a homogenous Universe when averaged on such scales.

A spatially homogeneous and isotropic geometry in 4-dimensions can be considered to be $\mathbb{R} \times \Sigma$ where $\mathbb{R}$ is the time direction and Σ is the maximally symmetric spacelike 3-manifold. We therefore have a metric

$$\mathrm{d}s^2 = -\mathrm{d}t^2 + \bar{a}^2(t)\mathrm{d}\sigma^2, \tag{1.1}$$

where $\mathrm{d}\sigma^2$ is the metric for the 3-dimensional foliating manifold, Σ and $\bar{a}(t)$ is the scale factor. By using the fact that maximally symmetric metrics obey

$$^{(3)}R_{ijkl} = k(\gamma_{ik}\gamma_{jl} - \gamma_{il}\gamma_{jk}), \tag{1.2}$$

where $k = {}^{(3)}R/6$ is a measure of the constant Gaussian curvature of the spatial 3-manifold, Σ, with metric $\mathrm{d}\sigma^2 = \gamma_{ij}\mathrm{d}x^i\mathrm{d}x^j$, $i, j \in \{1, 2, 3\}$. The metric can be written in a spherically symmetric form, such that,

$$\mathrm{d}\sigma^2 = \frac{\mathrm{d}\bar{r}^2}{1 - k\bar{r}^2} + \bar{r}^2\mathrm{d}\Omega^2, \tag{1.3}$$

where $\mathrm{d}\Omega^2 = \mathrm{d}\theta^2 + \sin^2\theta\mathrm{d}\phi$ is the metric on the 2-sphere[2]. The value of k can be normalised using the freedom in $\bar{a}(t)$ such that $k \in \{-1, 0, 1\}$. The $k = -1$, $k = 1$ and $k = 0$ cases correspond to negative, positive and flat spatial curvature respectively.

The Friedmann-Lemaître-Robertson-Walker (FLRW) geometry is given by

$$\mathrm{d}s^2 = -\mathrm{d}t^2 + \bar{a}^2(t)\left[\frac{\mathrm{d}\bar{r}^2}{1 - k\bar{r}^2} + \bar{r}^2\mathrm{d}\Omega^2\right]. \tag{1.4}$$

The metric (1.4) is invariant under the transformations

$$\begin{aligned} \bar{a} &\rightarrow \omega^{-1}\bar{a}, \\ \bar{r} &\rightarrow \omega\bar{r}, \\ k &\rightarrow \omega^{-2}k. \end{aligned} \tag{1.5}$$

[2]See [3, 4] for details.

This is convenient because it allows one to decide which variables to consider dimensionless. In (1.4) the scale factor has units of distance while the radial coordinate is dimensionless. Sometimes it is preferable to make the transformations

$$\begin{aligned} a(t) &= \frac{\bar{a}(t)}{\bar{a}_0}\,, \\ r &= \bar{a}_0 \bar{r}, \\ \kappa &= \frac{k}{\bar{a}_0^2}\,, \end{aligned} \tag{1.6}$$

where $\bar{a}_0$ normalises the scale factor to a convenient epoch, generally the present epoch. We now have a dimensionless scale factor, $a(t)$, a radial coordinate, r, with dimensions of distance and a curvature parameter, κ, with dimensions of (distance)$^{-2}$. Hence the metric (1.4) becomes

$$\mathrm{d}s^2 = -\mathrm{d}t^2 + a^2(t)\left[\frac{\mathrm{d}r^2}{1-\kappa r^2} + r^2 \mathrm{d}\Omega^2\right]. \tag{1.7}$$

To understand the dynamics of a universe with the metric, (1.7) one has to solve the Einstein equation with an appropriate energy-momentum tensor. The general assumption made is that the matter and energy can be modelled by a perfect fluid. This is again a simplification of grand proportions, one which is valid if the Universe is exactly isotropic and homogeneous. Hence, in suitable local frames, there are no off-diagonal terms in the energy-momentum tensor. The energy-momentum tensor for a perfect fluid is given by

$$T_{\mu\nu} = (\rho + p) U_\mu U_\nu + p g_{\mu\nu}, \tag{1.8}$$

where, in a local frame, the 4-velocity is $U^{\hat{a}} = (1, 0, 0, 0)$ with ρ and p being the density and pressure respectively. By the assumption of homogeneity, $\rho = \rho(t)$ and $p = p(t)$.

Energy conservation is given by the zeroth component of the conservation equation $\nabla_\mu T^\mu{}_0 = 0$,

$$\begin{aligned} \nabla_\mu T^\mu{}_0 &= \partial_\mu T^\mu{}_0 + \Gamma^\mu_{\mu\nu} T^\nu{}_0 - \Gamma^\nu_{\mu 0} T^\mu{}_\nu, \\ &= -\dot{\rho} - 3\frac{\dot{a}}{a}(\rho + p) = 0. \end{aligned} \tag{1.9}$$

where overdot is differentiation with respect to t. For perfect fluids one generally assumes a linear equation of state, $p = w\rho$. In FLRW models the parameter w is

independent of time. However, in extensions to quintessence models (see section 2.3.1) time dependence is allowed. In the present context we have a conservation of energy equation

$$\frac{\dot{\rho}}{\rho} = -3(1+w)\frac{\dot{a}}{a}. \tag{1.10}$$

Ordinary matter is assumed to be dust-like; i.e., it is collision–less and non-relativistic. This means that $p_{\text{matter}} = 0$, or equivalently $w_{\text{matter}} = 0$. For radiation, one obtains $w_{\text{radiation}} = 1/3$ from the energy-momentum tensor for electromagnetism. Vacuum energy is the component of the total energy density of the universe that most closely resembles a perfect fluid in reality. It has the equation of state $p_\Lambda = -\rho_\Lambda$. This negative pressure is often attributed to being the source of the current acceleration of the expansion of the Universe.

One can integrate (1.10), for $w \neq -1$, with respect to time to obtain

$$\rho \propto a^{-3(1+w)}. \tag{1.11}$$

For dust-like matter, radiation and vacuum energy the following relations between the energy density and the scale factor are obtained,

$$\begin{aligned} \rho_{\text{matter}} &\propto a^{-3}, \\ \rho_{\text{radiation}} &\propto a^{-4}, \\ \rho_\Lambda &= \text{const.} \end{aligned} \tag{1.12}$$

Hence one can see that while the densities of radiation and matter with decrease quickly with increasing size of the Universe, the vacuum energy has a constant density and therefore in an eternally expanding universe will eventually dominate.

Now if we consider Einstein's equation written in the form

$$R_{\mu\nu} = 8\pi G\left(T_{\mu\nu} - \frac{1}{2}\,g_{\mu\nu}T\right), \tag{1.13}$$

we get

$$\begin{aligned} -3\frac{\ddot{a}}{a} &= 4\pi G(\rho + 3p), \\ \frac{\ddot{a}}{a} + 2\left(\frac{\dot{a}}{a}\right)^2 + 2\frac{\kappa}{a^2} &= 4\pi G(\rho - p), \end{aligned} \tag{1.14}$$

from the tt and ij components respectively. Simplifying the ij equation with respect to the tt equation we get the familiar Friedmann equations,

$$\left(\frac{\dot{a}}{a}\right)^2 = \frac{8\pi G}{3}\,\rho - \frac{\kappa}{a^2}\,, \tag{1.15}$$

$$\frac{\ddot{a}}{a} = -\frac{4\pi G}{3}\,(\rho + 3p). \tag{1.16}$$

A number of important parameters can be defined with respect to these equations. The Hubble parameter, $H = \dot{a}/a$, which has units of $(time)^{-1}$, conventionally measured in km/sec/Mpc, is an important measure of the expansion rate of the universe. It is also useful to have a parameter dependent on the second derivative of $a(t)$ to measure the rate of change of the expansion rate. This is the deceleration parameter

$$q = -\frac{a\ddot{a}}{\dot{a}^2}\,, \tag{1.17}$$

which is positive for a decelerating universe. We also define the density parameter in any matter or radiation component, A, as

$$\Omega_A \equiv \frac{8\pi G}{3H^2}\,\rho_A = \frac{\rho_A}{\rho_{\text{critical}}}\,, \tag{1.18}$$

where the critical density is

$$\rho_{\text{critical}} \equiv \frac{3H^2}{8\pi G}\,. \tag{1.19}$$

If $\Lambda = 0$, the three different FLRW geometries can be characterised by the value of the density parameter. This is a direct result of (1.15) and gives

$$\begin{aligned}
\rho < \rho_{\text{critical}} &\;\leftrightarrow\; \Omega < 1 \;\leftrightarrow\; \kappa < 0 \;\leftrightarrow\; \text{“open” geometry,}\\
\rho > \rho_{\text{critical}} &\;\leftrightarrow\; \Omega > 1 \;\leftrightarrow\; \kappa > 0 \;\leftrightarrow\; \text{“closed” geometry,}\\
\rho = \rho_{\text{critical}} &\;\leftrightarrow\; \Omega = 1 \;\leftrightarrow\; \kappa = 0 \;\leftrightarrow\; \text{spatially flat geometry.}
\end{aligned}$$

The terminology “open” and “closed” in reference to the ultimate fate of the Universe is a nomenclature which derives from the case with no vacuum energy. If $\Lambda > 0$ then the Universe may expand forever even if the Universe is “closed”.

The current *concordance model* of cosmology is considered to be the so called Λ-Cold-Dark-Matter (ΛCDM) model where the geometry is considered to be flat with particular *concordance parameters*. This model has been shown to be in very good

agreement with many observations, especially the cosmic microwave background[3]. The present day make up of the universe for the flat-ΛCDM model which most closely agrees with the WMAP 3 year data set of the Cosmic Microwave Background (CMB) is given by the following parameters [5]

$$\begin{aligned} H_0 &= 73.2^{+3.1}_{-3.2}\text{km/sec/Mpc} \\ \Omega_\Lambda &= 0.759 \pm 0.034 \\ \Omega_{\text{matter}} &= 0.241 \pm 0.034 \\ \Omega_{\text{baryon}}h^2 &= 0.02229 \pm 0.00073 \end{aligned}$$

where h is defined by $H_0 = 100h$ km sec^{-1} Mpc^{-1}. When other data sets are included – particularly the supernovae Ia data, various galaxy surveys and alternative observations of the CMB[4] - the cosmological parameters currently claimed by the WMAP team [16] are

$$\begin{aligned} H_0 &= 70.4^{+1.5}_{-1.6}\text{km/sec/Mpc} \\ \Omega_\Lambda &= 0.732 \pm 0.018 \\ \Omega_{\text{matter}} &= 0.268 \pm 0.018 \\ \Omega_{\text{baryon}}h^2 &= 0.02186 \pm 0.00068 \end{aligned}$$

The concordance ΛCDM model calls for a dominant contribution from the vacuum energy or cosmological constant. Current observation seems to support an accelerating universe, and the cosmological constant is the physical mechanism within the ΛCDM model responsible for driving it. The model also has a significant proportion of cold dark matter. Non–baryonic dark matter is expected to make up 23% of the matter–energy content or 83% of ordinary clumped matter in the ΛCDM model when fitted to the observations [16]. The generally observed ingredient of the universe, baryonic matter, is only expected to make up 4.4% of the matter–energy content of the universe. Note that ΛCDM is flat, $\Omega_\Lambda + \Omega_{\text{matter}} = 1$ (at the present epoch radiation is negligible,

[3]However, some critical comments on this will be made in chapter 5.

[4]The included datasets are WMAP [6, 7], 2df Galaxy Redshift Survey [8], BOOMERang [9] + ACBAR [10], CBI [11] + VSA [12], Sloan Digital Sky Survey [1, 13], Supernova Legacy Survey [14] and the Riess 04 "Gold Sample" Supernova [15].

$\Omega_{\text{radiation}} \sim 10^{-4}$), which fits with both the WMAP observation and the theoretical requirements of inflation.

1.2 Inhomogeneous Cosmology

Over the years inhomogeneous cosmological models have been studied from many different viewpoints [see ref. [17] for a review]. There is significant observational evidence for an inhomogeneous matter distribution in the large scale struture of the Universe at the present epoch [18, 19]. The most widely studied approaches for dealing with inhomogeneity are discussed below.

1.2.1 Perturbation theory

If the background geometry can be assumed close to an FLRW model then one can consider inhomogeneous perturbations,

$$g_{\mu\nu} = g^{\text{FLRW}}_{\mu\nu} + h_{\mu\nu}. \tag{1.20}$$

where $|h_{\hat{a}\hat{b}}| \ll 1$ in a orthornormal frame. Perturbation theory must be directly relevant at early times given the evidence from the CMB for homogeneity in the early Universe. It is therefore very widely studied and the subject of many reviews and texts [20, 21, 22].

At the present epoch, initial perturbations that give rise to galaxy clusters have gone far into the non-linear regime and thus other approaches to dealing with inhomogeneity must be considered.

1.2.2 Exact inhomogeneous solutions to Einstein's equation

Here one assumes a metric which is inhomogeneous but still has some residual symmetry – such as spherical symmetry in the case of the widely studied Lemaître-Tolman-Bondi (LTB) models [23]. Given that exact spherical symmetry about our point is highly unlikely such models have limited applicability although a number of attempts have been made to apply these to the whole Universe [24, 25]. More realistic inhomogeneous

exact solutions with less symmetry have also been extensively studied, in particular the families of exact solutions discovered by Szekeres [26] and Szafron [27]. These solutions consider a perfect inhomogeneous fluid in comoving coordinates. Initially Szekeres solved the Einstein equations for a dust source and $\Lambda = 0$, and it was generalised to $p \neq 0$ by Szafron.

While LTB solutions are of limited values as models of the entire Universe, they are useful in modelling single voids or single overdense regions. More generally the problem of exact solutions representing stars or galaxies embedded in an expanding background has a long history going back to the work of McVittie [28]. In these cases one often constructs exact geometries with the desired properties, leaving the nature of the energy-momentum tensor on the right hand side of Einstein's equations the object to be determined and interpreted. An extensive discussion of such models has been recently given by Faraoni and Jaques [29].

1.2.3 Swiss cheese models

One can also construct solutions in which the energy-momentum tensor is directly specified in various regions which are cut and pasted together by junction conditions at a boundary. The first example of this, the original "Swiss cheese" model, was constructed by Einstein and Straus [30]. Their technique was to cut spherical holes out of the dust in FLRW models and replace them by central Schwarzschild solutions, which have a mass equal to that cut out of the fluid. The boundary of the Einstein-Straus vacuoles expands outwards in order to satisfy the junction conditions if the background universe is expanding. The Einstein-Straus model would be very realistic if the Universe did correspond to isolated galaxies moving uniformly away from each other in a completely smooth fluid background. However, it does not correspond to the observed structure of galaxy clusters in walls surrounding voids. Nonetheless, it is widely used in various studies due to its simplicity.

1.2.4 Averaged cosmologies

The question of extracting the correct average from a general inhomogeneous cosmology is an important problem since the average geometry will differ from that of FLRW models in general. Such approaches have recently become the focus of much interest [24, 31] as they may provide an alternative explanation for the apparent cosmic acceleration observed at present. This is closely related to the effects of "back–reaction" [32] of inhomogeneities on the average geometry of the Universe.

Of particular interest for this thesis are the effects of back–reaction on observed quantities. As the Einstein equations are local and nonlinear, one should take an initial inhomogeneous energy-momentum distribution and evolve this forward in time. This is not equivalent generally to taking the average of the equations initially, and time-evolving that average. Mathematically, if one considers an inhomogeneous scalar quantity, Φ, in general $\langle\Phi^2\rangle - \langle\Phi\rangle^2 \neq 0$ where angle brackets denote the average over a relevant domain. This non-commutativity results in a back–reaction term in the Einstein equations. The degree to which this back–reaction term affects the observational parameters of the universe is a topic of much current debate. The effect of this term may in fact be sufficient to cause apparent acceleration without the requirement of any dark energy [25, 33].

There are a number of methods for averaging spatial or null cone volumes, involving different foliations by hypersurfaces. Schemes for averaging both tensor quantities [34] and scalars [35] have been developed. Buchert [35] has developed a scheme for irrotational dust cosmologies, considering spatial averages of the scalar quantities: energy density $\rho(t,x)$, expansion, $\theta(t,x)$, and shear, $\sigma(t,x)$, over a spatial hypersurface of constant average time, t and spatial 3-metric ${}^3g_{ij}(x)$. The average cosmic evolution is then given by

$$3\frac{\dot{\bar{a}}^2}{\bar{a}^2} = 8\pi G\langle\rho\rangle - \frac{1}{2}\langle R\rangle - \frac{1}{2}Q, \tag{1.21}$$

$$3\frac{\ddot{\bar{a}}}{\bar{a}} = -4\pi G\langle\rho\rangle + Q, \tag{1.22}$$

$$\partial_t\langle\rho\rangle + 3\frac{\dot{\bar{a}}}{\bar{a}}\langle\rho\rangle = 0, \tag{1.23}$$

where $\bar{a}(t) \equiv [\mathcal{V}(t)/\mathcal{V}(t_0)]^{1/3}$ with $\mathcal{V}(t) \equiv \int_D \mathrm{d}^3x\sqrt{\det{}^3g}$. The back–reaction term, Q,

is given by

$$\begin{aligned} Q &\equiv \frac{2}{3}\langle(\theta-\langle\theta\rangle)^2\rangle - 2\langle\sigma\rangle^2 \\ &= \frac{2}{3}\left(\langle\theta^2\rangle - \langle\theta\rangle^2\right) - 2\langle\sigma\rangle^2. \end{aligned} \tag{1.24}$$

The angle brackets denote the spatial volume average, hence

$$\langle R\rangle \equiv \left(\int_D \mathrm{d}^3x\sqrt{\det{}^3g}R(t,x)\right)/\mathcal{V}(t) \tag{1.25}$$

is the average spatial curvature.

1.2.5 Fractal Bubble model

Wiltshire has recently proposed an approach to cosmological averaging which takes into account, not just back–reaction, but the possibility that there can be systematic differences between measurements of cosmological parameters made within local systems and at the volume average position in freely expanding space [36, 37]. This is done through systematic consideration of differences in the quasilocal gravitational energy between two scales: the very low density voids which dominate the Universe by volume at the present epoch, and the bubble walls and filaments which surround the voids. Wiltshire takes the present particle horizon volume as the domain of spatial averaging.

A crucial scale in Wiltshire's approach is the fiducial reference point for the definition of quasilocal gravitational energy gradients. It is defined as follows [37].

> With respect to a foliation of spacetime by spacelike hypersurfaces, finite infinity is identified with the set of *timelike boundaries* of (disjoint) compact domains, $\mathcal{F}_I$, within which the *average* expansion vanishes, while being positive outside:
>
> $$\begin{aligned} &\text{(i)}\ \ \langle\theta(p)\rangle_{\mathcal{F}_I} = 0; \\ &\text{(ii)}\ \exists\ \mathcal{D}_I \text{ such that } \mathcal{F}_I \subset \mathcal{D}_I \text{ and } \theta(p) > 0 \quad \forall\ p \in \mathcal{D}_I \setminus \mathcal{F}_I \end{aligned} \tag{1.26}$$

This is shown diagrammatically in Fig. 1.1. Physically, finite infinity regions should be considered as the analogue of the Einstein-Straus vacuoles. The principal difference is that no assumptions about homogeneity are made beyond finite infinity. Finite infinity may be understood as the demarcation scale between a bound system, or

strictly speaking a potentially bound system, and freely expanding space. The idea is that the density of matter averaged over a finite infinity domain is the "true critical density". Since the Universe was homogeneous and isotropic at last scattering it possessed an almost uniform initial expansion velocity. This means that the notion of a universal initial density of matter for gravity to overcome this initial uniform expansion is well-defined. However, as cosmological evolution no longer occurs via the Friedmann equation, ρ_{critical} cannot be naively equated to the mean Hubble parameter at a volume-averaged position according to (1.19).

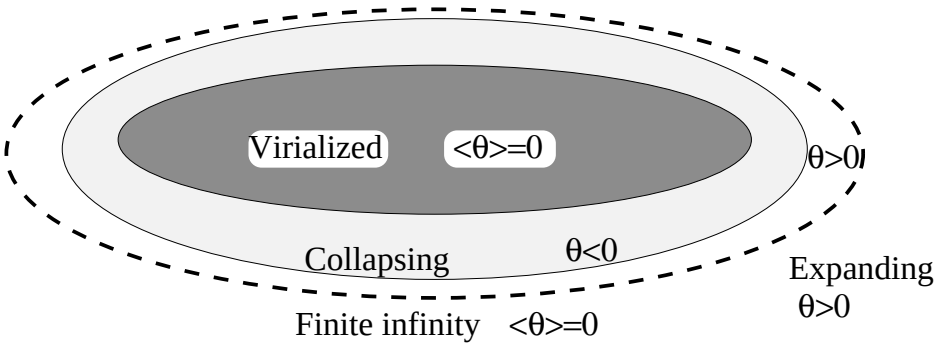

Figure 1.1: *The dotted line represents finite infinity, the boundary between the voids and the walls. Galaxies are expected to exist within the virialised region with a further collapsing region and then expanding region required within the bounds of finite infinity to give* $\langle\theta\rangle = 0$.

The local average geometry within finite infinity regions in bubble walls is assumed to be well-described, on average, by the spatially flat metric

$$\mathrm{d}s^2_{\mathcal{F}_I} = -\mathrm{d}\tau_w^2 + a_w^2(\tau_w)\left[\mathrm{d}\eta_w^2 + \eta_w^2\mathrm{d}\Omega^2\right], \tag{1.27}$$

where τ_w is strictly speaking the proper time of an ideal isotropic observer at the finite infinity boundary and η_w is an appropriate radial coordinate. The related scale factor is $a_w(\tau_w)$. While the clocks of observers within galaxies will differ slightly from those at finite infinity, it is assumed that these differences are small, since gravitational binding energy is conventionally neglected. The break with conventional assumptions comes from allowing significant spatial curvature gradients between finite infinity and the centres of voids. Quasilocal energy differences will arise, as a consequence, between finite infinity and the volume average.

The Buchert scale factor, $\bar{a}$, which appears in (1.21)–(1.23), is taken to be

$$\bar{a}^3 = f_{vi} a_v^3 + f_{wi} a_w^3, \tag{1.28}$$

in the 2-scale average. Here a_w is the scale factor relevant for finite infinity regions, as in (1.27), while a_v is a measure of the local geometry within voids, given similarly by

$$\mathrm{d}s_v^2 = -\mathrm{d}\tau_v^2 + a_v^2(\tau_v) \left[\mathrm{d}\eta_v^2 + \sinh^2(\eta_v) \mathrm{d}\Omega^2 \right]. \tag{1.29}$$

The constants f_{vi} and f_{wi} which appear in (1.28) are respectively the initial void fraction, $f_{vi} \ll 1$, and the initial wall fraction, $f_{wi} \equiv 1 - f_{vi}$ at last scattering.

The crucial argument of Wiltshire's solution to the averaging problem involves the assumption that the underlying expansion of the Universe is still uniform, when defined in terms of locally observed quantities, on scales larger than finite infinity. However, both local clocks and quasilocal spatial curvature can vary. Negative spatial curvature is associated with positive gravitational energy, which feeds back on clock rates to make clocks tick faster in voids relative to finite infinity.

By Wiltshire's assumptions the underlying locally measured Hubble flow is uniform and coincides with that measured at the volume average,

$$\bar{H} = \frac{1}{3} \langle \theta \rangle_{\mathcal{H}} = f_w H_w + f_v H_v, \tag{1.30}$$

where $\bar{H} = \dot{\bar{a}}/\bar{a}$, and $H_w \equiv \dot{a}_w/a_w$, and $H_v \equiv \dot{a}_v/a_v$ are the expansion rates of walls and voids referred to volume average clocks, $\langle \theta \rangle_{\mathcal{H}}$ is the average expansion over the particle horizon volume, and $f_w(t)$ and $f_v(t)$ are the wall and void fractions respectively[5].

The Buchert equations, (1.21)–(1.23), are now implemented with respect to the volume average position. The independent Buchert equations are [38]

$$\frac{\dot{\bar{a}}^2}{\bar{a}^2} + \frac{Q}{6} - \frac{\alpha^2 f_v^{1/3}}{\bar{a}^2} = \frac{8\pi G}{3} \bar{\rho}_0 \frac{\bar{a}_0^3}{\bar{a}^3} \tag{1.31}$$

$$\ddot{f}_v + \frac{\dot{f}_v^2 (2f_v - 1)}{2f_v(1 - f_v)} + 3\frac{\dot{\bar{a}}}{\bar{a}} \dot{f}_v - \frac{3\alpha^2 f_v^{1/3}(1 - f_v)}{2\bar{a}^2} = 0 \tag{1.32}$$

where

$$Q = \frac{2\dot{f}_v^2}{3 f_v (1 - f_v)}, \tag{1.33}$$

[5]The overdot throughout the Fractal Bubble formalism is defined to be differentiation with respect to proper time at the volume average, t.

$\alpha = -k_v f_{vi}^{2/3}$, and k_v is the curvature parameter in the voids defined by $\langle R\rangle_v = 6k_v/a_v^2$. A curvature parameter for the walls k_w is defined in a similar manner but is zero by the definition of the finite infinity boundary.

Once an underlying uniform expansion is assumed, the relationship or "dressing", of cosmological parameters between finite infinity and the volume average is determined. The volume average is located in voids, somewhere between their centres and the finite infinity regions along their boundaries. A metric for the volume-average geometry is reconstructed from solutions to Buchert's equations, and is given by

$$\begin{aligned} \mathrm{d}s^2 &= -\mathrm{d}t^2 + \bar{a}^2(t)\mathrm{d}\bar{\eta}^2 + A(\bar{\eta},t)\mathrm{d}\Omega^2 \\ &= -\bar{\gamma}_w^2(\tau_w)\mathrm{d}\tau_w^2 + \bar{a}^2(\tau_w)\mathrm{d}\bar{\eta}^2 + A(\bar{\eta},\tau_w)\mathrm{d}\Omega^2, \end{aligned} \tag{1.34}$$

where t and $\bar{\eta}$ are the temporal and radial coordinates of the averaged geometry while $\bar{a}$ and $A(\bar{\eta},t)$ are the volume averaged scale factor and area function respectively. The second line of (1.34) shows the line element as a function of the time parameter, τ_w, measured within the finite infinity region. The average lapse function, $\bar{\gamma}_w(\tau_w) = \mathrm{d}t/\mathrm{d}\tau_w$, describes the difference in the rate of the usual cosmic time, t, measured in the volume average, and τ_w, the proper time at finite infinity. This lapse function is no longer negligible once the possibility of quasilocal gravitational energy differences are considered.

When the geometry (1.27) is related to the average geometry (1.34) by conformal matching of radial null geodesics it may be rewritten

$$\mathrm{d}s^2_{\mathcal{F}_I} = -\mathrm{d}\tau_w^2 + \frac{\bar{a}^2}{\bar{\gamma}^2}\left[\mathrm{d}\bar{\eta}^2 + r_{\mathrm{w}}^2(\bar{\eta},\tau_w)\,\mathrm{d}\Omega^2\right] \tag{1.35}$$

where $r_{\mathrm{w}} \equiv \bar{\gamma}\,(1-f_{\mathrm{v}})^{1/3}\,{f_{\mathrm{wi}}}^{-1/3}\eta_{\mathrm{w}}(\bar{\eta},\tau_w)$. Two sets of cosmological parameters are relevant: those relative to an ideal observer at the volume–average position in freely expanding space using the metric (1.34), and conventional dressed parameters using the metric (1.35). The conventional metric (1.35) arises in our attempt to fit a single global metric (1.27) to the universe with the assumption that average spatial curvature and local clock rates everywhere are identical to our own, which is no longer true. One important consequence is that the dressed matter density parameter, $\Omega_{_M}$, differs from the bare volume–average density parameter, $\bar{\Omega}_M$, according to $\Omega_{_M} = \bar{\gamma}^3\bar{\Omega}_M$. The

difference between these two parameters has direct implications for the calibration of the baryonic density parameter from primordial nucleosynthesis: the value predicted in the standard FLRW analysis is the volume–average, $\bar{\Omega}_B$, which is smaller than the conventional dressed parameter, Ω_B.

The conventional dressed Hubble parameter, H, of the metric (1.35) differs from the bare Hubble parameter, $\bar{H}$, of (1.34) according to

$$H = \bar{\gamma}\bar{H} - \tfrac{\mathrm{d}}{\mathrm{d}t}\,\bar{\gamma} = \bar{\gamma}\bar{H} - \bar{\gamma}^{-1}\,\tfrac{\mathrm{d}}{\mathrm{d}\tau}\,\bar{\gamma}\,. \tag{1.36}$$

Since the bare Hubble parameter characterises the uniform "locally measured" Hubble flow, for observers in galaxies its present value coincides with the value of the Hubble constant they would obtain for measurements averaged solely within the plane of an ideal local bubble wall, on scales dominated by finite infinity regions. The numerical value of $\bar{H}$ is smaller than the global average, H, which includes both voids and bubble walls. Eq. (1.36) thus also quantifies the apparent variance in the Hubble flow below the scale of homogeneity. Measurements across single dominant local voids (on scales $30h^{-1}\,\mathrm{Mpc}$) should give a Hubble "constant" which exceeds the global average H_0 by an amount commensurate to $H_0 - \bar{H}_0$. As voids are dominant by volume, an isotropic average will produce a Hubble "constant" greater than H_0 until the scale of homogeneity ($\sim 200\,\mathrm{Mpc}$) is reached: a "Hubble bubble" feature [39, 40, 41].

1.3 Cosmological Observations

- **Type Ia Supernovae**

  Observations of Type Ia supernovae have been the main piece of evidence supporting the current view that the expansion of the Universe appears to be accelerating. This is a major result as it poses major challenges for our fundamental understanding of physics. It is possible that it demands changes to our understanding of the forces of nature, or modifications to gravity. Type Ia Supernovae are the brightest standard candle known[6], giving information about the behaviour out

[6] Attempts have recently been made to use gamma–ray bursts as standard candles [42]. These are much brighter and could be used to large redshifts. However, it is not yet clear whether the intrinsic systematic variations in their luminosities are well enough understood.

to a redshift of $z \sim 1.5$, far beyond the observable distance of other standard candles: cepheid variables, RR Lyrae variables and eclipsing binaries. Given the central importance of the Type Ia Supernovae observations, we will give a review of their relevant astrophysical properties.

Type Ia Supernovae are believed to be ignited by white dwarf stars in binary systems. A white dwarf is the stable remnant of a star that has completed its life cycle, with nuclear fusion having ended. The white dwarf must have a mass below the Chandrasekhar limit of ~ 1.38 solar masses so that electron degeneracy pressure is not overcome, restarting nuclear fusion. If these white dwarves start accreting matter from a binary companion, they can approach the Chandrasekhar limit, at which point it is believed that carbon fusion of the core starts to occur. This causes a runaway reaction leading to a supernova. This mechanism results in the supernova displaying very consistent characteristics, the peak luminosity being of particular interest for the purposes of using Type Ia Supernovae as standard candles[7].

Although Type Ia Supernovae display very similar peak luminosities, it is not without some dispersion. The apparent similarity was noticed in the early 1980s leading to hopes that Type Ia Supernovae could be used as a standard candles. However, it was soon discovered by studying nearby events, which could be compared to other standard candles, that the peak absolute magnitudes varied by 0.3-0.5 mag [44]. In 1993 Phillips *et al.* [45] discovered an empirical relation between the rate of decline of the light curve over 15 days and the peak luminosity. This has been further refined [46] and has, hence, allowed the use of Type Ia Supernovae as standard candles leading to the results in 1997.

Interest in Type Ia Supernovae observations increased markedly with the release of results in 1997 indicating the expansion of the Universe appears to be accelerating [47, 48]. Similar studies since have come to the same conclusion [14, 15, 49, 50, 51]. There is still part of the community that disputes not only the mechanism put forward for the observed acceleration, the cosmological constant or another form of dark energy, but the results themselves.

[7]Reviews of the physical mechanisms predicted in Type Ia Supernovae can be found in [43].

Recently, further analysis of the Type Ia Supernovae observations has led to a number of interesting conclusions. A large variation in the interpretation of the results is possible, dependent on the techniques used in the analysis, to the extent that an accelerating Universe "is not supported *beyond reasonable doubt*" [52] when the raw data is carefully analysed. The issues covered by Cattoen and Visser [52] are:

- The distance scale

  The value of the best-fit χ^2 for a given model is shown to vary significantly dependent on whether one uses the luminosity distance, proper motion distance (photon count distance), angular diameter distance or a number of other cosmological distance definitions. These alternative definitions lead to alternative versions of the Hubble law, and differing results.

- The dependence of the deceleration parameter

  It is shown that the value of the inferred deceleration parameter is affected by whether one considers the redshift, z, or a parameter argued for as an improvement on theoretical grounds, $y = z/(1+z)$.

- Systematic Errors

  The systematic errors quoted for the Type Ia Supernovae results, when combined with the usually displayed statistical errors, indicate that the level of confidence for cosmic acceleration may be significantly overstated.

- **Cosmic Microwave Background**

The Cosmic Microwave Background (CMB) is perhaps the most important known phenomenon in the study of modern cosmology. It was one of the most famous accidental discoveries in physics, being attributed to Penzias and Wilson. The Nobel Prize winning discovery was made while trying to find the source of background noise on a microwave receiver at Bell Telephone Laboratories in New Jersey in 1965 [53]. In 1941 McKellar actually detected the CMB while studying the properties of an interstellar gas cloud without realising what he had found [3, 54]. The CMB had been theorised and values predicted on a number of

occasions before the 1965 discovery [55], in fact, Wilkinson and Roll at Princeton University had begun construction of a Dicke radiometer to measure it in 1964.

Since the discovery of the CMB many observations have been conducted. The two most famous of these are the Cosmic Background Explorer (COBE) and Wilkinson Microwave Anisotropy Probe (WMAP), both satellite missions undertaken with the backing of NASA. Other notable experiments are the balloon based BOOMERanG experiment, and the ground based observations by the Very Small Array, the Degree Angular Scale Interferometer (DASI) and the Cosmic Background Imager. Due to the apparent importance of the CMB to studies of cosmology, more experiments are planned with the Planck Surveyor satellite due to be lauched in 2008 and ground based experiments, Clover and Atacama Cosmology Telescope, which saw first light on the 8th of June 2007.

The radiation, which peaks in the microwave regime at 1.9mm at the current epoch, is, to current limits of experimental accuracy, a perfect blackbody spectrum. At times earlier than roughly 300,000 years, the average temperature of the Universe was at energy scales above the binding energy of hydrogen. Consequently the Universe was filled with an ionised plasma, with photons and electrons undergoing Thomson scattering, and was opaque. As the Universe expanded, it cooled so that $k_B T$ was reduced below the binding energy of hydrogen, and the first atoms formed, the beginning of recombination. The Universe then became transparent, as the free electrons were bound to nuclei, decoupling matter and radiation. The photons which scattered from the last free electrons have been travelling to us ever since. Hence this epoch is referred to as the *time of last scattering*. These photons have since cooled due to the expansion of the Universe but have retained a very nearly isotropic mean temperature, 2.725 K at the present epoch. There is a dipole variation of order 10^{-3} in this temperature, which is assumed to be almost completely due to our local motion with respect to the cosmic rest frame[8]. When this dipole is subtracted, temperature variations

[8]It is possible that there is a 1-2% error in the dipole substraction due to foreground inhomogeneities [56]. Via the Rees-Sciama effect this may account for anomalies in the low multipole moments of the CMB anisotropy spectrum, which have been dubbed the "axis of evil" [57].

of the order 10^{-5} are seen.

The power of the fluctuations $\Delta T/T$ for 2-point variations as a function of angular scale is shown in the well-known CMB anisotropy spectrum in figure 1.2. These fluctuations are believed to be intrinsic to the plasma at the time of last scattering. The structure of peaks can be modelled from acoustic oscillations in the matter-radiation plasma before last scattering.

Under the assumption that the CMB is the remnant of last scattering a number of deductions can be made. The first, and perhaps most significant, is that we live in a universe which underwent a Big Bang as opposed to being in a steady state. This resulted in a major change in direction for much of the community in the 1960s when it was discovered. Within the context of a cosmological model, the Doppler peaks in the angular anisotropy spectrum encode a lot of information. These predictions include the dark matter content of the universe, the epoch of reionisation by population III stars and the ratio of photons to baryons.

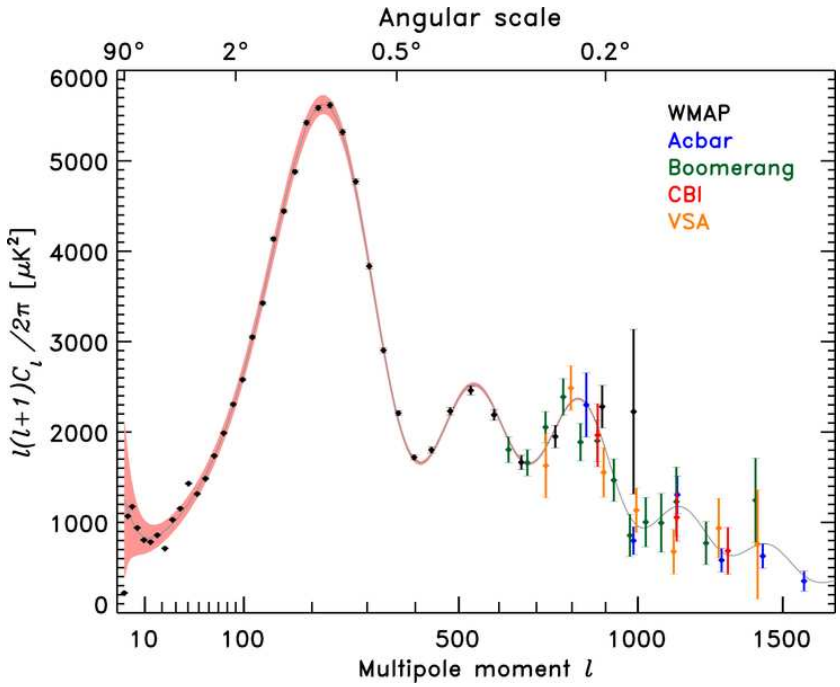

Figure 1.2: *The power spectrum of the anistropies in the CMB. The data shown is from WMAP (2006), Acbar (2004) Boomerang (2005), CBI (2004) and VSA (2004) instruments.*

The determination of the geometry of the Universe arises on account of the overall

focussing of light rays which determines the angular scale of the Doppler peaks. The first peak corresponds roughly to the angular diameter of the sound horizon. WMAP results have quoted values with respect to the ΛCDM model for both the size of the sound horizon at decoupling, $r_s = 147 \pm 2$Mpc, and the distance from decoupling, $d_A = 14.0^{+0.2}_{-0.3}$Gpc [6]. This gives an angular scale of the sound horizon, $\delta = 0.0105^{+0.0003}_{-0.0004}$ at the present epoch.

- **Baryon Acoustic Oscillations**

  Analysis of the Sloan Digital Sky Survey (SDSS) data [1, 2] reveals a slight departure from Gaussian statistics in the average distribution of galaxies in the Universe. The overdensity or baryon acoustic oscillation (BAO), appears to occur at distances comparable to the expected size of the remnant of the largest acoustic oscillation in the baryon-photon plasma at the time of decoupling, once intervening expansion of the Universe is taken into account. Since the angular scale of the first Doppler peak corresponds to a standard ruler at the time of last scattering, whereas the BAO scale gives a standard length scale at recent epochs, we have a powerful tool for directly determining the expansion of the Universe in the interim. This puts strong constraints on any cosmological model. The distance between the areas of overdensity is found to be about $100h^{-1}$Mpc [1]. This result seems to match with reasonable accuracy estimates using the ΛCDM model.

1.4 Schwarzschild and Reissner-Nordström Black Holes

Classically black holes are defined as trapped regions in the spacetime manifold. These are compact regions bounded by horizons that in the classical description of physics are inescapable once crossed. A number of different definitions of black holes horizons exist. Nielsen [58] gives a review of the major candidates. The version of the horizon that has been perhaps the most deeply studied is the *event horizon*: a hypersurface which separates the trapped region from regions of the manifold in which points are

connected by at least one possible timelike path to future null infinity [59]. Event horizons exist not only for black holes but also in models of the universe in which the rate of expansion is accelerating, most notably the de-Sitter universe.

Event horizons are a global property of the manifold. While sufficient for many applications, the global definition can cause difficulties if one wishes to consider interacting black holes. Furthermore, the physical interpretation of an event horizon in dynamical situations can be somewhat strange. Because the event horizon is defined as the boundary of the causal past of future null infinity, in the case of black hole creation, an event horizon may first develop before matter falls across the horizon as seen by a local observer. There have been many attempts to provide more local definitions of the horizon, beginning with the notable example of apparent horizons [59]. More recently other locally defined horizons have become an area of interest [58]. They may hold clues to the resolution of the information paradox in quantum gravity. They also have applications for numerical work, especially in multi-body problems. Event horizons, however, give a very good approximation for many applications. Other types of horizons can be defined within general relativity including the particle horizon, the acceleration horizon and Cauchy horizon. The particle horizon constitutes the relevant domain of averaging used in section 1.2. Otherwise these alternative notions of horizon are not considered in depth in this thesis.

Black hole horizons are associated with quantities that obey laws analogous to those of thermodynamics. In particular, the surface gravity can be thought of as a temperature, and the area of the horizon as an entropy [60]. At the level of classical general relativity this is a purely formal analogy. However, once quantum field theory is included black holes may evaporate via the Hawking effect and the correspondence to thermodynamics becomes exact.

The Schwarzschild solution [61] is the simplest black hole solution for Einstein's vacuum equations in 4-dimensions being uncharged, static, asymptotically flat and spherically symmetric. The Schwarzschild metric is given by

$$\mathrm{d}s^2 = -\left(1 - \frac{2GM}{r}\right)\mathrm{d}t^2 + \frac{\mathrm{d}r^2}{\left(1 - \frac{2GM}{r}\right)} + r^2\mathrm{d}\theta^2 + r^2\sin^2\theta\mathrm{d}\phi^2, \tag{1.37}$$

where we are using the $3+1$ split of Schwarzschild coordinates, M is the Arnowitt–

Deser–Misner (ADM) mass [62]. The Schwarzschild coordinates obviously break down at $r = 2GM$, which actually corresponds to the horizon. The Schwarzschild geometry has three rotational Killing vectors of $SO(3)$. In addition, it has a fourth Killing vector, $\frac{\partial}{\partial t}$, as a result of Birkhoff's theorem.

In general relativity one must be extremely careful about coordinate dependent statements. The Schwarzschild coordinate singularity at $r = 2GM$ can be removed by going to other coordinates such as the Painlevé-Gullstrand or Eddington-Finkelstein coordinates. Other coordinate systems may also possess coordinate singularities. In the case of Schwarzschild geometry, the double null Kruskal-Szekeres coordinates (u, v, θ, ϕ),

$$\mathrm{d}s^2 = -\frac{32G^3M^3}{r}\,\mathrm{e}^{-r/2GM}\mathrm{d}u\mathrm{d}v + r^2\Omega^2, \tag{1.38}$$

with transformations

$$\begin{aligned} v(t,r) &= \left(\frac{r}{2GM} - 1\right)^{1/2}\mathrm{e}^{(r+t)/4GM}, \\ u(t,r) &= \left(\frac{r}{2GM} - 1\right)^{1/2}\mathrm{e}^{(r-t)/4GM}, \end{aligned}$$

for $r > 2GM$ and

$$\begin{aligned} v(t,r) &= \left(1 - \frac{r}{2GM}\right)^{1/2}\mathrm{e}^{(r+t)/4GM}, \\ u(t,r) &= \left(1 - \frac{r}{2GM}\right)^{1/2}\mathrm{e}^{(r-t)/4GM}, \end{aligned}$$

for $r < 2GM$, in fact, cover the entire spacetime including the past singularity and an additional asymptotic region. One may readily see from (1.38) that for fixed θ, ϕ, $u =$ const and $v =$ const surfaces are null hypersurfaces, which are respectively outgoing and ingoing. Thus $r = 2GM$, $t = +\infty$, corresponds to the null surface $u = 0$, the future horizon.

Coordinate independent measures of the curvature are useful for detecting singularities. The Kretschmann scalar, $R^{abcd}R_{abcd}$, is one such invariant. For the Schwarzschild solution it is given by

$$R^{abcd}R_{abcd} = \frac{48G^2M^2}{r^6}. \tag{1.39}$$

This diverges as $r \to 0$ and hence implies the existence of a curvature singularity at $r = 0$. Most physicists do not regard singularities as physical infinities, but rather

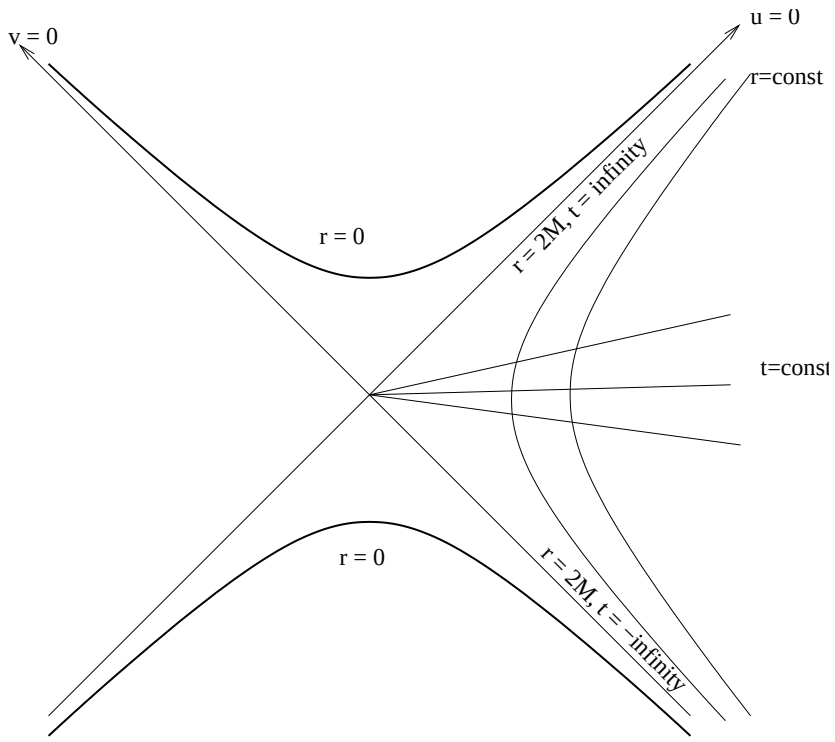

Figure 1.3: The Schwarzschild geometry in Kruskal-Szekeres coordinates.

a signal that the underlying theory – general relativity – is incomplete. In quantum gravity one may hope to eliminate such singularities. Singularities are not considered part of the manifold and are also conjectured, regardless of their physical nature, to exist within a trapped region bounded by the horizon. The *cosmic censorship hypothesis* states, in particular, that naked singularities cannot form in gravitational collapse from generic, initially non-singular states in an asymptotically flat spacetime obeying the dominant energy condition [63, 64].

The region of most theoretical interest is the *domain of outer communications* outside the horizon as this is the only region, at least classically, in which it is possible to make observations for use in discriminating between theories. The Schwarzschild geometry has been very successful for modelling phenomena seen within the solar system, where one can model the planets and comets as point particles since $r > r_{sun} \gg 2GM_{sun}$. The perihelion precession of Mercury is the most well-known local verification of general relativity, and is predicted to high accuracy by the Schwarzschild geometry. Other examples are: (i) the Shapiro time delay, detected when bouncing radar signals off Venus when it is behind the sun; (ii) the bending of light by the sun,

first seen during eclipses, which is correctly predicted to be twice the Newtonian value. Strictly speaking, a complete description of the local geometry is more sophisticated than the Schwarzschild geometry, since at the very least angular momentum should be included. However, these effects are negligible in the solar system.

The 'no-hair' theorems hypothesise that all black holes, under certain premises, can be uniquely defined by four asymptotic parameters, the mass, M, electric and magnetic monopole charges, Q and P, and the angular momentum, J. The Kerr-Newman solution is the relevant unique analytic solution of the vacuum Einstein equation.

We are interested in the case of a non-rotating charged black hole, parameterised by M, Q and P: the Reissner-Nordström solution. It should be noted that Q and P are generally considered together as they parametrise the electromagnetic charges as a whole and are just different components of the electromagnetic field tensor, $F_{\mu\nu}$. It is therefore usual to consider black holes as parameterised by three asymptotic parameters. Of course, magnetic monopoles have not been observed yet in nature. But they remain a theoretical possibility.

The 4-dimensional Reissner-Nordström metric in Schwarzschild coordinates is

$$\mathrm{d}s^2 = -\Delta \mathrm{d}t^2 + \Delta^{-1}\mathrm{d}r^2 + r^2\mathrm{d}\theta^2 + r^2\sin^2\theta\mathrm{d}\phi^2, \tag{1.40}$$

where

$$\Delta = 1 - \frac{2GM}{r} + \frac{G(Q^2+P^2)}{r^2}. \tag{1.41}$$

As with the Schwarzschild solution, provided we have been careful with our selection of spatial coordinates and have a timelike Killing vector, we can take $g^{rr} = 0$ as the null hypersurface that coincides with the horizon. In this case we get two horizons, the outer and inner horizons, r_+ and r_- respectively where

$$r_\pm = GM \pm \sqrt{G^2M^2 - G(Q^2+P^2)}. \tag{1.42}$$

There is a critical case at $GM^2 = Q^2 + P^2$. If $GM^2 < Q^2 + P^2$ there are no horizons as g^{rr} is always positive, so the metric remains regular for all values of $r > 0$. However, there is a problem as the Kretschmann scalar diverges at a curvature singularity at $r = 0$. Since there are no horizons this would represent a naked singularity, in violation of the cosmic censorship conjecture. If the conjecture holds, such solutions are unphysical.

When $GM^2 > Q^2 + P^2$ both event horizons exist and the singularity at $r = 0$ is timelike. The inner horizon is unstable to small perturbations [65]. It is an example of a Cauchy horizon – points to its future can also be influenced by the timelike singularity, leading to a loss of predictability for Cauchy initial values set at $r = r_-$.

The extremal Reissner-Nordström solutions have zero temperature and therefore do not emit Hawking radiation. The extremal solutions have a different topology to the non-extremal ones. Locally the geometry in the neighbourhood of the horizon is $\mathrm{AdS}_2 \times S^2$, equivalent to the Bertotti-Robinson metric. The region between the horizon and the singularity may be thought of as an infinitely long throat or equivalently, the geodesic distance is infinite. This property makes extremal black holes useful for string theoretic calculations.

Chapter 2

Extensions to General Relativity

2.1 Kaluza-Klein Compactification

Scalar fields appear in many parts of physics from statistical mechanical concepts such as temperature and pressure, potential fields in Newtonian gravity and electrostatics through to representations of spin-0 particles in quantum field theory and the phenomenology of symmetry breaking and compactification in string theory. We are largely interested in the last of these examples, which arises through various mechanisms when string theory is considered the underlying fundamental physical theory. There are three main classes of scalar fields attributed to the manifestation of string theory in 4 dimensions, the dilaton, the axion and the moduli fields. Firstly, however, we will present the well-known example of Kaluza-Klein compactification in five dimensions, as it demonstrates a number of the essential features common to compactification in more complex string theory scenarios.

The number of dimensions the Universe possesses is an interesting question for fundamental physics. While we observe four spacetime dimensions, one temporal and three spatial, a number of unified theories of gravity and the other forces which were developed in the 20th century require or allow more dimensions. These extra dimensions have generally been considered to be 'rolled-up' or compactified to such a degree that they are not observable at current experimental limits. It is worth noting that theories do exist with extended extra dimensions, the most notable example being

braneworlds [see Maartens [66] for a review]. In the context of M-theory braneworlds, all standard model particle excitations – including spin-1 bosons – are confined to a brane with three spatial dimensions: the Universe in which we live. However, gravity can probe all the dimensions.

The idea of extra dimensions in physics was introduced by Kaluza in 1921 [67]. He discovered that a fifth dimension allowed for a theory which contained both electromagnetism and gravity, the only known forces at the time. In 1926 Klein proposed the fourth spatial dimension to be curled up into a circle with a very small radius, leading to periodic boundary conditions for physical fields in the extra dimension [68]. In dimensions greater than five, this can be replaced by a more general Lie group, corresponding to a Yang-Mills gauge theory. In string theory compactifications, 6-dimensional Calabi-Yau spaces are favoured on a number of theoretical grounds [69].

Kaluza-Klein theory takes a standard Einstein action in five dimensions,

$$S_{(5)} = \frac{1}{4\bar{\kappa}^2} \int \mathrm{d}^5x\sqrt{-\bar{g}}\,{}^{\mathbf{5}}\mathbf{R}, \tag{2.1}$$

where $\bar{g} \equiv |\det(\bar{g}_{AB})|$ and $\bar{\kappa} = 4\pi\bar{G}$ with $\bar{G}$ being the 5-dimensional Newton constant[1]. The five dimensional metric, $\bar{g}_{AB}$ can be separated into the 4-dimensional metric $g_{\mu\nu}$, a vector, $\bar{g}_{\mu 4}$ and a scalar, $\bar{g}_{44}$ and is given by

$$\mathrm{d}s^2 = \bar{g}_{AB}\mathrm{d}x^A\mathrm{d}x^B = \bar{g}_{44}\left(\mathrm{d}x^4 + 2\kappa A_\mu \mathrm{d}x^\mu\right)^2 + \beta(\sigma)g_{\mu\nu}\mathrm{d}x^\mu\mathrm{d}x^\nu, \tag{2.2}$$

where $\bar{g}_{\mu 4} = 2\kappa\bar{g}_{44}A_\mu$ and $\kappa = 4\pi G$. The form of the metric, (2.2), is the most general invariant under translations in x^4. For later convenience we take $\beta(\sigma) = \exp(-2\kappa\sigma/\sqrt{3})$ and $\bar{g}_{44} = \exp(4\kappa\sigma/\sqrt{3})$ where σ can be thought of as some scalar which corresponds to the $\bar{g}_{44}$ component of the metric. The fourth spatial dimension, x^4, is considered to be periodic,

$$x^4 \cong x^4 + 2\pi R_\kappa. \tag{2.3}$$

Since the internal manifold is $U(1)$ under this assumption we can take Fourier series

[1]In this section, capitalised Latin indices, $A, B, ...$ run over all D-dimensions, $0, ..., D-1$, while Greek indices, $\alpha, \beta, ...$, are the d-noncompact dimensions $0, ..., d-1$ with $D = 5$ and $d = 4$ for the Kaluza-Klein theory.

expansions of the fields σ, A_μ, and $g_{\mu\nu}$ in x^4

$$\begin{aligned}
\sigma(x^A) &= \sum_{n=-\infty}^{\infty} \sigma^{(n)}(x^\lambda) \exp\left(\frac{inx^4}{R_\kappa}\right), \\
A_\mu(x^A) &= \sum_{n=-\infty}^{\infty} A_\mu^{(n)}(x^\lambda) \exp\left(\frac{inx^4}{R_\kappa}\right), \\
g_{\mu\nu}(x^A) &= \sum_{n=-\infty}^{\infty} g_{\mu\nu}^{(n)}(x^\lambda) \exp\left(\frac{inx^4}{R_\kappa}\right).
\end{aligned} \tag{2.4}$$

Making the ansatz that $g_{\mu\nu}$ is independent of x^4 we can then use the equivalent assumption that we can consider just the zero-modes of the expansions in (2.4). This corresponds to the low energy limit of the theory. From (2.2) and (2.4) we obtain the effective 4-dimensional action of the zeroth-order approximation,

$$S_{(4)} = \int \mathrm{d}^4x\sqrt{-g}\left(-\frac{{}^{\mathbf{4}}\mathbf{R}}{4\kappa^2} - \frac{1}{4}\,\exp(2\sqrt{3}\kappa\sigma)F_{\mu\nu}F^{\mu\nu} + \frac{1}{2}\,g_{\mu\nu}\partial^\mu\sigma\partial^\nu\sigma\right). \tag{2.5}$$

The metric (2.2) preserves symmetry under the coordinate reparametrisations

$$x^\mu \to x'^\mu(x^\nu), \qquad x'^4 \to x^4 + \Lambda(x^\nu), \tag{2.6}$$

which in turn give the 4-dimensional coordinate transforms and the $U(1)$ gauge transformations

$$A_\mu \to A'_\mu = A_\mu + \frac{1}{2\kappa}\,\partial_\mu\Lambda, \tag{2.7}$$

in the effective 4-dimensional theory. This is the *Kaluza-Klein* mechanism, proposed by Kaluza in 1921, which generates electromagnetism in the effective 4-dimensional theory.

If one considers an additional complex scalar field, ϕ, coupled to the 5-dimensional theory it is possible to determine the radius, R_κ, if the ansatz, $\bar{g}_{\mu 4} = 2\kappa\bar{g}_{44}A_\mu$, is followed to its natural conclusion. We consider the Fourier series expansion about x^4,

$$\phi(x^A) = \sum_{n=-\infty}^{\infty} \phi^{(n)}(x^\lambda) \exp\left(\frac{inx^4}{R_\kappa}\right), \tag{2.8}$$

again in order to find the 5-dimensional scalar Lagrangian

$$\mathcal{L}_{(5)\phi} = \sqrt{\bar{g}}\bar{g}^{AB}\partial_A\phi^*\partial_B\phi. \tag{2.9}$$

This reduces to

$$\mathcal{L}_{(4)\phi} = \sum_{n=-\infty}^{\infty} \sqrt{-g} \left\{ (D^\mu \phi^n)^* D_\mu \phi^n - n^2 \phi^{n*} \phi^n \exp\left(\frac{-2\kappa\sigma}{\sqrt{3}} \right) \right\}, \tag{2.10}$$

in the effective 4-dimensional theory where the covariant derivative is given by

$$D_\mu = \partial_\mu - \frac{2i\kappa n}{R_\kappa} A_\mu. \tag{2.11}$$

If we compare this to the 4-dimensional form of D_μ in relativistic quantum mechanics [70] we find the elementary charge is quantised in units of $e = 2\kappa/R_\kappa$ and hence $R_\kappa \simeq 3.78 \times 10^{-34}\,\mathrm{m} \simeq 23.4\,\ell_{\mathrm{Planck}}$ which is well beyond the current detectable limits of experiment.

In the effective 4-dimensional Lagrangian, (2.10), the non-zero modes correspond to massive charged particles with masses,

$$m_n = \frac{n^2}{R_\kappa} \exp\left(\frac{-2\kappa\sigma}{\sqrt{3}} \right). \tag{2.12}$$

This infinite tower of mass states is position dependent with charges and masses being integer multiples of e and $m_0 = 2\kappa e$. These are the the *Kaluza-Klein excitations*. Similar mass states will exist if one takes the non-zero modes in the expansion (2.4) in the free theory given by (2.5). These excitations can be shown to be pure spin-2 [71] and while Kaluza-Klein is not a realistic theory, such features are present in more sophisticated unified theories.

It would appear that the Kaluza-Klein excitations are stable [72, 73] which would indicate that if such mass states exist they should be observable as remnants of compactification if it is in fact an actual physical phenomena. This places constraints on the underlying theories requiring compactification, as no such excitations are currently observed [72]. In the standard Kaluza-Klein scenario the masses would be so large that they would also still be unobservable at the Large Hadron Collider (LHC) which will start operation soon. However, other proposals – including brane worlds and other scenarios with large extra dimensions – do give rise to the possibility of modifying the spectrum of Kaluza-Klein excitations in such a way that they would be observable at LHC energies. The fact that ordinary Kaluza-Klein modes have masses proportional to their charges, would cause difficulties for being dark matter candidates, given that dark matter appears not to interact strongly via electromagnetic interactions. Different scenarios need to be looked at phenomenologically on a case-by-case basis.

2.2 Dilaton, Axion and Moduli Fields

The labels dilaton and moduli refer to scalar fields, and are often used in a sloppy fashion. The dilaton was originally introduced by Isham, Salam and Strathee [74]. It arose through the development of an effective lagrangian which respected conformal and $[SU(2)\times SU(2)]$ or $[SU(3)\times SU(3)]$ chiral symmetry. The resulting physical theory had a number of features including massless, even-parity, spin-zero and chiral invariant Goldstone particles corresponding to spontaneous symmetry breaking. The relevant particle was named the "dilaton".

In a string context the dilaton is a scalar appearing in 10-dimensional string theory effective actions, which may also be obtained by dimensional reduction of M-theory on a circle in 11 dimensions. In 10 dimensions it is associated with the dilation symmetry. However, the word has loosely come to be associated with any scalar field coupled to gravity in any dimension.

The dilaton field[2], ϕ, defines the string coupling constant, α, such that,

$$\alpha = \exp(\langle\phi\rangle), \tag{2.13}$$

and hence is vital component for the physical realisation of string theory. This is a novel situation in that the coupling constant is not constant but dynamical, varying with position. It contrasts with the situation in quantum field theory where coupling constants are exactly that, constant. When supersymmetry is unbroken the value of the scalar field is arbitrary, however, breaking of supersymmetry will usually create a potential associated with the dilaton field which contains a minimum restricting the behaviour of the field to energy states localised in this region.

Moduli fields[3] are another form of theoretical scalar fields defined as having arbitrary values as the associated potential is flat. In string theory compactifications, moduli fields encode information about the shape and size of the compactified dimensions, particularly Calabi-Yau manifolds, when compactifing from 10-dimensional string theory to a 4-dimensional effective theory.

[2]Note the change in notation here due to convention, σ in the previous section is the dilaton in a compactification of 11-dimensional M-theory to a 10-dimensional string theory.

[3]Generally denoted σ in this thesis.

The final scalar field we consider here is the axion. The axion arose in the standard model formulation of the strong interaction in quantum chromodynamics (QCD). QCD has a non-trivial vacuum structure that allows violation of the charge conjugation and parity symmetries (CP). This violation would have a value that could be measured, in theory, as a dipole induced within the neutron. No such dipole is observed to a high degree of accuracy, which means that the degree of CP violation must be $\lesssim 10^{-9}$, if it is non-zero [75]. Since this value should be arbitrary in the range, 0 to 2π, this seems rather unnatural.

It was suggested by Peccei and Quinn [76] that by adding a new global symmetry that is spontaneously broken, resulting in a particle, the axion, the value of the CP violating term could be taken to zero. This particle turns out to be a spin-0 pseudo-Goldstone boson, as the symmetry is not exact as due to instanton effects, and therefore carries a small mass.

It has been suggested that the axion could be a dark matter candidate. Axions should have been created in great numbers during the Big Bang. In the post-inflation universe it is theorised they would have become a very cold Bose-Einstein condensate, which could be be a source of dark matter in the modern universe. Current experiments have not yet been able to make observations at the expected very low masses, although halo axions have been ruled out at masses above 1.9×10^{-6}eV [77], which is at the higher end of the expected order.

2.3 Scalar Fields Coupled to Gravity

2.3.1 Cosmology

The inclusion of scalar fields in cosmological solutions is relatively recent. This is partly due to the current "golden era of cosmology" leading to increased theoretical focus on the subject in the past two decades. However, another primary motivation was a change in the consensus about the underlying cosmological model around 1998. Prior to this there was only relatively slim observational evidence to suggest that the Universe could not be explained by a standard open $\Lambda = 0$ FLRW model. With the release of the type

Ia supernovae results in 1997 [47, 48] that indicated the Universe appeared to be was undergoing accelerating expansion, consensus swung in favour of "dark energy" as a cause for cosmic acceleration. Scalar fields were an obvious candidate.

Much work had previously be done on the subject of scalar fields in cosmology, most notably as a mechanism to drive inflation [78], the so-called *slow-roll inflation*. [See Linde [79] for a review.] The scalar field present during inflation, however, was not thought to have any relevance beyond the very early universe since the energy scale is vastly different to any residual dark energy today.

Late-time homogenous scalar fields in cosmology were studied in earnest from the mid 1980s onwards. The pioneers included Wetterich [80] and Pebbles and Ratra [81] who introduced a time-dependent scalar with a time-varying equation of state parameter lying in the range $-1 < w_\phi < 1$. The term *quintessence* was later coined [82] to describe such late-time fields, and became a major area of research immediately following the 1997 results. Quintessence is generally postulated as a form of dark energy which drives cosmic acceleration at the present epoch. It is generally dependent on all spacetime coordinates and has a varying equation of state, which must enter into the regime, $w_Q < -1/3$ that violates the strong energy condition. By comparison, the cosmological constant is fixed such that $w_\Lambda = -1$.

Quintessence may also weaken the cosmological constant problem. Most of the solutions show tracker behaviour until the epoch of matter-radiation equality at which point the field becomes independent of the evolution of the other background fields and starts to behave as dark energy. The energy density attributed to such a field is expected to be lower than estimates of the vacuum energy.

The strong energy condition, $w > -1/3$, is satisfied by all classical matter and radiation and is required for fields to focus light rays. An exotic form of matter, such as quintessence, may violate the strong energy condition while satisfying the dominant energy condition which requires $-1 \leqslant w \leqslant 1$ for perfect fluids. Physically the dominant energy condition is required for the speed of sound to be less than or equal to the speed of light.

Recently a number of people have considered cosmological models in which the dominant energy condition is violated, giving rise to *phantom* cosmologies, with $w <$

-1 [83, 84]. Such models are not new. In fact, they formed the basis of the Hoyle-Narlikar models in the early 1960s [85]. At the time the models were of interest due to the negative kinetic energy $C(x)$ field which was considered a mechanism for energy creation. The violation of energy conservation was seen as a benefit by Hoyle and Narlikar, as it allowed for the continuous creation of matter.

Cosmologies with $w < -1$ have some potentially serious problems. Causality and stability of the system are no longer guaranteed by the Hawking-Ellis vacuum conservation theorem [59, 86] and the dominant energy condition. In a physical sense this means the speed of the energy flow can exceed the speed of light allowing closed causal loops. Another problem is that the classical Hamiltonian can be unbounded below depending on the system, but particularly for phantom matter with a negative kinetic energy. Such a system has a negatively infinite ground state meaning no stable vacuum solution exists [87, 88]. One cosmological implication, if such a fluid existed and came to dominant the late time evolution of the Universe, is the *big rip*. The expansion of the Universe would accelerate at such a rate that the event horizon due to acceleration would eventually shrink to the point that all bound systems are ripped apart, as no particle can remain causally connected to any other particle.

Solutions which violate the dominant energy condition need a quantum field theory and hence a vacuum, before they can seriously be considered as a viable theory. Such solutions are, however, an area of interest and the issues mentioned above are not necessarily terminal, as pointed out, but need analysis on a case-by-case basis. Measurements of the current equation of state parameter, although rather haphazard and model dependent in nature, indicate w could be less than -1 in certain situations [83, 89]. It is worth noting, however, if the Universe has an equation of state parameter $w = -1$ or slightly larger, any observations would possess some variance and systematic errors and therefore likely include the region $w < -1$ within the error limits. Data supporting $w < -1$ should therefore be treated with care as the physics inherent in such a Universe would be significantly different to the status quo. We consider some cosmological models, which enter this regime for certain parameter values, when considering perturbative terms in a 4-dimensional effective string theory action in chapter 4.

Another approach taken by many authors [90] is to consider the 4-dimensional effective actions motivated by string theory [91][4]. These approaches, through necessity, generally consider truncated perturbative effective theories following compactification. The focus of much of this work pre-1997 was to examine the behaviour in the inflationary and pre-inflationary universe. Many of these solutions show non-singular behaviour at the beginning of the Big Bang, in contrast to many of the more traditionally derived solutions. The scalar fields apparent in both the 10-dimensional and effective 4-dimensional theories also give a natural mechanism to drive inflation, although many solutions do not possess a *graceful exit* to end the inflationary period. In recent years, string motivated cosmologies have gained interest, this is due to a multitude of reasons, many interrelated. The motivation relevant here is that the scalar fields present in the effective 4-dimensional theory may help explain the late-time acceleration of the Universe along with the earlier inflationary periods. Other motivations include the advances within string theory itself which have allowed construction of more explicit cosmological scenarios which obey the microphysical constraints of string theory. These advances include flux-compactifications of Calabi-Yau manifolds and the popularisation of brane-worlds [92].

2.3.2 Black holes

Black hole solutions to Kaluza-Klein theory were first considered in 1960 [93], though such results were largely forgotten until higher dimensions became the vogue in the late 1980s with the advent of supergravity theories. One reason why black hole solutions with scalar fields were not widely studied earlier was due to the "no-hair" theorems [94]. In particular it was shown in the early 1970s for a number of different models involving gravity plus scalars that static, spherically symmetric solutions with regular horizons do not exist [95]. Generally the scalar field diverges at the putative horizon, making it singular.

Kaluza-Klein black holes avoid the no-hair theorems by virtue of the coupling

[4]Obviously the scalars considered in string theoretic motivated situations can often fit the definition of quintessence. We separate them here due to original inspiration where quintessence is motivated by cosmological interest rather than an underlying fundamental theory.

between the scalar field and other gauge fields, such as the $U(1)$ field in the case of the 5-dimensional theory. The scalar charge depends on the electric and magnetic charges and must vanish if these fields are both set to zero. Thus the scalar charge is deemed to be a "secondary hair" in contrast to the "primary hair" that is ruled out by the no-hair theorems.

Following the first "string theory revolution" in 1984, interest in the physical viability of black hole solutions with scalar fields grew. Stable black hole solutions in the low energy limit of string theory are generally considered a necessity, though phenomenologically this only needs to be the case in the compactified theory.

In 1988 Gibbons and Maeda took a systematic approach to black hole solutions in higher dimensional theories with scalar fields [96]. The solutions, which are of interest in this thesis are 4-dimensional solutions for scalar fields coupled to gravity and a $U(1)$ gauge field. In reference [96], Gibbons and Maeda initially considered the arbitrary dimensional model with the following action

$$\begin{aligned} S &= \int \mathrm{d}^D x\sqrt{-g}\Bigg[\frac{R}{2\kappa^2} - \frac{4}{(D-2)\kappa^2}\,(\nabla\phi)^2 - \frac{1}{4}\,\exp\left(-\frac{4}{D-2}\,g_2\phi\right)F_{\mu\nu}F^{\mu\nu} \\ &- \frac{1}{2(D-2)!}\,\exp\left(-\frac{4}{D-2}\,g_{D-2}\phi\right)F_{\mu_1,..,\mu_{D-2}}F^{\mu_1,..,\mu_{D-2}} - V(\phi)\Bigg]. \end{aligned} \tag{2.14}$$

where g_2 and g_{D-2} are coupling constants of the dilaton ϕ to the 2-form $\mathbf{F}$ and $(D-2)$-form $\mathbf{F_{D-2}}$ respectively.

For generality the potential has been included here although it is set to $V(\phi) = 0$ for the systems we are interested in. When the potential is absent the action has scale invariance under the transformation,

$$\begin{aligned} g_{\mu\nu} &\rightarrow \Omega g_{\mu\nu}, \\ F_{\mu\nu} &\rightarrow \Omega^{[1+2g_2k/(D-2)]}F_{\mu\nu}, \\ F_{\mu_1,..,\mu_{D-2}} &\rightarrow \Omega^{[D-3+2g_2k/(D-2)]}F_{\mu_1,..,\mu_{D-2}}, \\ \phi &\rightarrow \phi + k\ln\Omega, \end{aligned} \tag{2.15}$$

where k is arbitrary and non-zero. A non-zero potential will, in general, break this scale invariance. Non-zero potentials will arise in compactification schemes; the question of the physical relevance of solutions with $V = 0$ is therefore open to debate. However,

exact solutions are readily found when $V = 0$, making them the object of the first studies.

Asymptotically flat analytic solutions are found to both the electrically and magnetically charged cases in Gibbons and Maeda. These solutions are dependent on the values of M and Q with no dependence on the charge of the scalar field. In fact the scalar field only exists in the situation where either $Q \neq 0$ or $P \neq 0$; i.e. they are an example of "secondary hair".

The solutions themselves show some interesting thermodynamical properties. In the case where $g_2 < \sqrt{D-3}$ the isotherms in the $M - Q$ plot show Reissner-Nordström type behaviour [97] with zero temperature extremal black holes and a change in sign in the specific heat, $C \equiv (\partial M/\partial T)|_Q$. When this limit is exceeded the the solutions are Kaluza-Klein-like [98] with infinite temperature extremal black holes and a negative definite specific heat. The limiting case, $g_2 = \sqrt{D-3}$, is interesting in that the isotherms end on the extremal limit, this means the extremal case has finite varying temperature. The solutions for the electric case have a duality with the magnetic case such that $(g_2, Q) \rightarrow (g_{D-2}, P)$.

2.4 Higher-order Gravity

Theories of gravity based on modifications to the Einstein-Hilbert action have a long history. One primary consideration is the need for field equations, second-order in the derivatives of the metric. Theories based on field equations with higher-derivatives generally have problems with causality, and conservation of energy at the classical level, or a loss of unitarity when quantised[5].

In 1971 Lovelock considered the problem of finding the most general field equations in D-dimensions which contain, at most, second derivatives of the metric. In four dimensions, the Einstein equations with a possible cosmological term are unique in this respect. However, if $D > 4$ then additional divergence-free second-order symmetric tensors, $A_{\mu\nu}$, can be found [100]. For a D-dimensional manifold it is shown that n such tensors can be constructed from the metric and its first and second derivatives where

[5]See Barth and Christian [99] for a brief historical review.

$n = D/2$ for even D and $n = (D+1)/2$ for odd D,

$$A^{\nu}{}_{\mu} = \sum_{p=1}^{n-1} a_p \delta^{\nu\nu_1\ldots\nu_{2p}}_{\mu\mu_1\ldots\mu_{2p}} R_{\nu_1\nu_2}{}^{\mu_1\mu_2} R_{\nu_3\nu_4}{}^{\mu_3\mu_4} \ldots R_{\nu_{2p-1}\nu_{2p}}{}^{\mu_{2p-1}\mu_{2p}} + a\delta^{\nu}{}_{\mu}, \tag{2.16}$$

where a_p and a are arbitrary constants.

The quadratic curvature correction is obtained through variation of the Gauss-Bonnet term in the action given by

$$R^2_{GB} = R_{\mu\nu\gamma\lambda} R^{\mu\nu\gamma\lambda} - 4R_{\mu\nu} R^{\mu\nu} + R^2. \tag{2.17}$$

It can be shown that the Gauss-Bonnet term is the only possible quadratic order correction to Einstein gravity in a low energy effective string theory if a ghost-free expansion in the slope parameter is demanded [101]. Ghosts are particles with negative definite kinetic energy. Other higher order terms can also be expected in the perturbative expansion but as the quadratic term is the leading order correction it tends to garner the highest level of interest.

In four dimensions the Gauss-Bonnet term is a topological invariant and therefore is only of interest in pure gravity when considering dimensions greater than four. It can, however, appear in effective 4-dimensional theories when coupled to another field. There has therefore been great interest in Gauss-Bonnet terms coupled to moduli and dilaton fields for both cosmological and black hole solutions as these fields are present in the effective 4-dimensional theory of string theory and may couple to the higher order gravity terms. One also observes such couplings when considering Jordan-Brans-Dicke type gravity [102, 103] which has a Lagrangian analogous to that of the Jordan string frame. If a conformal transformation to the Einstein frame is performed in the presence of higher order gravity terms such couplings can also be expected.

Chapter 3

Multi-scalar Black Holes

3.1 Introduction

Black hole solutions with scalar fields are usually constrained to possessing only *secondary hair* by the "no-hair conjectures" [94]. Early attempts to find black hole solutions coupled solely to a scalar field found solutions where the scalar field diverged at the putative horizon [95]. Hence, technically such solutions cannot actually be considered black hole solutions due to a lack of a regular horizon. They are unlikely to have any physical relevance [104]. The original "no-hair conjectures" have since been violated in a number of cases, either via coupling the scalar fields to gauge fields, or through violation of the dominant energy condition. When the existence of scalar hair depends on a non-vanishing gauge field, and is entirely fixed by the mass, gauge charge and angular momentum, it is called secondary hair [105]. Here we discuss a solution with contingent primary hair [106], that is to say the scalar hair depends on the existence of a non-vanishing gauge field but its behaviour is not entirely fixed by the values of the other asymptotic parameters. We briefly list some further "hairy" black hole solutions.

- Scalar fields coupled to higher order gravity have been heavily investigated due to the applicability to low energy effective 4-dimensional theories of string theory. The Gauss-Bonnet term, which is the only ghost-free leading order curvature correction, has naturally been of particular interest [107, 108].

- Minimally coupled scalar fields with dominant energy condition violating potentials have been shown to allow non-trivial hair [109, 110, 111, 112]. Examples have been found both analytically and numerically provided there is at least one global minimum with $V(\phi) < 0$.

- Theories which couple gravity to non-Abelian gauge fields such as Einstein-Yang-Mills, Einstein-Yang-Mills-Higgs and Einstein-Skyrme, usually contain nonlinear self-interactions and admit "hairy" black holes. Einstein-Yang-Mills-Higgs and Einstein-Skyrme also include scalar fields. These vanish exponentially at infinity, however, and thus they do not have "Gauss-like" scalar charge. These hairy black holes were thought to be generally unstable but it has been shown that some branches of solutions of the Einstein-Skyrme black holes are linearly stable [113]. Whether they are non-linearly stable remains an open question.

- Scalar fields non-minimally coupled to an Abelian gauge theory have been shown to admit hairy black hole solutions [96, 114, 115, 116]. Such theories arise naturally in Kaluza-Klein theories and effective low-energy limits of string theory with a non-trivial dilaton.

Despite the solutions listed above being beyond the premises of the original "no-hair conjecture", they are still considered interesting as tests of the limits of the conjectures. Stability is still an open problem in most cases.

Gibbons and Maeda found the solution to a non-rotating, static black hole with a single scalar field coupled to the $U(1)$ electromagnetic gauge field [96]. This solution is not a member of the Reissner–Nordström class but is entirely specified by the values of M, Q and P and hence, possesses only secondary hair. Adding an extra scalar field was shown to give more freedom [117] and a version of scalar hair that falls between the definitions of primary and secondary hair. This was called *contingent primary hair* and has been generalised to incorporate N scalar fields, with linear stability being shown [106]. Here we present numerical solutions to this model and discuss some of the features. We use the notation of [106] and define $c = 4\pi\kappa^2 = 1$.

3.2 Model

The general Lagrangian density for the N-scalar field case is

$$\mathcal{L} = \frac{1}{4}\Bigg[R \;-\; 2\Lambda - 2\sum_{i=1}^{N}\partial^{\mu}\Phi_i\partial_{\mu}\Phi_i \\ -\; \left(\sum_{i=1}^{N}\lambda_i^2\right)^{-1}\sum_{i=1}^{N}\lambda_i^2 e^{-2g_i\Phi_i}F_{\mu\nu}F^{\mu\nu}\Bigg], \tag{3.1}$$

where R is the Ricci scalar and $F_{\mu\nu}$ is the electromagnetic field strength. Initially we consider the $N = 2$ case with no cosmological constant, i.e., $\Lambda = 0$. For simplicity we split the representation of the scalar fields such that

$$\mathcal{L} = \frac{1}{4}\left[R - 2\partial^{\mu}\Phi\partial_{\mu}\Phi - 2\partial^{\mu}\Psi\partial_{\mu}\Psi - \frac{\lambda_1^2 e^{-2g_1\Phi} + \lambda_2^2 e^{-2g_2\Psi}}{\lambda_1^2 + \lambda_2^2}F_{\mu\nu}F^{\mu\nu}\right], \tag{3.2}$$

Since there is no potential dependent on any of the scalar fields, the Lagrangian density has the same scale invariance as the Gibbons-Maeda solution [96]. This invariance applies under global re-scalings of the metric $g_{ab} \to \omega^2 g_{ab}$ where $\nabla_a\omega = 0$.

The coupling between the scalar fields and the electromagnetic sector should be considered a "toy model" or at least a simplification of more physical well-motivated models. The construction of such an action is discussed by Cadoni and Mignemi [118], one of the precursors to the work presented here. The action presented in (3.2, with only minimal coupling of Ψ, can be found through a redefinition of the scalar fields when considering the four-dimensional low-energy action from heterotic string theory presented by Witten [119]. While there is no motivation at the string tree level to include a non-minimal coupling of Ψ, at the one-loop level it can arise. This was considered as a method of dealing with the supersymmetrisation of anomaly cancelling terms by Ibañez and Nilles [120]. More recently such a exponential coupling has been shown to arise when one integrates out the heavy modes of the string spectrum and be a necessary component to dynamical symmetry breaking [121]. The case considered here is a simplified version of the couplings which arise in these cases. It does, however, allow some progress to be made in finding black hole solutions and testing the validity of the no-hair conjectures.

We use a standard metric ansatz for static, spherically symmetric Schwarzschild

coordinates following the formalism of [122].

$$\mathrm{d}s^2 = -A^2(r)\left(1-\frac{2m(r)}{r}\right)\mathrm{d}t^2 + \frac{1}{1-\frac{2m(r)}{r}}\,\mathrm{d}r^2 + r^2\mathrm{d}\Omega^2 \tag{3.3}$$

where $\mathrm{d}\Omega^2 = \mathrm{d}\theta^2 + \sin^2\theta\mathrm{d}\phi^2$ and $m(r)$ is the familiar Misner-Sharp mass function. In order for non-trivial solutions to exist we take the magnetic monopole field ansatz

$$F_{\theta\phi} = P\sin\theta \tag{3.4}$$

where P is the magnetic charge. This is equivalent to the ansatz

$$B(r) = F_{\hat{\theta}\hat{\phi}} = \frac{P}{r^2} \tag{3.5}$$

in an orthonormal basis. Hence it can be seen explicitly that the magnetic field is radial and falls as $1/r^2$. Since the scalar field is assumed to be radial with no θ or ϕ dependence the Maxwell-like equation is still satisfied. The choice to use the magnetic monopole ansatz is made out of convenience. Due to the scalar coupling to the electromagnetic sector, the electric ansatz includes dependence on the scalar fields and is therefore non-trivial, the magnetic ansatz, being the $\theta\phi$ components of the electromagnetic tensor, avoids these complications. There is no longer a simple duality between the magnetic and electric solutions although solutions for the electric solution should still be tractable if the magnetic solutions exist. We could, of course, also consider a situation where both are non-zero. As in the single scalar field case of [96] the scalar fields will vanish if $Q = P = 0$.

The $G_t{}^t$ component of the Einstein equations gives

$$\frac{2m'}{r^2} = \left(1-\frac{2m(r)}{r}\right)\left(\Phi'^2+\Psi'^2\right) + \left(\frac{\lambda_1^2 e^{-2g_1\Phi}+\lambda_2^2 e^{-2g_2\Psi}}{\lambda_1^2+\lambda_2^2}\right)\frac{P^2}{r^4}\,. \tag{3.6}$$

The linear combination $G_t{}^t - G_r{}^r$ of components of the Einstein equations gives

$$\frac{A'}{A} = r\left(\Phi'^2+\Psi'^2\right), \tag{3.7}$$

while the two scalar field equations are

$$\partial_r\left(\left(1-\frac{2m(r)}{r}\right)Ar^2\partial_r\Phi\right) = -A\lambda_1^2 g_1 e^{-2g_1\Phi}\frac{P^2}{r^2} \tag{3.8}$$

and

$$\partial_r\left(\left(1-\frac{2m(r)}{r}\right)Ar^2\partial_r\Psi\right) = -A\lambda_2^2 g_2 e^{-2g_2\Psi}\frac{P^2}{r^2}\,. \tag{3.9}$$

Prime denotes differentiation with respect to r. We note these generalise to $N+2$ field equations for the system given in (3.1),

$$\frac{2m'}{r^2} = \left(1 - \frac{2m(r)}{r}\right)\left(\sum_{i=1}^{N} \Phi_i'^2\right) + \left(\sum_{i=1}^{N} \lambda_i^2\right)^{-1} \sum_{i=1}^{N} \lambda_i^2 e^{-2g_i\Phi_i} \frac{P^2}{r^4} + \Lambda, \tag{3.10}$$

$$\frac{A'}{A} = r \sum_{i=1}^{N} \Phi_i'^2 \tag{3.11}$$

and

$$\partial_r \left(\left(1 - \frac{2m(r)}{r}\right) A r^2 \partial_r \Phi_i\right) = -A\lambda_i^2 g_i e^{-2g_i\Phi_i} \frac{P^2}{r^2}\,. \tag{3.12}$$

3.3 Numerical Solutions

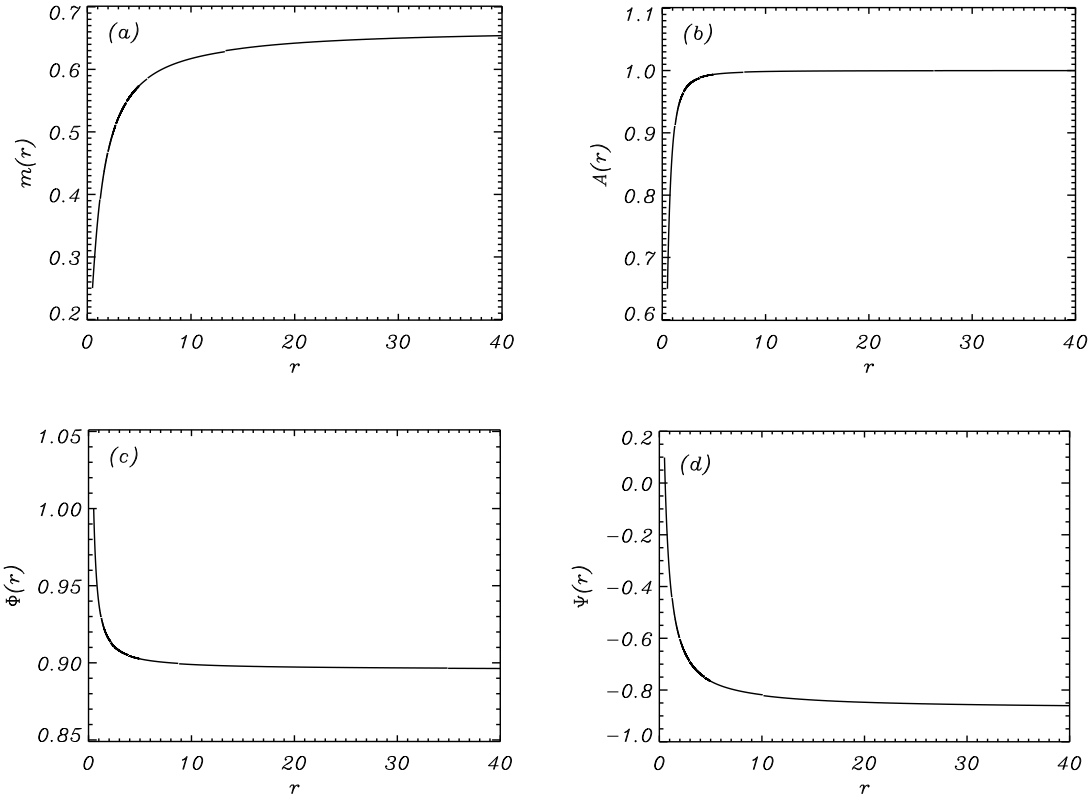

Figure 3.1: *Solution given by* $\lambda_1 = \lambda_2 = g_1 = g_2 = 1.0$ *with horizon values* $m(r_h) = 0.25$, $\Phi(r_h) = 1.0$, $\Psi(r_h) = 0.1$ *with* $P = 0.5$. $P_\infty = 0.8611$ *and* $M_{ADM} = 0.6674$ *while* $A(r_h) = 0.6490$ *as found by the shooting method: (a)* $m(r)$*; (b)* $A(r)$*; (c)* $\Phi(r)$*; (d)* $\Psi(r)$.

The $N = 2$ solutions can be obtained numerically with the help of the following

expansions near the horizon;

$$\begin{aligned} m(r) &= m_h + m_1(r-r_h) + m_2(r-r_h)^2 + ..., \\ A(r) &= A_h + A_1(r-r_h) + A_2(r-r_h)^2 + ..., \\ \Phi(r) &= \Phi_h + \Phi_1(r-r_h) + \Phi_2(r-r_h)^2 + ..., \\ \Psi(r) &= \Psi_h + \Psi_1(r-r_h) + \Psi_2(r-r_h)^2 + ... \end{aligned} \tag{3.13}$$

In figure 3.1 we show the general form of the solutions for a non-extremal case.

The solution is uniquely defined by 3 asymptotic charges in the $N = 2$ case and by $N + 1$ charges in the general case. The Arnowitt, Deser and Misner (ADM) mass, M_{ADM}, is given by the asymptotic value of $m(r)$, while the asymptotic Gauss-like magnetic charge is given by

$$P_\infty = \sqrt{\frac{(\lambda_1^2 e^{-2g_1\Phi_\infty} + \lambda_2^2 e^{-2g_2\Psi_\infty})}{(\lambda_1^2 + \lambda_2^2)}}\, P. \tag{3.14}$$

These two asymptotic charges along with the coefficient Φ_{-1} of the $1/r$ term in the Φ asymptotic expansion

$$\Phi = \Phi_\infty + \frac{\Phi_{-1}}{r} + \frac{\Phi_{-2}}{r} + ..., \tag{3.15}$$

uniquely define the solution. As shown in [106], Ψ_{-1} is constrained in the $N = 2$ case by

$$\Phi_{-1}^2 + \Psi_{-1}^2 + 2M_{ADM}\left(\frac{\Phi_{-1}}{g_1} + \frac{\Psi_{-1}}{g_2}\right) - \left(\frac{\Phi_{-1}}{g_1} + \frac{\Psi_{-1}}{g_2}\right)^2 = P_\infty^2. \tag{3.16}$$

and in general by

$$\sum_{i=1}^{N} \Phi_{-1,\,i}^2 + 2M_{ADM}\sum_{i=1}^{N}\frac{\Phi_{-1,\,i}}{g_i} - \left(\sum_{i=1}^{N}\frac{\Phi_{-1,\,i}}{g_i}\right)^2 = P_\infty^2, \tag{3.17}$$

where $\Phi_{-1,\,i}$ denotes the $1/r$ coefficient of the ith scalar field. This constraint limits the system to $N + 1$ degrees of freedom with these being, in the magnetic monopole case, M_{ADM}, P_∞ and $\{\Phi_{-1,\,1}$, $\Phi_{-1,\,2}$,...,$\Phi_{-1,\,N-1}\}$. The constraint, (3.17), holds throughout our numerical work to the accuracies required.

We use the shooting method to find solutions such that

$$\lim_{r\to\infty} A = 1, \tag{3.18}$$

where this condition is adhered to with a numerical accuracy of 10^{-7}. This exploits the rescaling freedom in $A(r_h)$ which can be seen in (3.7) – (3.9). This is a necessary

requirement for the surface gravity, κ, to be a well-defined quantity. The numerical limits used to define the asymptotic region are $m'(r) < 10^{-8}$ and $r > 500 r_h$.

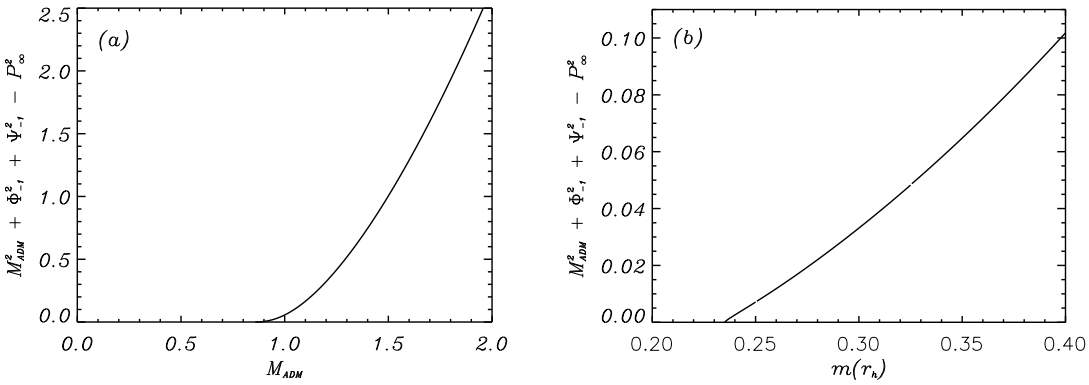

Figure 3.2: *Behaviour of constraint given in (3.23) for* $\lambda_1 = \lambda_2 = g_1 = g_2 = 1.0$*: (a)* $P_\infty = 1.2$*; shows the solution approaching the limit as it reaches the extremal case at* $M_{ADM} = 0.849$ *(numerical accuracy of* 10^{-5} *used for finding* P_∞ *and* M_{ADM}*), note that although (a) shows the expected behaviour it does not allow comparison with the expected values for* $\kappa = 0$ *as all quantities are defined at infinity; (b)* $P = 0.5$*; approaches the limit* $m(r_h) = 0.233$ *while the required value for* $\kappa = 0$ *from (3.22) is* $m(r_h) = 0.173$*.*

We have also found solutions to both the $N = 3$, $\Lambda = 0$ and $N = 2$, $\Lambda = -1$ cases. The solutions for the $N = 3$, $\Lambda = 0$ case are shown in figure 3.3. It is noted that there are no particular additional features when compared to the solutions in figure 3.1 beyond the obvious additional freedom in both the coupling and scalar charge. From these results, however, we would assume that solutions, with $N > 2$ scalar fields, exist, having $N + 1$ degrees of freedom. This may be of interest to string theory motivated work, where, in many cases a large or infinite number of scalar fields appear in the low energy effective 4-dimensional theory. [See [123] for a review.]

The anti-de-Sitter (adS) solutions, while attainable, have distinct numerical issues related to finding solutions over a wide parameter range. However, the critical temperature generally exhibited by adS solutions, due to the thermal bath, may result in interesting behaviour when Hawking evaporation is considered if the unique thermodynamic features of the $N = 2$, $\Lambda = 0$ system shown below are also manifest in the $\Lambda < 0$ case. A particular solution with $\Lambda = -1$ is shown in figure 3.4. Note that the

mass plot given for the $\Lambda = -1$ case is not $m(r)$ but rather,

$$M(r) = m(r) - \frac{\Lambda}{6} r^3, \tag{3.19}$$

The asymptotic mass is given by $M_\infty \equiv M(r_\infty)$, where the asymptotic region in the numerical integration is defined as $dM(r)/dr < 10^{-6}$.

3.4 Thermodynamic Behaviour

The surface gravity[1] for a black hole in these coordinates is given by [122]

$$\kappa = \frac{A(r_h)}{4m(r_h)} \left(1 - 2m'(r_h)\right) \tag{3.20}$$

Clearly we will have zero-temperature black hole solutions ($\kappa = 0$) if $m'(r_h) = 1/2$. In the horizon expansion given above this would correspond to $m_1 = 1/2$, while from the equations of motion we find

$$m_1 = \frac{P^2}{2r^2} \left(\frac{\lambda_1^2 e^{-2g_1\Phi_\infty} + \lambda_2^2 e^{-2g_2\Psi_\infty}}{\lambda_1^2 + \lambda_2^2} \right). \tag{3.21}$$

Hence, $\kappa = 0$ when

$$m(r_h)\Big|_{\kappa=0} = \frac{P}{2} \sqrt{\frac{\lambda_1^2 e^{-2g_1\Phi_h} + \lambda_2^2 e^{-2g_2\Psi_h}}{\lambda_1^2 + \lambda_2^2}}, \tag{3.22}$$

where we have used $r_h = 2m(r_h)$. We have denoted this limiting case as $m(r_h)|_{\kappa=0}$ as it turns out not to be the extremal case. Here we define the "extremal solution" as the solution existing with the maximal electromagnetic charge for a given mass and scalar charge. This varies from the alternative definition often used in a thermodynamic context, the solutions with $\kappa = 0$. We show that, while in many solutions these definitions coincide, they are not in general the same.

We find that the separate condition given by Mignemi and Wiltshire [106],

$$P_\infty^2 \leq M_{ADM}^2 + \sum_{i=1}^{N} \Phi_{-1,\,i}^2, \tag{3.23}$$

[1] We are considering surface gravity here, temperature may not be well-defined due to the lack of $T = 0$ black holes. In the discussion we use temperature and surface gravity interchangeably as $T \propto \kappa$ still holds.

is the constraint for extremal black holes. This constraint has no thermodynamic significance but the equality indicates the degenerate horizon. This is a novel situation as when (3.22) and (3.23) are considered we find $P_{\infty,\,\mathrm{extremal}} < P_{\infty,\,\kappa=0}$ for a given mass and scalar charge. For the degenerate horizon, given by the equality in (3.23), we find that the horizon becomes singular and hence does not have a well-defined surface gravity. This is indicated by divergence of the coefficient m_1 in (3.13).

The limiting behaviour due to (3.23) is shown in figure 3.2, where Φ_{-1} is defined by

$$\Phi_{-1} = g_1 \lambda_1^2 P^2 \int_{r_h}^{\infty} \frac{e^{-2g_1\Phi}}{r^2}\, A\partial r, \tag{3.24}$$

and similarly for Ψ_{-1} [106].

Contour plots of the surface gravity show Reissner-Nordström-like solutions when $g_1 = g_2 = 1$ and Kaluza-Klein-like solutions when $g_1 = g_2 = 3$ in figure 3.5(a) and figure 3.5(b) respectively. The 'specific heat', defined as $C \propto (\partial M_{ADM}/\partial\kappa)|_{P_\infty}$, changes sign in figure 3.5(a) while it is always negative for figure 3.5(b). Unfortunately we do not possess the computational power to find the limit of the coupling gradients that produce these two types of solutions.

The extremal limit in these cases is not an 'isotherm' but instead tends to finite non-zero values where the surface gravity is decreasing with increasing P_∞. If one was to consider the "thermodynamic" definition of extremal black hole solutions, $\kappa = 0$, these do not exist. The contours mimic those found in [96] but with a region excluded due to the constraint (3.23). Figure 3.6 shows this graphically. However, we would caution that the extremal solution falls into a different class from those solved by the numerical method implemented here. As the value of $m'(r_h)$ diverges we do not have well-defined solutions and hence the surface gravity is not defined. We therefore only comment on the limiting behaviour for the extremal cases.

3.5 Discussion

We have numerically demonstrated linearly stable black hole solutions with contingent primary hair. The condition, (3.17), as previously derived in [106], gives $N+1$ asymptotic charges for N scalar fields with two being M_{ADM} and P_∞ (in the non-zero magnetic

monopole solution considered here) with the other $N-1$ charges being the $1/r$ coefficients of the asymptotic expansion of $N-1$ of the scalar fields, $\{\Phi_{-1,1},\Phi_{-1,2},...,\Phi_{-1,N-1}\}$. This violation of the no-hair conjectures is, however, not entirely within the confines of the premise under which the conjectures were originally derived as we have non-minimal coupling between the scalar field and the $U(1)$ gauge field.

The solutions here may help to shed some light on black hole solutions to the low energy effective 4-dimensional theory of string theory when coupled with further corrections, such as, higher-order gravity terms [108], another $U(1)$ field or the inclusion of scalar potentials. Chen *et al.* have found constraints on the value of the coupling in the single scalar case when a Gauss-Bonnet term is introduced. This appears to limit the applicability in string theory motivated situations. However, this constraint would possibly be weakened by additional scalar fields, similar to the case for the slope of the potential when additional scalar fields are considered in cosmology [124].

The result of major interest is that the solutions are bounded by (3.23) and do not contain the $\kappa = 0$ case. At the extremal limit no surface gravity is defined. It does, however, limit to finite, non-zero values for a general coupling, g_i. Previously this behaviour has only been seen in [96] when considering the limiting case between Reissner-Nordström and Kaluza-Klein type solutions for a single scalar field with $g = \sqrt{D-1}$. Although (3.17) limits the number of independent asymptotic charges, it does not allow us further insight into the nature of the horizon. The Gibbons-Maeda solution allowed analysis of the horizon in the extremal case, indicating a singularity. This would seem likely in the present case as $m'(r)$ diverges at the horizon indicating a curvature singularity.

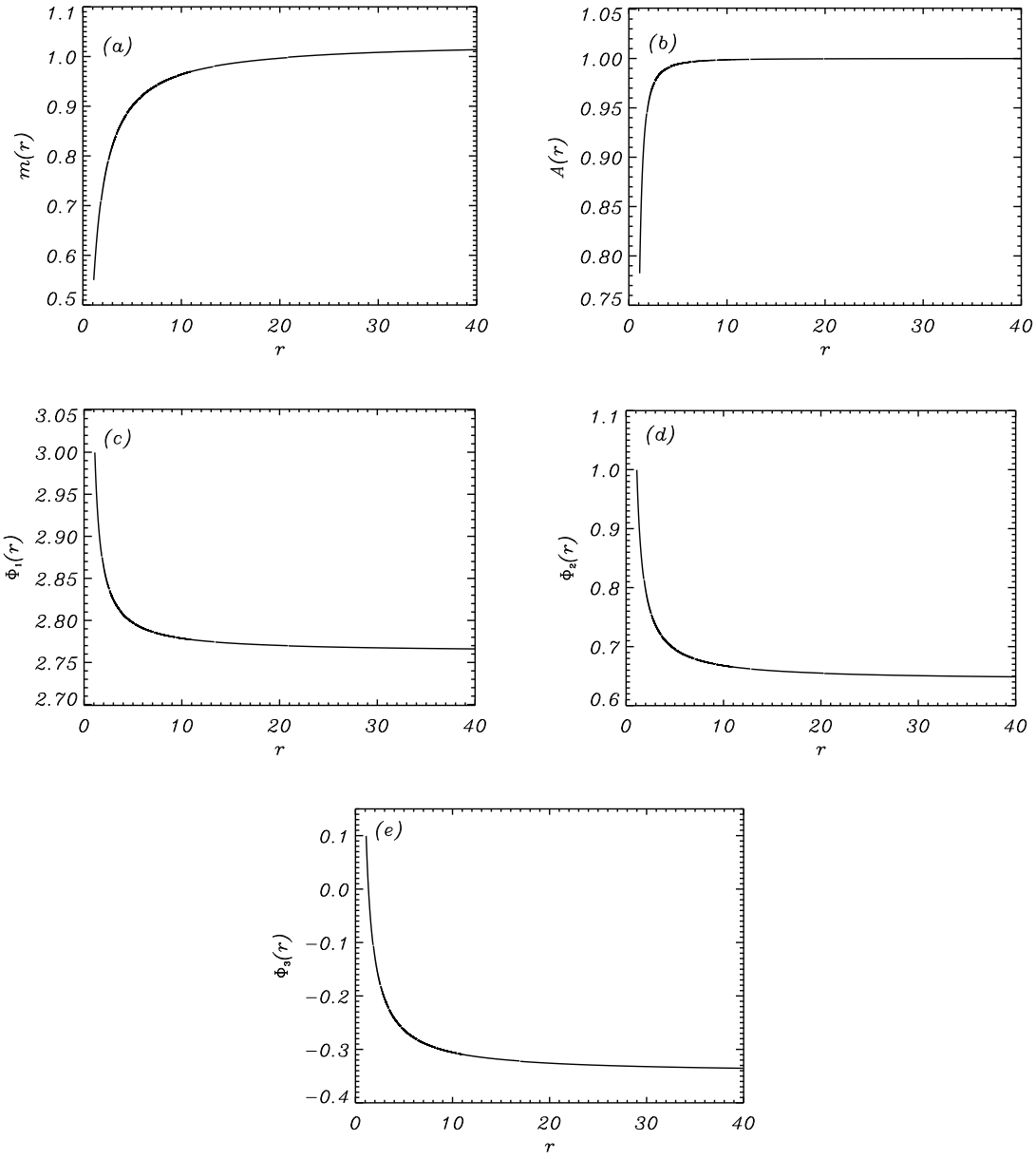

Figure 3.3: *Solution for* $N = 3$, $\Lambda = 0$, *where* $\lambda_1 = \lambda_2 = \lambda_2 = 1.0$, $g_1 = g_2 = 0.1$, $g_3 = 1.0$ *with horizon values* $m(r_h) = 0.25$, $\Phi(r_h) = 1.0$, $\Psi(r_h) = 0.1$ *with* $P = 0.5$. $P_\infty = 1.0728$ *and* $M_{ADM} = 1.0316$ *while* $A(r_h) = 0.7818$ *as found by the shooting method: (a)* $m(r)$*; (b)* $A(r)$*; (c)* $\Phi_1(r)$*; (d)* $\Phi_2(r)$*; (e)* $\Phi_3(r)$.

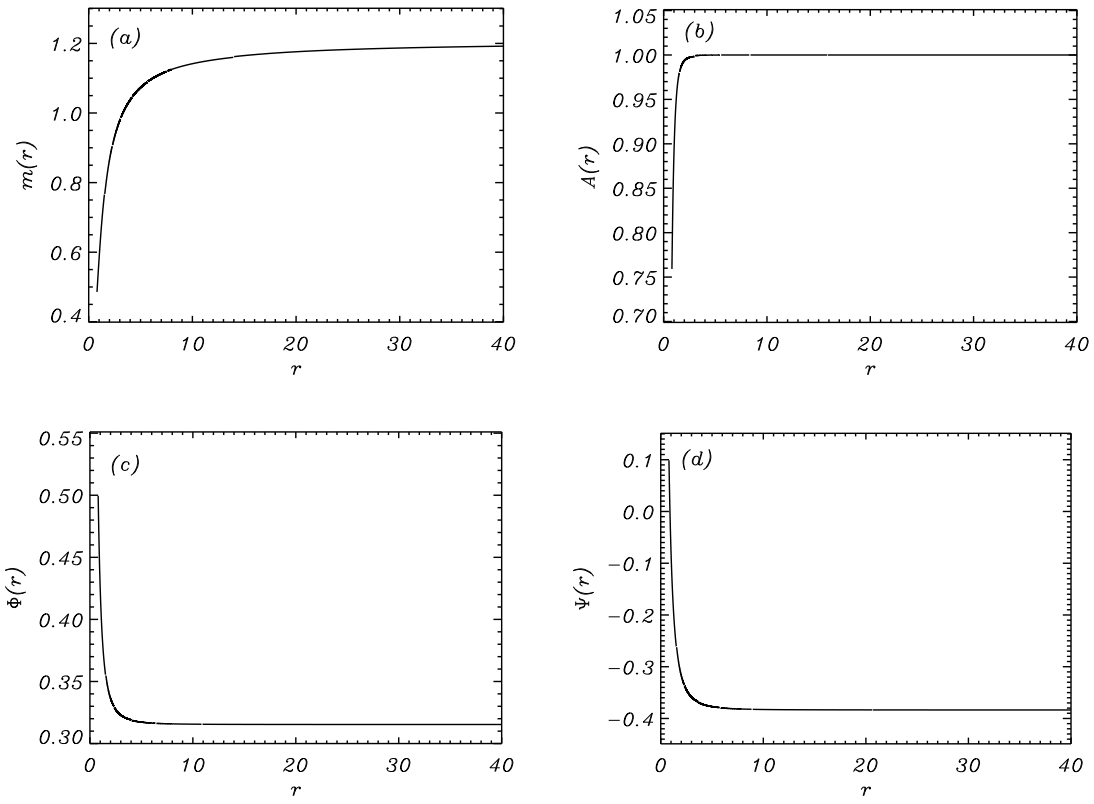

Figure 3.4: *Solution for* $N = 2$, $\Lambda = -1$, *where* $\lambda_1 = \lambda_2 = g_1 = g_2 = 1.0$ *with horizon values* $m(r_h) = 0.4$, $\Phi(r_h) = 0.1$, $\Psi(r_h) = 0.1$ *and* $P = 1.0$. $P_\infty = 1.1589$ *and* $M_\infty = 1.2092$ *while* $A(r_h) = 0.7582$ *as found by the shooting method: (a)* $M(r)$*; (b)* $A(r)$*; (c)* $\Phi(r)$*; (d)* $\Psi(r)$.

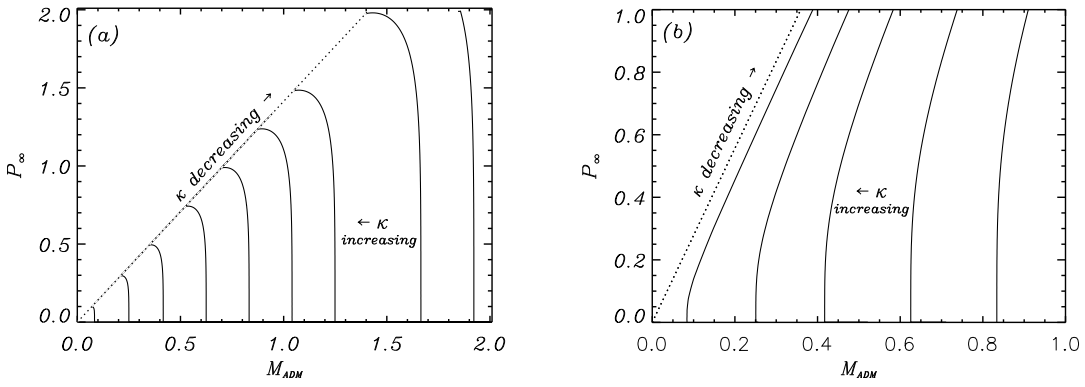

Figure 3.5: *"Isotherm" contour plots showing the behaviour of the surface gravity;* $\lambda_1 = \lambda_2 = 1.0$ *with horizon values* $\Phi(r_h) = 1.0$ *and* $\Psi(r_h) = 0.1$*: (a)* $g_1 = g_2 = 1.0$*; (b)* $g_1 = g_2 = 3.0$*. Note the change in behaviour from Reissner-Nordström-like solutions in (a) where the specific heat changes sign for* $P_\infty = const$ *as it moves away from the extremal limit while in (b) the specific heat for* $P_\infty = const$ *is always negative and mimics the well-known Kaluza-Klein examples. The extremal limit is shown as a dotted line as it is not an 'isotherm', instead the surface gravity limits to the case where it decreases with increasing* P_∞*.*

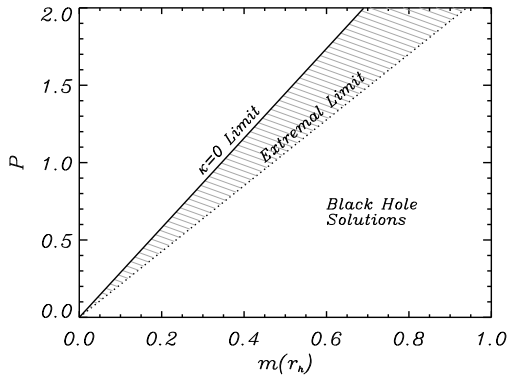

Figure 3.6: *The dotted line shows the constraint (3.23) while the solid line indicates the limit imposed by (3.22) for* $\lambda_1 = \lambda_2 = g_1 = g_2 = 1.0$*,* $\Phi(r_h) = 1.0$ *and* $\Psi(r_h) = 0.1$ *while varying over horizon values for* $m(r_h)$ *and the 'bare'* P *values.*

Chapter 4

Gauss-Bonnet Cosmology

4.1 Introduction

If we follow standard assumption that dark energy is due to a perfect cosmological fluid with an equation of state which violates the strong energy condition, then dark energy and its associated cosmic acceleration problem presents three main conundrums for modern cosmology:

- Why does the effective equation of state w_{eff} appear to have a value so close to -1?

- Why is the dark energy density comparable to the matter density at the current epoch? The current accelerating epoch began following a period of deceleration and matter domination. If this acceleration had begun earlier structure would not have had time to form. This is the so-called *cosmic coincidence problem.*

- Why is the cosmological vacuum energy extremely small and positive?

The fact that the expansion of our universe is accelerating after a long period of deceleration is inferred by the observations of type Ia supernovae, gravitational weak lensing and cosmic microwave background (CMB) anisotropies [15, 51, 126]; for a review see Padmanabhan [127].

Some possible mechanisms[1] to cause this acceleration have already been discussed in section 2.3.1. A number of further cosmological scenarios have expanded on these ideas within the context of modified theories of scalar-tensor gravity such as, coupled quintessence [129], k-inflation or dilatonic-ghost model [130], scalar-phantom model [131], Gauss-Bonnet dark energy [132] and its various generalizations [133, 135, 136]. These ideas are interesting as, like quintessence, they offer a possible solution to the cosmic coincidence problem. The proposals in [131, 132, 133, 135, 136] are promising because they may lead to the observationally supported equation of state, $w \approx -1$, while more interestingly provide a natural link between cosmic acceleration and fundamental particle theories, such as superstring theory. We focus primarily on the first two questions raised above within the context of a generalized theory of scalar-tensor gravity including non-minimal coupling to the Gauss-Bonnet curvature invariant.

The question of whether the gravitational vacuum energy is something other than a pure cosmological term will not be central to our discussion. But we note that Einstein's general relativity supplemented with a cosmological constant term does not appear to have any advantages over scalar-tensor gravity containing a standard scalar potential. The recent observation that the dark energy equation of state parameter w is ≈ -1 does not necessarily imply that the dark energy is in the form of a cosmological constant; it is quite plausible that after inflation the scalar field φ has almost frozen, so that $V(\varphi) \approx \text{const} = \Lambda$. In a cosmological background, there is no deep reason for expecting the energy density of the gravitational vacuum to be a constant, instead perhaps it can be determined by the underlying theory, as in the case where a scalar potential possesses many minima. It is thus worth exploring dynamical dark energy models, supporting both $w < -1$ and $w > -1$, and also $dw/dz \neq 0$ (where z is the redshift parameter).

The expansion of the universe is perhaps best described by a monotonically decreasing Hubble expansion rate, implying that $\dot{H} \equiv \ddot{a}/a - \dot{a}^2/a^2 \leq 0$, where $a = a(t)$ is the scale factor of a four-dimensional FLRW universe[2] and $H = \dot{a}/a$. In the presence of a barotropic fluid of pressure p and energy density ρ, this last inequality implies

[1] Also see the references [128] for further review of quintessence.

[2] Overdot represents a derivative with respect to the cosmic time t throughout this chapter.

that the cosmic expansion obeys the dominant energy condition (DEC), $p+\rho \geq 0$, and hence $w \equiv p/\rho \geq -1$. The standard view is that the Hubble expansion rate increases as we consider earlier epochs until it is of a similar order to that of the Planck mass, $m_{Pl} \sim 10^{18}\,\mathrm{GeV}$. However, in strong gravitational fields, such as, during inflation, the Einstein description of gravity is thought to break down and quantum gravity effects are expected to become important. This provides a basis for the assumption that the expansion of the universe is inseparable from the issue of the ultraviolet completion of gravity. In recent years, several proposals have been made in order to establish such a link. For instance, Creminelli *et al.* and Arkani-Hamed *et al.* [137] introduced a system of a derivatively coupled scalar Lagrangian which violates the condition $\dot{H} \leq 0$ spontaneously: the model would involve a short-scale (quantum) instability associated with a super-luminal cosmic expansion (see also Aref'eva and Volovich [138]).

The beauty of Einstein's theory is in its simplicity. It has been remarkably successful as a classical theory of gravitational interactions from scales of millimeters through to kiloparsecs. Thus any modification of Einstein's theory, both at small and large distance scales, must be consistent with known tests. Several proposals in the literature [137, 139] do not seem to fall into this category as these ideas would involve modifications of Einstein's theory in a rather non-standard (and nontrivial) way.

We motivate our work through the theoretical insights of superstring or M-theory as it would appear worthwhile to explore the cosmological implications of such models. In particular we examine whether we can achieve observationally supported cosmological perturbations in the low-energy string effective action, which includes a nontrivial interaction between dynamical scalar fields and a Riemann invariant of the Gauss-Bonnet form, and study its phenomenological viability as a dark energy model. It is appreciated that a generalized theory of scalar-tensor gravity, featuring one or several scalar fields coupled to a spacetime curvature, or a Riemann curvature invariant, can easily account for an accelerated universe with quintessence ($w > -1$), cosmological constant ($w = -1$) or phantom ($w < -1$) equation of state without introducing the wrong sign on the scalar kinetic term.

In the following section we discuss a general scalar-field Lagrangian framework and write equations of motion that describe gravity and a scalar field φ, allowing nontrivial

matter-scalar couplings. We discuss some astrophysical and cosmological constraints on the model. In section 3 we present the construction of a number of scalar potentials for some specific constraints, in an attempt to gain insight into the behaviour of the scalar potential for late time cosmology. In section 4 we discuss inflationary cosmologies for specific cases and study the parameters related to cosmological perturbations of the background solution. The problem of suitable initial conditions, given stable observationally viable solutions with a full array of background fields for the general system is considered in section 5 using numerical and analytic techniques for both minimal and non-minimal scalar-matter couplings. In section 6 we present several remarks about the existence of superluminal propagation and/or small-scale negative instabilities for the tensor modes. Section 7 is devoted to the discussions of our main results.

4.2 Essential Ingredients

An unambiguous and natural way of modifying general relativity in four dimensions is to introduce one or more fundamental scalar fields and their interactions with the leading order curvature terms in the string parameter expansion, as arising in string or M theory compactifications from ten- or eleven-dimensions to four-dimensions. The string parameter is defined by the expectation value of the dilaton field, $\alpha = \exp(\langle\varphi\rangle)$, in 10-dimensional string theory. In the low energy limit a perturbative expansion in α is possible as it is generally expected to take values $\alpha \ll 1$. The simplest version of such scalar-tensor gravities is given by the following general action

$$S = S_{grav} + S_m, \tag{4.1}$$

with

$$S_{grav} = \int d^4x\sqrt{-g}\left(\frac{R}{2\kappa^2} - \frac{\gamma}{2}\,(\nabla\varphi)^2 - V(\varphi) - \frac{1}{8}\,f(\varphi)\mathcal{R}^2_{GB}\right), \tag{4.2}$$

$$S_m = S(\varphi, A^2(\varphi)g_{\mu\nu}, \psi_m) \tag{4.3}$$

where $\mathcal{R}^2_{GB} \equiv R^2 - 4\,R_{\mu\nu}\,R^{\mu\nu} + R_{\mu\nu\rho\sigma}\,R^{\mu\nu\rho\sigma}$ is the Gauss-Bonnet (GB) curvature invariant. The matter component of the Lagrangian has been presented by Steinhardt and Turok [134] heuristically as

$$S_m = \int d^4x\sqrt{-g}\left(A^4(\varphi)\,(\rho_m + \rho_r)\right), \tag{4.4}$$

One should be careful with this formulation as it is not a "true" Lagrangian as the presence of the densities indicate it is not covariant. However, it does allow one to see the explicitly the coupling between the scalar and matter fields. This sector of the theory is more accurately a component of the energy-momentum tensor.

Above we shall assume that φ is a canonical field, so $\gamma > 0$. The coupling $f(\varphi)$ between φ and the GB term is a universal feature of all 4-dimensional manifestations of heterotic superstring and M theory [140, 141]. For example, such a form arises at heterotic string tree-level if φ represents a dilaton, and at one-loop level if φ represents the average volume modulus; in a known example of heterotic string theory, one has $f(\varphi) \propto \sum_{n=1} c_n \, e^{(n-2)\varphi} > 0$ in the former case, while $f(\varphi) \propto \varphi - \frac{\pi}{3} \, e^{\varphi} + 4 \sum_{n=1} \ln\left(1 - e^{-2n\pi \, e^{\varphi}}\right) + \ln 2 < 0$ in the latter case (see discussions in references [142] for further details). As discussed in [135, 136], a nontrivial or non-constant $f(\varphi)$ is useful not only for modelling a late time cosmology, but is also desirable for embedding the model in a fundamental theory, such as superstring theory. Here we also note that from a model building point of view, only two of the functions $V(\varphi), f(\varphi)$ and $A(\varphi)$ are independent; these can be related through the equations of motion below.

The Hubble value at the time of nucleosynthesis is thought to be $H \approx 1MeV \approx 10^{-21} m_{Pl}$ and has decreased until the present epoch where it has a value $H \approx 10^{-33} eV \approx 10^{-60} m_{Pl}$, where we are considering Planck Mass units in the action due to the choice $2\kappa = 1$. These values are obviously much less than unity. As $R \propto H^2(2\dot{H}^2 + \dot{H}/H^2)$ and $R^2_{GB} = 24H^2(H^2 + \dot{H})$, to leading order we have $R \propto H^2$ (under the assumption that $\epsilon \sim \mathcal{O}(1)$) and $R_{GB} \propto H^4$. The linear curvature term therefore dominates over the contribution of the quadratic term and all other higher order terms in the post-inflation universe, if curvature is minimally coupled to all other fields[3]. It is the strength of the coupling $f(\phi)$ which leads to a contribution from the quadratic curvature correction term. The $f(\phi)H^2$ term must be less than unity for the $f(\phi)R_{GB}$ term to remain subdominant, as would be expected throughout the evolution of the Universe. This allows *very large* values of $f(\phi)$ as $H^2 \sim 10^{-120} m_{Pl}$ at the present epoch. The value of

[3]This is purely a comment on the relative orders of the terms and only has relevance in the four dimensional case when the higher order curvature corrections are non-minimally coupled. In four dimensions the minimally coupled Gauss-Bonnet term is a scalar invariant and therefore makes no contribution, as with all other ghost-free higher order corrections as discussed in section 2.4.

$f(\phi)H^2$, being the important parameter with regard to the effect of the Gauss-Bonnet term on the evolution of the Universe, is treated as an independent variable throughout most of the work that follows. The initial value is set to values which result in physically interesting solutions and is hence a type of tuning.

One can supplement the above action with other higher derivative terms, such as those proportional to $f(\varphi)(\nabla_\lambda\varphi\nabla^\lambda\varphi)^2$ and curvature terms, but in such cases it would only be possible to get approximate (asymptotic) solutions, so we limit ourselves to the above action. In the model previously studied by Antoniadis *et al.* [140], $V(\varphi)$ and S_m were set to zero. However, the states of string or M theory are known to include extended objects of various dimensionalities, known as "branes", beside trapped fluxes and nontrivial cycles or geometries in the internal (Calabi-Yau) spaces. It is also natural to expect a non-vanishing potential to arise in the four-dimensional string theory action due to some non-pertubative effects of branes and fluxes. With supersymmetry broken, such a potential can have isolated minima with massive scalars. This then avoids the problem with runway behaviour of φ after inflation.

We allow φ to couple with both an ordinary dust-like matter and a relativistic fluid. The model under consideration is shown to be sufficient to make inroads into all major cosmological conundrums of concordance cosmology, notably the transition from matter dominance to a dark energy regime and the late time cosmic acceleration problem attributed to dark energy, satisfying $w_{\text{eff}} \approx -1$.

4.2.1 Basic equations

In order to analyse the model we take a four-dimensional spacetime metric in standard FLRW form: $ds^2 = -dt^2 + a^2(t)\sum_{i=1}^{3}(dx^i)^2$, where $a(t)$ is the scale factor of the universe. The equations of motion that describe gravity, the scalar field φ, and the background fluid (matter and radiation) are given by

$$-\frac{3}{\kappa^2}H^2 + 3\dot{\varphi}f_{,\varphi}H^3 + \frac{\gamma}{2}\dot{\varphi}^2 + V(\varphi) + A_b^4(\varphi)\rho_b = 0, \quad (4.5)$$

$$\frac{1}{\kappa^2}(2\epsilon+3)H^2 + \frac{\gamma}{2}\dot{\varphi}^2 - V(\varphi) - \ddot{f}H^2 - 2\dot{\varphi}Hf_{,\varphi}(1+\epsilon) + w_b A_b^4(\varphi)\rho_b = 0, \quad (4.6)$$

$$\gamma(\ddot{\varphi} + 3H\dot{\varphi}) + V_{,\varphi} + 3(1+\epsilon)f_{,\varphi}H^4 - \eta Q_m A_m^4(\varphi)\rho_m = 0, \quad (4.7)$$

where $f_{,\varphi} \equiv dV/d\varphi$, $V_{,\varphi} \equiv dV/d\varphi$, $\ddot{f} \equiv f_{,\varphi\varphi}\,\dot{\varphi}^2 + f_{,\varphi}\,\ddot{\varphi}$, η is a numerical parameter which we define below and

$$\epsilon = \frac{\dot{H}}{H^2}\,, \quad w_b \equiv \frac{p_b}{\rho_b}\,, \quad Q \equiv \frac{d\ln A(\varphi)}{d\varphi}\,, \tag{4.8}$$

where b stands for the background matter and radiation. For convenience we also define the following quantities

$$x = \frac{\dot{\varphi}}{H}\,, \quad y = \frac{V(\varphi)}{H^2}\,, \quad u \equiv f_{,\varphi}H^2,$$
$$\Omega_b \equiv \frac{\rho_b A^4(\varphi)}{3H^2}\,, \quad \Omega_\varphi \equiv \frac{\rho_\varphi}{3H^2} = \frac{\gamma x^2 + 2y}{6}\,, \qquad \Omega_{GB} = \dot{\varphi}Hf_{,\varphi} = ux \equiv \mu, \tag{4.9}$$

so that the constraint equation (4.5) reads $\Omega_\varphi + \Omega_{GB} + \Omega_b = 1$. The density fraction Ω_b may be split into radiation and matter components: $\Omega_b = \Omega_r + \Omega_m$ and $w_b\Omega_b = w_m\Omega_m + w_r\Omega_r$. Similarly, in the component form, $Q\rho_m = Q_i\rho_m^{(i)}$. Stiff matter for which $w_m = 1$ may also be included. The analysis of Steinhardt and Turok [143] neglects such a contribution, where only the ordinary pressureless dust ($w_m = 0$) and radiation ($w_r = 1/3$) were considered, in a model with $f(\varphi) = 0$. The implicit assumption above is that matter couples to $A^2(\varphi)g_{\mu\nu}$ with scale factor $\hat{a}$, where $\hat{a} \equiv aA(\varphi)$, rather than the Einstein metric $g_{\mu\nu}$ alone, and $\rho_r \propto 1/\hat{a}^4$, so ρ_r does not enter the φ equation of motion, (4.7). That is, by construction, the coupling of φ to radiation is vanishing. This is, in fact, consistent with the fact that the quantity Q couples to the trace of the matter stress tensor, $g^{\mu\nu}_{(i)}T^{(i)}_{\mu\nu}$, which vanishes for the radiation component, $T^\mu_\mu = -\rho_r + 3P_r = 0$. We also note that, in general, $\rho \propto 1/\hat{a}^{3(1+w)}$, thus, for ordinary matter or dust ($w = 0$) we have $\eta = 1$, for a highly relativistic matter ($w = 1$) we have $\eta = -2$, and for radiation ($w = 1/3$), we have $\eta = 0$, while, for any other relativistic matter with pressure $\rho > p > \rho/3$, $-2 < \eta < 0$.

Equations (4.5) – (4.7) may be supplemented with the equation of motion for a barotropic perfect fluid, which is given by

$$\hat{a}\frac{d\rho_b}{d\hat{a}} = \frac{1}{H}\frac{\partial\rho_b}{\partial t} + \frac{\dot{\varphi}}{H}\frac{\partial\rho_b}{\partial\varphi} = -3(1+w_b)\rho_b, \tag{4.10}$$

where p_b is the pressure of the fluid component with energy density ρ_b. In the case of

minimal scalar-matter coupling, the quantity $\partial\rho_b/\partial\varphi \to 0$ [4] and hence

$$\Omega_b' + 2\epsilon\Omega_b + 3(1+w_b)\Omega_b = 0, \tag{4.11}$$

where the prime denotes a derivative with respect to $N = \ln[a(t)/a_0]$. In this case the dynamics in a homogeneous and isotropic FLRW spacetime may be determined by specifying the field potential $V(\varphi)$ and/or the scalar-GB coupling $f(\varphi)$.

For $A(\varphi) \neq$ const, there exists a new parameter, Q; more precisely,

$$\frac{\partial\rho_m^{(i)}}{\partial\varphi} = -\eta\rho_m^{(i)}Q_i, \quad \frac{\partial\rho_r}{\partial\varphi} = 0. \tag{4.12}$$

The variation in the energy densities of the ordinary matter, $\rho_m^{(d)}$, and the relativistic fluid, $\rho_m^{(s)}$, and their scalar couplings Q_i are not essentially the same[5]. Thus, hereafter, we denote the Q by Q_d for an ordinary matter (or dust) and Q_s for a relativistic matter (or stiff fluid coupled to φ). Equation (4.10) may be written as

$$\Omega_s' + 2\epsilon\Omega_s + 3(1+w_s)\Omega_s = -3\eta Q_s\Omega_s\varphi', \tag{4.13}$$

$$\Omega_d' + 2\epsilon\Omega_d + 3\Omega_d = -3Q_d\Omega_d\varphi', \tag{4.14}$$

$$\Omega_r' + 2\epsilon\Omega_r + 4\Omega_r = 0. \tag{4.15}$$

In the following we adopt the convention $\kappa^2 = 8\pi G = 1$, unless shown explicitly.

4.2.2 Cosmological and astrophysical constraints

Scalar-tensor gravity models of the type considered are generally constrained by various cosmological and astrophysical observations, including the big bang nucleosynthesis bound on the φ-component of the total energy density and the local gravity experiments. However, the constraints obtained in a standard cosmological setup (for instance, by analyzing the CMB data), which assumes general relativity, that is, $Q = 0$, cannot be straightforwardly applied to the present model. The distance of the last scattering surface can be (slightly) modified if the universe at the stage of

[4] Recently, Sami and Tsujikawa analysed the model numerically by considering $Q \to 0$ [144]. The authors also studied the case $Q =$ const, but without modifying the Friedmann constraint equation.

[5] From this point on the subscripts s and d will refer to stiff, relativistic matter and ordinary matter (dust) respectively with the m subscript being dropped.

Big Bang Nucleosynthesis (BBN) contained an appreciable amount if energy in the φ-component [145]).

The coupling Q_d can be constrained by taking into account cosmological and solar system experiments. Observations are made of objects that can be classified as visible matter or dust [146, 147]; hence a value of $Q_d^2 \ll 1$ is required to agree with the current observational limits on deviations from the equivalence principle. If we also require $Q_s^2 \ll 1$, then the non-minimal coupling of φ with a relativistic fluid may be completely neglected at present, since $\Omega_s \ll \Omega_d$.

Under parameterised post-Newtonian (PPN) approximations [148], the local gravity constraints on Q_d and its derivative loosely imply that

$$m_{Pl}^2 Q_d^2 \lesssim 10^{-5}, \qquad m_{Pl}\,|dQ_d/d\varphi| \lesssim \mathcal{O}(1). \tag{4.16}$$

If $A(\varphi)$ is sufficiently flat near the current value of $\varphi = \varphi_0$, then these couplings have modest effects on large cosmological scales. Especially, in the case that $A(\varphi) \propto e^{\zeta\kappa\varphi}$, the above constraints may be satisfied only for a small ζ ($\ll 1$) since $Q_d = \zeta$ is constant. On the other hand, if $A(\varphi) \propto \cosh[\zeta\kappa\varphi]$, then Q_d is only approximately constant, at late times. Another possibility is that $Q_d \propto e^{-\zeta\kappa\varphi}$; in this case, however, for the consistency of the model, one also requires a steep potential. In the particular case of $A(\varphi) \propto e^{\zeta\kappa\varphi}$ with $\zeta \sim \mathcal{O}(1)$ (as one may expect from string theory or particle physics beyond the standard model), it may be difficult to satisfy the local gravity constraints (under PPN approximation), unless there is a mechanism like the one discussed by Khoury *et al.* [149] and Mota *et al.* [150].

4.3 Construction of Inflationary Potentials

In this section we study the model in the absence of background matter (and radiation). Equations (4.5) – (4.7) form a system of two independent equations of motions, as given by

$$\gamma x^2 + 2y + 6\mu - 6 = 0, \tag{4.17}$$

$$\mu' + (\epsilon - 1)\mu - \gamma x^2 - 2\epsilon = 0. \tag{4.18}$$

The equation of state (EoS) parameter can be written in terms of ϵ such that for a flat, FLRW model,

$$w \equiv \frac{p}{\rho} = -\frac{3H^2 + 2\dot{H}}{3H^2} = -1 - \frac{2}{3}\,\epsilon. \tag{4.19}$$

The solution $\epsilon = 0$, therefore, corresponds to a cosmological constant term, for which $w = -1$. The universe accelerates for $w < -1/3$, or equivalently, for $\epsilon > -1$. It is possible to attain $w < -1$, or equivalently $\epsilon > 0$, for the action (4.2) without introducing a wrong sign to the kinetic term. We shall assume that the scalar potential is non-negative, so $y \geq 0$. Evidently, with $x^2 > 0$, as is the case for a canonical φ, the inequality $\mu < 1$ holds at all times. Here $\mu = 1$ is a saddle point for any value of ϵ. Thus, an apparent presence of ghost states (or short-scale instabilities) at a semi-classical level, as discussed in Calcagni *et al.* [151], with further discussion in references [152], is not physical. We shall return to this point in more detail, in our latter discussions on small scale instabilities incorporating superluminal propagations or ghost states.

We are interested in the possibility that one can explain inflation in the distant past through the inclusion of a modified Gauss-Bonnet theory. To carry this out analytically we require some physically motivated ansätze

$$x \equiv x_0\, e^{\alpha N/2}, \quad \mu \equiv \mu_0\, e^{\beta N}, \tag{4.20}$$

where x_0, μ_0, α and β are all arbitrary constants. The implicit assumption is that both x and μ decrease exponentially with N, or the expansion of the universe. We then find

$$\epsilon = \frac{2(\beta - 1)\mu - \gamma x^2}{2(2 - \mu)}\,. \tag{4.21}$$

From this we can see that a transition between the $\epsilon > 0$ and $\epsilon < 0$ phases is possible if $\mu \neq 0$. Moreover, the first assumption in (4.20) implies that $\alpha N = 2\ln\varphi + \ln\varphi_1$, where φ_1 is an arbitrary constant. The scalar potential is then given by

$$V(\varphi) = H(\varphi)^2 \left(3 - \lambda_0\varphi^2 - \lambda_1\, \varphi^{\,2\beta/\alpha}\right), \tag{4.22}$$

where λ_0, λ_1 are (arbitrary) constants. For a canonical φ, so $x^2 > 0$, we have $\lambda_0 > 0$, whereas the sign of λ_1 is determined by the sign of μ_0. Note that $\alpha = \beta$ is a special case for which the potential takes the form $V(\varphi) \equiv H^2(\varphi)\,(3 - (\lambda_0 + \lambda_1)\varphi^2)$. The quantity

ϵ (and hence $1+w$) cannot change its sign in this case. Typically, if $\beta = 2\alpha$, then the scalar potential would involve a term which is fourth power in φ, i.e., $V \propto H^2(\varphi)\,\varphi^4$. At this point we also note that the potential (4.22) is different from a symmetry breaking type potential $V \propto (\Lambda \pm m_\varphi^2\varphi^2 + \lambda_1\varphi^4 + \cdots)$ generally considered. Here it is multiplied by $H^2(\varphi)$. An inflationary potential of the form $V \propto \varphi^4$ is already ruled out by recent WMAP results, at 3σ-level [156]. In the view of this result, rather than the monomial potentials, namely $V(\varphi) \propto (\varphi/\varphi_0)^p$, a scalar potential of the form $V(\varphi) \propto H^2(\varphi)(\varphi/\varphi_0)^p$, with $p \geq 2$, as implied by the symmetries of Einstein's equations, is worth studying in the context of the inflationary paradigm.

It may also be possible to use the modified Gauss-Bonnet theory to explain the ongoing accelerated expansion of the universe. We note that, especially at late times, the rolling of φ can be modest. In turn, it is reasonable to suppose that $\dot{\varphi}/H \simeq$ const, or $x \simeq x_0$. Hence

$$V(\varphi) = \frac{H^2}{2}\,\left(6 - \gamma {x_0}^2 + 6\mu_0\,\mathrm{e}^{\beta\phi}\right) \equiv H(\varphi)^2\,\left(\Lambda_0 + \Lambda_1\,\mathrm{e}^{\beta\phi}\right), \tag{4.23}$$

where $\phi \equiv (\varphi - \varphi_0)/x_0$ and the Hubble parameter is given by

$$H = H_0\,\left(1 - \mu_0\,e^{\beta\varphi}\right)^{(2+x_0)/2\beta - 1}\,e^{-\,x_0\varphi/2}, \tag{4.24}$$

with H_0 being an integration constant. Interestingly, a non-vanishing $f(\varphi)$ not only supports a quartic term in the potential, proportional to $H^2(\varphi)\,\varphi^4$, but its presence in the effective action also allows the possibility that the equation of state parameter w switches its value between the $w > -1$ and $w < -1$ phases. We shall analyse the model with the choice (4.23) and in the presence of matter fields, where we will observe that the universe can smoothly pass from a stage of matter dominance to dark energy dominance.

In the case where φ is rolling with a constant velocity, $\varphi' \equiv c$, satisfying the power-law expansion $a(t) \propto t^{1/p}$, or equivalently $H \equiv H_0\,e^{-\,pN}$ and $p \neq 1$, we find that the scalar potential and the scalar-GB coupling evolve as

$$V = V_0\,e^{-\,2p\phi} + 3(3p+1)f_1H_0^2\,e^{\,(1-p)\phi}, \tag{4.25}$$

$$f = f_0\,e^{\,2p\phi} - \frac{f_1}{H_0^2}\,e^{\,(1+3p)\phi} + f_2, \tag{4.26}$$

where $\phi \equiv (\varphi - \varphi_0)/c$, f_1 and f_2 are arbitrary constants, and

$$V_0 \equiv \frac{(6 - 6p + 5c^2 - pc^2)H_0^2}{2(1+p)}\,, \quad f_0 \equiv \frac{2p - c^2}{2p(p+1)H_0^2}\,. \tag{4.27}$$

The potential is a sum of two exponential terms. Such a potential may arise, for example, from a time-dependent compactification of 10 or $11d$ supergravities on factor spaces [153]. In general, both $V(\varphi)$ and $f(\varphi)$ pick up additional terms in the presence of matter fields, but they may retain similar structures. In fact, various special or critical solutions discussed in the literature [132] correspond to the choice $f_1 = f_2 = 0$.

We can be more specific here. Let us consider the following ansatz [132],

$$a \propto (t + t_1)^\alpha, \qquad \varphi = \varphi_0 + \beta \ln(t + t_1), \tag{4.28}$$

for which obviously both ϵ and φ' are constants,

$$\epsilon \equiv \dot{H}/H^2 = -1/\alpha, \quad \varphi' \equiv \frac{\dot{\varphi}}{H} = \frac{\beta}{\alpha}\,. \tag{4.29}$$

For $\epsilon < 0$, one can take $t_1 = 0$; the Hubble parameter is given by

$$H = |\alpha|\, \mathrm{e}^{-\frac{1}{\beta}(\varphi - \varphi_0)}. \tag{4.30}$$

The scalar potential is double exponential, which is given by

$$V = V_0\, \mathrm{e}^{-2\phi} + V_1\, \mathrm{e}^{(\alpha-1)\phi}, \tag{4.31}$$

where $\phi \equiv (\varphi - \varphi_0)/\beta$ and

$$V_0 \equiv \frac{6\alpha^2(\alpha-1) + \beta^2(5\alpha - 1)}{2(\alpha+1)}\,, \quad V_1 \equiv -3(\alpha+3)\alpha c_1. \tag{4.32}$$

The scalar-GB coupling $f(\varphi)$ may be given by

$$f = f_0\, \mathrm{e}^{2\phi} + f_1\, \mathrm{e}^{(\alpha+3)\phi} + f_2, \tag{4.33}$$

with

$$f_0 \equiv \frac{2\alpha - \beta^2}{2(1+\alpha)\alpha^2}\,, \quad f_1 \equiv \frac{c_1}{\alpha^2(\alpha+3)}\,, \quad f_2 \equiv \frac{c_2}{\alpha^2}\,. \tag{4.34}$$

Of course, the numerical coefficient f_2 does not contribute to Einstein's equations in four dimensions but, if non-zero, it will generate a nontrivial term for the effective potential.

In the case $\epsilon > 0$ (or $\dot{H} > 0$), the above ansatz may be modified as

$$a \propto (t_\infty - t)^\alpha, \qquad \varphi = \varphi_0 + \beta \ln(t_\infty - t), \tag{4.35}$$

where $\alpha < 0$. The Hubble parameter is then given by $H = -\alpha(t_\infty - t)^{-1}$. Such a solution to dark energy is problematic. Although this solution avoids the initial singularity at $t = 0$, it develops a big-rip type singularity in the asymptotic future, $t = t_\infty$. This is not a physically appealing case. The above critical solution may also be unstable under inhomogeneous cosmological perturbations, which often leads to a super-luminal expansion and violates all energy conditions.

The reconstruction scheme presented in Nojiri *et al.* [154] was partly based on some special ansatz, e.g., (4.28), which may therefore suffer from one or more future singularities. However, as we show below, for the model under consideration there exists a more general class of cosmological solutions without any cosmological singularities.

4.4 Inflationary Cosmology: Scalar Field Dynamics

Inflation is now a well established paradigm of a consistent cosmology, which is strongly supported by recent WMAP data[6] [6]. It is also generally believed that the small density fluctuations which developed during inflation naturally lead to the formation of galaxies, stars and other structure in the present Universe. It is therefore interesting to consider the possibility of achieving observationally supported cosmological perturbations in low-energy string effective actions. For the model under consideration, this can be done by using the standard method of studying the tensor, vector, and scalar modes. We omit the details of our calculations because they are essentially contained in the references [152].

4.4.1 Inflationary parameters

One may define the slow roll parameters, such as ϵ_H and η_H, associated with cosmological perturbations in a FLRW background, using two apparently different versions of

[6]The small inhomogeneities observed for primordial density or temperature fluctuations in the CMB provide support for the concept of inflation.

the slow-roll expansion. The first (and more widely used) scheme in the literature takes the potential as the fundamental quantity, while the second scheme takes the Hubble parameter as the fundamental quantity. A real advantage of the second approach [155] is that it also applies to models where inflation results from the term(s) other than the scalar field potential. Let us define these variables in terms of the Hubble parameters [7],

$$\epsilon_H \equiv 2\left(\frac{H_\varphi}{H}\right)^2 = \frac{2\epsilon^2}{\varphi'^2}\,, \quad \eta_H \equiv \frac{2H_{\varphi\varphi}}{H} = \frac{2}{\varphi'^2}\left(\epsilon' + \epsilon^2 - \epsilon\frac{\varphi''}{\varphi'}\right) \tag{4.36}$$

(in the units $\kappa = 1$). Here, as before, the prime denotes a derivative with respect to e-folding time $N \equiv \ln[a(t)/a_0]$. One also defines the parameter ξ_H, which is second order in slow-roll expansion,

$$\xi_H \equiv \frac{1}{2}\left(\frac{H_\varphi H_{\varphi\varphi\varphi}}{H^2}\right)^{1/2} = \left(\epsilon_H\eta_H - \sqrt{2\epsilon_H}\,\frac{\eta_H'}{\varphi'}\right)^{1/2}. \tag{4.37}$$

These definitions are applicable in both the cases, $V(\varphi) \neq 0$ and $V(\varphi) = 0$, and are based on the fact that inflation occurs as long as $\frac{\mathrm{d}}{\mathrm{d}t}\left(\frac{1}{aH}\right) < 0$ holds. The above quantities $(\epsilon_H, \eta_H, \xi_H)$ are known as, respectively, the slope, curvature and jerk parameters.

Typically, in the case $f(\varphi) = 0$, or simply when $|\Omega_{GB}| \ll \Omega_\varphi$, so that the coupled GB term becomes subdominant to the field potential, the spectral indices of scalar and tensor perturbations to the second order in slow-roll expansion may be given by [155, 156]

$$\begin{aligned} n_\mathcal{R} - 1 &= -4\epsilon_H + 2\eta_H - 2(1+c)\epsilon_H^2 - \frac{1}{2}(3-5c)\epsilon_H\eta_H + \frac{1}{2}(3-c)\xi_H^2, \\ n_T &= -2\epsilon_H - (3+c)\epsilon_H^2 + (1+c)\epsilon_H\eta_H, \end{aligned} \tag{4.38}$$

where $c = 4(\ln 2 + \gamma) - 5 \approx 0.08$. For the solutions satisfying $\xi_H \simeq 0$, implying that both ϵ_H and η_H are much smaller than unity (at least, near the end of inflation) and their time derivatives are negligible, we have

$$n_\mathcal{R} - 1 \simeq -4\epsilon_H + 2\eta_H, \qquad n_T \simeq -2\epsilon_H. \tag{4.39}$$

In fact, $n_\mathcal{R}$ and n_T, along with the scalar-tensor ratio r, which is given by $r \approx 16\epsilon_H + 32c(\epsilon_H - \eta_H)\epsilon_H$, are the quantities directly linked to inflationary cosmology.

[7] The slow-roll variable is ϵ_H, not ϵ, the latter is defined by $\epsilon \equiv H'/H$.

We introduce the following quantities: [8]

$$\epsilon_1 = -\frac{\dot{H}}{H^2} = -\epsilon, \qquad \epsilon_2 = \frac{\ddot{\varphi}}{\dot{\varphi}H} = \frac{x' + \epsilon x}{x}, \qquad \epsilon_4 = \frac{\varrho'}{2\varrho},$$
$$\epsilon_5 \equiv \frac{\mu}{2(1-\mu)}, \qquad \epsilon_6 \equiv -\frac{\mu'}{2(1-\mu)}. \tag{4.40}$$

where

$$\varrho \equiv \gamma + \frac{3\mu^2}{2(1-\mu)x^2}, \qquad \mu \equiv \dot{f}H = f'H^2. \tag{4.41}$$

Even in the absence of the GB coupling ($\mu = 0$), hence $\epsilon_4 = \epsilon_5 = \epsilon_6 = 0$, there are particular difficulties in evaluating the spectral indices $n_{\mathcal{R}}$ and n_T, and the tensor-scalar ratio r, in full generality. In perturbation theory it is possible to get analytic results only by making one or more simplifying assumptions. In the simplest case, one treats the parameters ϵ_i almost as constants, so their time derivatives are (negligibly) small as compared to other terms in the slow-roll expansion. An ideal situation like this is possible if inflation occurred entirely due to the power-law expansion, $a(\tau) \propto |\tau|^{-1/(1+\epsilon)}$, where the conformal time $\tau \equiv -1/[aH(1+\epsilon)]$. In this case, the spectral indices of scalar and tensor perturbations are well approximated by

$$n_{\mathcal{R}} - 1 = 3 - \left| \frac{3 + \epsilon_1 + 2\epsilon_2 + 2\epsilon_4}{1 - \epsilon_1} \right|, \quad n_T = 3 - \left| \frac{3 - \epsilon_1 + 2\epsilon_6}{1 - \epsilon_1} \right|. \tag{4.42}$$

Note that not all ϵ_i are smaller than unity. Nevertheless, for various explicit solutions found in this chapter, the quantity ϵ_4 is close to zero, while ϵ_5, ϵ_6 can have small variations during the early phase of inflation. After a few e-folds of inflation, $\Delta N \gtrsim 5$, these all become much smaller than unity, so only the first two terms (ϵ_1, ϵ_2) enter into any expressions of interest. In any case, below we will apply the formulae (4.42) to some explicit cosmological solutions.

The above relations are only valid in the limit where the speeds of propagation for scalar and tensor modes, which may be given by

$$c_{\mathcal{R}}^2 = 1 + \frac{\mu^2[4\epsilon(1-\mu) + \ddot{f} - \mu]}{(1-\mu)[2\gamma(1-\mu)x^2 + 3\mu^2]}, \quad c_T^2 = \frac{1 - \ddot{f}}{1 - \dot{f}H} = \frac{1 - \mu' + \epsilon\mu}{1 - \mu}, \tag{4.43}$$

where $\mu = \dot{f}H$ and $x = \dot{\varphi}/H$, take approximately constant values. These formulae may be expressed in terms of the quantity, $\nu(vph) \equiv f(\varphi)H^2$, using the relation $\mu = \nu' - 2\epsilon\nu$.

[8] The parameter ϵ_3 defined in references [152, 157] is zero in our case since the action (4.1) is already written in the Einstein frame, and φ does not couple with the Ricci-scalar term in this frame.

The propagation speeds depend on the scalar potential only implicitly, i.e., through the background solutions which may be different for the $V(\varphi) = 0$ and $V(\varphi) \neq 0$ cases. In the case where $c_{\mathcal{R}}^2$ and c_T^2 are varying considerably, the derivative terms like $\dot{\epsilon_5}$, $\ddot{\epsilon_5}$ are non-negligible, for which there would be nontrivial corrections to the above formulae for $n_{\mathcal{R}}$ and n_T. Furthermore, the spectral indices diverge for $\epsilon_1 \sim 1$, thus the results would apply only to the case where $\epsilon_1 \ll 1$. In this rather special case, which may hold after a few e-folds of power-law expansion through to near the end of inflation, we find that the tensor-to-scalar ratio is approximately given by

$$r \equiv \frac{A_T^2}{A_{\mathcal{R}}^2} \approx 16 \frac{2\gamma x^2(1-\mu) + 3\mu^2}{(2-\mu)^2} \left(\frac{c_{\mathcal{R}}}{c_T}\right)^3 . \tag{4.44}$$

This is also the quantity directly linked to observations, other than the spectral indices $n_{\mathcal{R}}$ and n_T. The WMAP data put the constraint $r < 0.55$ at 2σ level. The results for inflation in the presence of an exponential coupling to the Gauss-Bonnet term are presented below. The cases of a vanishing potential and an exponential potential were also covered [158], but this work was largely carried out by my collaborator, Ishwaree Neupane, and hence is not included here.

4.4.2 Inflating with an exponential coupling

Let us take the scalar-GB coupling of the following form,

$$f_{,\varphi} = f_0 \, e^{2\varphi/\varphi_0}, \tag{4.45}$$

but without specifying the potential, $V(\varphi)$. With this choice, the system of autonomous equations is given by

$$\frac{du}{dN} = \frac{2(x + \epsilon\varphi_0)}{\varphi_0} \, u, \tag{4.46}$$

$$\frac{dx}{dN} = \frac{2\epsilon + \gamma x^2}{u} + (1 - 3\epsilon)x - \frac{2x^2}{\varphi_0} , \tag{4.47}$$

$$y = 3 - \frac{\gamma}{2} \, x^2 - 3ux. \tag{4.48}$$

These equations admit the following de Sitter (fixed-point) solution

$$x = 0, \quad V = \Lambda_0, \quad H = \sqrt{\frac{\Lambda_0}{3}} , \quad u = u(\varphi), \tag{4.49}$$

which corresponds to the case of a cosmological constant term, for which $w = -1$. In the following we consider two special cases,

- Suppose that $\mu \equiv$ const, that is, $\Omega_{GB} = \text{const} \equiv \mu_0$. Then we find

$$\epsilon = \frac{\mu_0 + \gamma x^2}{\mu_0 - 2}\,, \quad \frac{dx}{dN} = \frac{2(\gamma\varphi_0 x^3 - (2-\mu_0)x^2 + 2\mu_0\varphi_0 x)}{(2-\mu_0)\varphi_0}\,. \tag{4.50}$$

These equations may be solved analytically[9] for $\mu_0 = 2/3$. As the solutions are still messy to write, we only show the behavior of w in Mathematica plots. In the next section we will numerically solve the field equations, in the presence of matter, allowing us to consider all values of μ_0. We should at least mention that the above system of equations has a pair of fixed point solutions:

$$x_1 = \frac{2-\mu_0 - \sqrt{(2-\mu_0)^2 - 8\gamma\varphi_0\mu_0}}{2\gamma\varphi_0}, \quad x_2 = \frac{2-\mu_0 + \sqrt{(2-\mu_0)^2 - 8\gamma\varphi_0\mu_0}}{2\gamma\varphi_0}. \tag{4.51}$$

The fixed point x_1 is an attractor, while the x_2 is a repeller provided that x_1, x_2 are real. In the case where $8\gamma\varphi_0\mu_0 > (2-\mu_0)^2$ the solution diverges. The solution also diverges for initial values of x such that $x < 0$ and $x > x_2$. If these conditions are not violated, the solutions would always converge to the attractor fixed point $x = x_1$. The evolution of the solution is monotonic from the initial value of ϵ to the ϵ given by the attractor fixed point at $x = x_1$. The initial value of w for a wide range of μ_0 and initial values of x may be read from figure 4.1(a), and evolve to the w given in figure 4.1(b) for a specific value of μ_0.

- Next suppose that $u = \text{const} \equiv u_0$, instead of $ux = \mu = $const. In this case, the quantity x decreases quickly with the expansion of the universe; the GB density fraction, Ω_{GB}, also decreases with the number of e-folds. The explicit solution is

$$\epsilon = -\frac{x}{\varphi_0}\,, \qquad x = \frac{2 - u_0\varphi_0}{\gamma\varphi_0 + u_0 + (2 - u_0\varphi_0)u_1\, e^{(2/u_0\varphi_0 - 1)N}}\,, \tag{4.52}$$

where u_1 is an integration constant. Without any surprise, as $x \to 0$, $\epsilon \to 0$; the model then corresponds to the cosmological constant case.

Inflation is apparently future eternal for the solutions above for much of the parameter range. However, in a more viable cosmological scenario, the contribution of

[9]This is actually a critical point in the phase space, which may be seen also in cosmological perturbation analysis, see, e.g., [159].

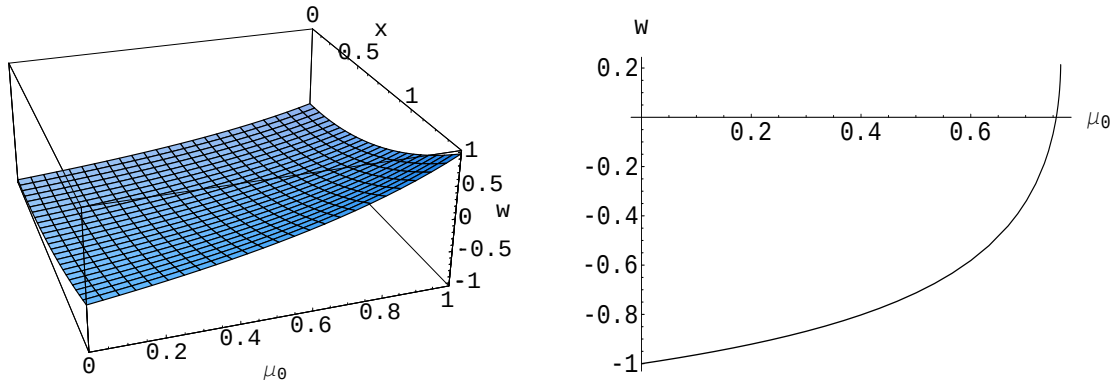

Figure 4.1: *The left panel (a) shows the initial equation of state parameter* w *with various initial conditions for* $\Omega_{GB} = \mu_0$ *and* x*, while, the right panel (b) shows a possible variation of* w *for a particular value of* μ_0*; solutions evolve to these values regardless of* x_{ini} *provided the fixed points exist and* $0 < x_{ini} < x_2$*. We have taken* $\varphi_0^{-1} = 2$ *and* $\gamma = 1$

the matter field may not be completely negligible. This is because, during inflation, the field φ, while slowly evolving down its potential, which satisfies $\Delta\varphi \propto \Delta N$, decays into lighter particles and radiation. The inflaton may even decay to heavier particles, especially, if the reheating of the universe was due to an instance preheating [160]. In turn, a significant amount of the energy density in the φ component might be transforming into the radiation and (baryonic plus dark) matter, with several hundreds of degrees of freedom and with all components present, e.g., stiff matter ($p = \rho$) and radiation ($3p = \rho$). In turn, the slow roll type parameter ϵ would receive a nontrivial contribution from the matter fields. Explicitly, we find

$$\epsilon = -\frac{3}{2}\,(1+w)\Omega_b - \frac{\varphi'^2}{2}\,, \tag{4.53}$$

where $\Omega_b = \Omega_m + \Omega_r$ and $w \equiv (p_m + p_r)/(\rho_m + \rho_r)$. Inflation ends when there is a significant fraction of matter and radiation, making $\epsilon < -1$.

Before proceeding to next section we also wish to make a clear separation between the inflationary solutions that we discussed above and the dark energy cosmologies that we will discuss in the following sections. Although it might be interesting to provide a natural link between the early universe inflation and the late time cosmic acceleration attributed to dark energy, postulating a string-inspired model of *quintessential inflation*, the time and energy scales involved in the gravitational dynamics may differ vastly. As we have seen, through the construction of potentials, the scalar potential

driving an inflationary phase at an early epoch and a second weak inflationary episode at late times could be due to a single exponential term or a sum of exponential terms, but the slopes of the potential of the leading terms could be very different. In fact, one of the very interesting features of an exponential potential is that the cosmological evolution puts stringent constraints on the slope of the potential, particularly during big-bang nucleosynthesis, but its coefficient may not be tightly constrained. That is, even if we use the potential $V(\varphi) = V_0\, e^{-\beta\varphi}$, with $\beta \sim \mathcal{O}(1-10)$, for explaining both the early and the late time cosmic accelerations, the magnitude of the coefficient V_0 can be significantly different, hence indicating completely different time and energy scales.

4.5 Non-vanishing Matter Fields

The above results were found in the absence of radiation and matter fields. It is thus natural to ask what happens in a more realistic situation, at late times, when both radiation and matter evolve together with the field φ. It may be possible to find a number of new and interesting background evolutions. Also some of the pathological features, like the appearance of super-luminal scalar modes, may be absent due to nontrivial scalar-matter couplings.

4.5.1 Non-minimally coupled scalar field

To investigate a possible post-inflation scenario, where the scalar field may couple non-minimally to a relativistic fluid or stiff-matter other than to ordinary matter or dust, we consider the following three different epochs: (i) background domination by a stiff relativistic fluid; (ii) radiation domination; (iii) a relatively long period of dust-like matter domination which occurred just before the current epoch of dark energy or scalar field domination. To this end, we define the fractional densities as follows: Ω_s for stiff-, relativistic matter, Ω_r for radiation and Ω_d for dust, where the respective equation of state parameters are given by $w_s = 1$, $w_r = 1/3$ and $w_d = 0$. Equations (4.13) – (4.13) may be written as

$$\Omega_s' + 2\epsilon\Omega_s + 3\Omega_s(1+w_s) \;=\; -3\eta_s Q_s \Omega_s \varphi', \tag{4.54}$$

$$\Omega_d' + 2\epsilon\Omega_d + 3\Omega_d = -3Q_d\Omega_d\varphi'. \tag{4.55}$$

$$\Omega_r' + 2\epsilon\Omega_r + 4\Omega_r = 0, \tag{4.56}$$

In order for current experimental limits on verification of the equivalence principle to be satisfied, the coupling must be small, $Q_d^2 \ll 1$, at present [146].

Superstring theory in its Hagedorn phase (a hot gas of strings), and also some brane models, naturally predict a universe filled with radiation and stiff-matter. To this end, it is not unreasonable to expect a nontrivial coupling of the field φ with the stiff-matter: highly relativistic fluids may have strong couplings of the order of unity, $Q_s \sim \mathcal{O}(1)$. As we do not observe a highly relativistic stiff-matter at the present time, i.e., $\Omega_s \approx 0$, the scalar-stiff-matter coupling Q_s in the order of unity is not ruled out and may have a quantifiable effect on the evolution of the early universe.

4.5.2 The $\Omega_{GB} = \text{const}$ solution

It is interesting to study the case of a constant Ω_{GB} as it allows us to evolve the potential without constraining it through an ansatz. An exponential potential is generally used in the literature due to the simplification it affords allowing a change of variables and hence a system of autonomous equations.

It is worthwhile to investigate whether a physically interesting result can be found without the need for an ansatz for the potential. To this end, let us take $\Omega_{GB} \simeq \text{const} \equiv \mu_0$. With the ansatz (4.45), we have

$$\frac{\mathrm{d}x}{\mathrm{d}N} = -2x(\epsilon + \frac{x}{\varphi_0}) \tag{4.57}$$

$$y = 3 - \frac{\gamma}{2}x^2 - 3\mu_0 - 3(\Omega_r + \Omega_s + \Omega_d), \tag{4.58}$$

where

$$\epsilon = \frac{\gamma x^2 + \mu_0 + 2x(\eta_s Q_s\Omega_s + \eta_d Q_d\Omega_d) + 3\Omega_r(1+w_r) + 3\Omega_s(1+w_s) + 3\Omega_d(1+w_d)}{\mu_0 - 2}, \tag{4.59}$$

in addition to the continuity equations (4.54) – (4.56) describing the system. We also note that, since $\epsilon = H'/H$, H is solved using (4.59), this allows us to find both the scalar field potential $V = yH^2$ and the effective potential $\Lambda(\varphi) \equiv V(\varphi) + 3f(\varphi)H^4(1+\epsilon)$

explicitly. We can see that there is a strong correlation between the length of dust-like matter domination and the parameter values, μ_0 and $\Omega_{d,\mathrm{ini}}$.

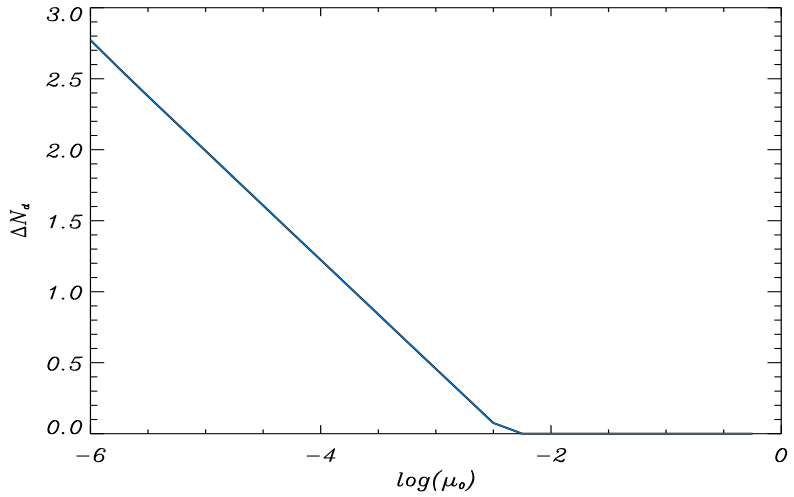

Figure 4.2: *The period of dust-like matter domination as a function of* μ_0 *for* $f_{,\varphi} = f_0\, e^{3\varphi}$, $\gamma = 1$, $Q_d^2 = 10^{-5}$ *and* $Q_s^2 = 0.01$. *The initial conditions are* $x = 10^{-7}$, $y = 10^{-15}$, $\Omega_d = 0.1$ *and* $\Omega_r = 0.45$.

The dust domination period is expected to last for about $5 - 7$ e-folds of expansion. However, in the above case, no parameter ranges meet this condition while still maintaining a relatively long period of radiation domination. This is problematic as at least some period of radiation domination appears to be a requirement for reconciling any cosmological model with observation. Our results here are therefore presented in the spirit of a toy model, which allow the evolution of an unconstrained potential for parameter ranges and give solutions with the expected qualitative features.

Figure 4.2 shows the period of dust domination observed for various values of μ_0. We see that, in the parameter range $\mu_0 \lesssim 10^{-3}$, there exist solutions supporting both radiation and stiff-matter domination prior to matter domination. For larger values of μ_0, the Gauss-Bonnet contribution suppresses the background fields and we observe a quick transition to scalar-field domination, with either the radiation dominated era or the matter dominated era, or both eras not occuring. For smaller values of μ_0, no solutions exist for the parameters used above due to constraints in the field equations. The behaviour of w_{eff} for varying μ_0 and the general evolution of the cosmology are

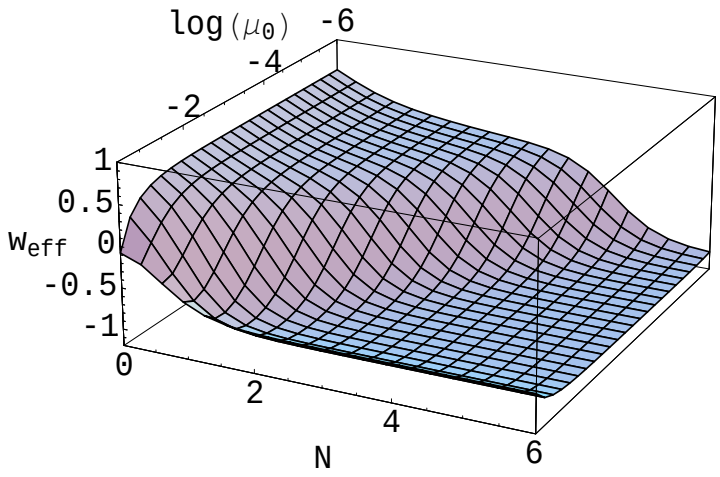

Figure 4.3: *The behaviour of* $w_{\rm eff}$ *for varying* μ_0 *for* $f_{,\varphi} = f_0\, e^{3\varphi}$, $\gamma = 1$, $Q_d^2 = 10^{-5}$ *and* $Q_s^2 = 0.01$. *The initial conditions are* $x = 10^{-7}$, $y = 10^{-15}$, $\Omega_d = 0.1$ *and* $\Omega_r = 0.45$.

shown in figure 4.3 and figure 4.4, respectively. In the cases where the second derivative of $w_{\rm eff}$ is monotonic there is no radiation domination ($w_{\rm eff} \sim 1/3$) or dust domination ($w_{\rm eff} \sim 0$). For lower values of μ_0, the second derivative of $w_{\rm eff}$ obviously changes sign and hence implies a period of background matter or radiation domination. We show the behaviour of the scalar potential and the corresponding effective potential in figure 4.5.

4.5.3 Simplest exponential potentials

We now wish to consider the evolution of the full system while putting minimal restrictions on the evolution of the cosmological constituents. To do this we employ simple single exponential terms for both the field potential and the scalar-GB coupling:

$$f_{,\varphi}(\varphi) = f_0\, e^{\alpha\varphi} \qquad \text{and} \qquad V(\varphi) = V_0\, e^{-\beta\varphi}. \tag{4.60}$$

The commonly invoked exponential potential ansatz has some physical motivation in supergravity and superstring theories as it could arise due to some nonperturbative effects, such as gaugino condensation and instantons. These choices are almost undoubtedly too naive to allow all the expected physical features of our universe from the inflation epoch to the present day. This is because generally the slopes of the potential considered in post-inflation scenarios are too steep to allow the required

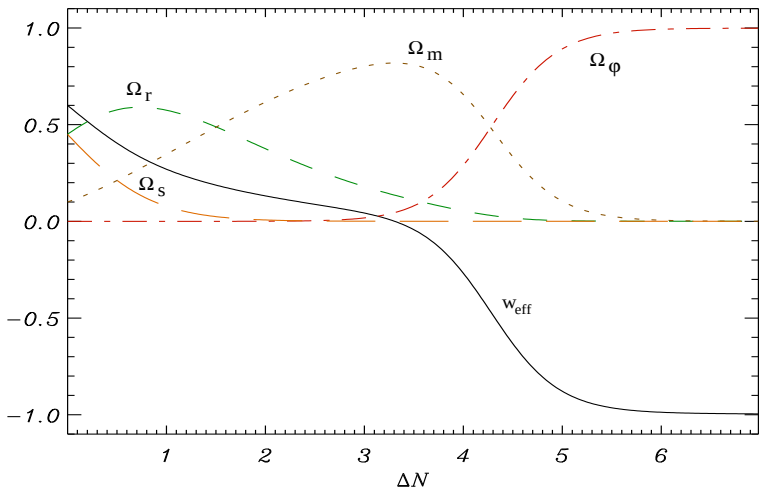

Figure 4.4: *The evolution of the fractional densities and* $w_{\rm eff}$ *(solid line) for a fixed* $\mu_0 = 10^{-6}$ *with parameters* $\gamma = 1$, $\varphi_0 = 2/3$, $Q_d^2 = 10^{-5}$ *and* $Q_s^2 = 0.01$, *and initial conditions as* $x = 10^{-7}$, $y = 10^{-15}$, $\Omega_d = 0.1$ *(dots) and* $\Omega_r = 0.45$ *(dashes).* Ω_s *is represented by long dashes and* Ω_φ *by dot-dash.*

number of e-folds of inflation in the early universe. As a post-inflation approximation, however, these may hold some validity, as one can replicate many observable physical features from nucleosynthesis to the present epoch while allowing nontrivial scalar-matter couplings. In section 4.5.5 we will discuss the possibility of a two-scalar fields model where the potential related to one scalar field meets the requirements of inflation while the other scalar drives the late time cosmology.

The ansätze (4.60) allow us to write an autonomous system

$$\begin{aligned}
\frac{\mathrm{d}x}{\mathrm{d}N} &= -\frac{1}{2\gamma}[2\gamma x\epsilon + 6\gamma x - 2\beta y + 6u(1+\epsilon) - 6\eta_s Q_s \Omega_s \\
&\quad +\eta_d Q_d\{\gamma x^2 + 2y + 6(ux + \Omega_r + \Omega_s - 1)\}] \qquad (4.61)\\
\frac{\mathrm{d}y}{\mathrm{d}N} &= -y(\beta x + 2\epsilon) \qquad (4.62)\\
\frac{\mathrm{d}u}{\mathrm{d}N} &= u(\alpha x + 2\epsilon) \qquad (4.63)
\end{aligned}$$

where

$$\begin{aligned}
\epsilon &= \frac{1}{6(2\gamma ux - 2\gamma - 3u^2)}\Big[18\gamma\,(1 + w_d - w_d\Omega_r - w_d\Omega_s + w_r\Omega_r + w_s\Omega_s) \\
&\quad +6\gamma ux - 6\gamma y + 3\gamma^2 x^2 + 18u^2 - 3\gamma^2 w_d x^2 - 6\beta uy - 6\gamma\alpha u x^2 - 18\gamma w_d ux - 6\gamma w_d y
\end{aligned}$$

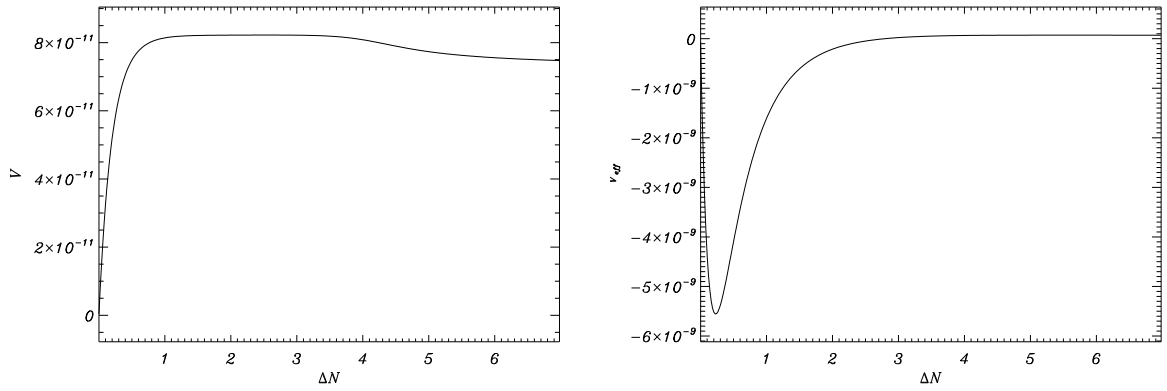

Figure 4.5: *The left panel shows the evolution of* $V(\varphi)$ *while the right panel shows the evolution of* $V_{\rm eff} \equiv V(\varphi) + 3f(\varphi)H^4(1+\epsilon)$ *for* $\mu_0 = 10^{-6}$, $\gamma = 1$, $f(\varphi) \propto e^{3\varphi}$, $Q_d^2 = 10^{-5}$ *and* $Q_s^2 = 0.01$ *with initial conditions* $x = 10^{-7}$, $y = 10^{-15}$, $\Omega_d = 0.1$, $\Omega_r = 0.45$, $H = 0.01$ *and* $f(\varphi)_{\rm ini} = 10^{-10}$.

$$-\eta_d Q_d(2\gamma^2 x^3 + 18u - 18u^2 x - 6uy - 18u\Omega_r - 12\gamma x + 4\gamma xy + 12\gamma x\Omega_r + 9\gamma u x^2)$$
$$-\left(\eta_d Q_d - \eta_s Q_s\right)\left(12\gamma x - 18u\Omega_s\right)\Big], \tag{4.64}$$

which along with the continuity equations (4.54) – (4.56) and the Friedmann constraint equation, $\Omega_d + \Omega_\varphi + \Omega_{GB} + \Omega_r + \Omega_s = 1$, allow us to proceed with numerical computation.

We look particularly at two values for β here, $\beta = \sqrt{2/3}$ and $\beta = \sqrt{3}$, while keeping the other parameters constant to limit the vast parameter space. These values may be motivated by various schemes of string or M theory compactifications [153]. We will discuss the effects of varying these other parameters and some of the physically relevant results. The evolution of the various constituents is shown in figures 4.6-4.7.

The $\beta = \sqrt{2/3}$ case appears to show a smoother evolution and has a short period during which there is acceleration and an appreciable amount of matter in the universe. In the table below we look at some of the features of the accelerating period for the solution given in figure 4.6. At the onset of acceleration, $w_{\rm eff} = -1/3$, we have $\Omega_d = 0.650$. Within the best-fit concordance cosmology the present observational data seem to require $w_{\rm eff} < -0.74$ [161]. However, in the above case, this requires less matter ($\Omega_d \lesssim 0.12$) than in ΛCDM model.

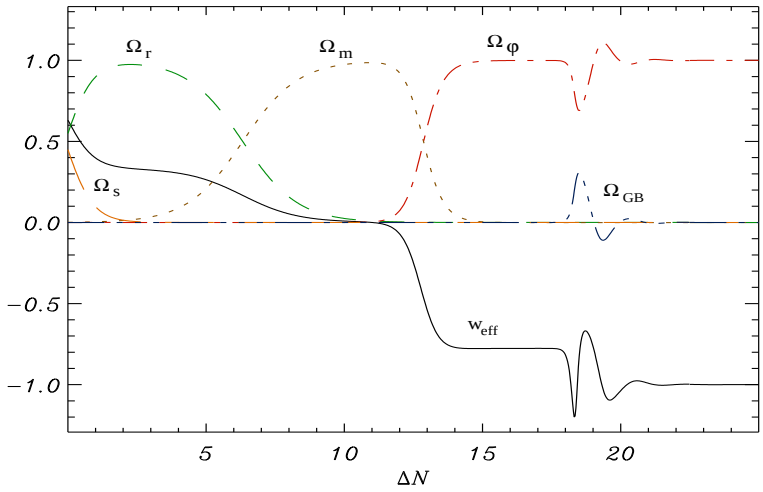

Figure 4.6: *Evolution of the fractional densities and* w_{eff} *(solid line) where* $\beta = \sqrt{2/3}$, $\gamma = 1$, $\alpha = 12$, $Q_d^2 = 10^{-5}$ *and* $Q_s^2 = 0.01$ *with initial conditions* $x = \sqrt{6} \times 10^{-4}$, $y = 5 \times 10^{-20}$, $u = 0.08$, $\Omega_r = 0.549$ *(dashes) and* $\Omega_s = 0.45$ *(long dashes).* Ω_d *is represented by dots,* Ω_φ *by dot-dash and* Ω_{GB} *by dot-dot-dot-dash.*

Condition imposed at present	$\Delta N_{\text{accelerating}}$	Implied w_{eff}	Implied Ω_d
$\Omega_d = 0.27$	0.582	-0.648	N/A
$w_{\text{eff}} = -0.74$	0.955	N/A	0.123
$w_{\text{eff}} = -0.9$	5.48	N/A	3.02×10^{-6}
$w_{\text{eff}} = -1.0$	5.55	N/A	2.46×10^{-6}
$\Delta N = 0.69$	N/A	-0.685	0.215
$\Delta N = 0.91$	N/A	-0.734	0.134

The recent type Ia supernovae observations [14, 51] appear to indicate that the universe may be accelerating out to a redshift of $z \sim 0.4 - 1$ [162]. In terms of the number of e-folds of expansion, this corresponds to $\Delta N = \ln(1+z) \sim 0.34 - 0.69$, if one assumes a rescaling of $N \to 0$ at the present epoch using the freedom in choosing the initial value of the scale factor, a_0. We have chosen the initial value of y, or the ratio $V(\varphi)/H^2$, such that the period of dust-like matter domination is $\Delta N_{\Omega_d} \sim 6.5$ as this corresponds to a total redshift of $z \sim 1100$, the epoch of matter-radiation equality.

The evolution with $\beta = \sqrt{3}$ does not seem to be in agreement with current cosmo-

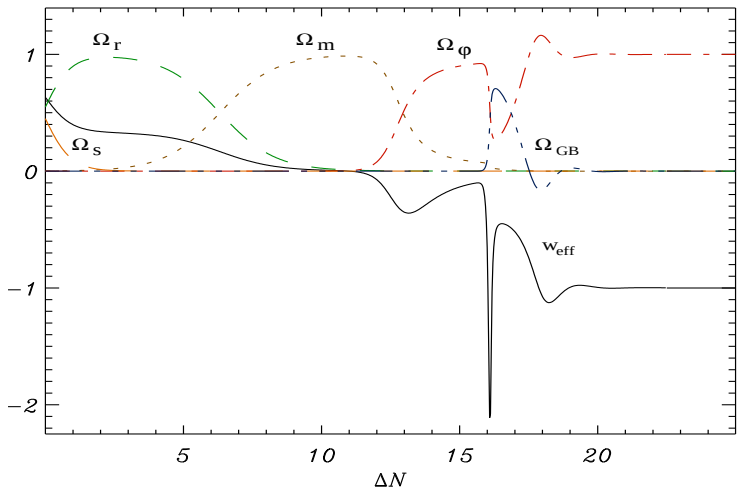

Figure 4.7: *Evolution of the fractional densities and* w_{eff} *(solid line) where* $\beta = \sqrt{3}$, $\gamma = 1$, $\alpha = 12$, $Q_d^2 = 10^{-5}$ *and* $Q_s^2 = 0.01$ *with initial conditions* $x = \sqrt{6} \times 10^{-4}$, $y = 5 \times 10^{-20}$, $u = 0.08$, $\Omega_r = 0.549$ *(dashes) and* $\Omega_s = 0.45$ *(long dashes).* Ω_d *is represented by dots and* Ω_φ *by dot-dash,* Ω_{GB} *by dot-dot-dot-dash.*

logical observations. The solution may undergo a period of sudden change in w_{eff} when the Gauss-Bonnet contribution becomes appreciable (or significant); this would have to occur around at the present epoch as to retrieve the current value of $w_{eff} \sim -1$. This result does not reconcile with either the supernovae data, which seem to indicate a longer period of acceleration, or with a constraint for the present value of Gauss-Bonnet density which requires that $\Omega_{GB} \lesssim 0.2$ [163], or with the present concordance value of Ω_d (~ 0.27).

We observe an oscillatory crossing of $w_{\text{eff}} = -1$ limit for all cases in which the Gauss-Bonnet contribution becomes appreciable, even momentarily. Such behaviour may be seen in variants of scalar-tensor models [164]. In our case, the amplitude of these oscillations corresponds to the amplitude of the oscillations seen in the Gauss-Bonnet contribution and hence is heavily dependent on the slope of the scalar-GB coupling; for large α we observe much larger oscillations. These oscillations damp quickly as the Gauss-Bonnet contribution becomes negligibly small, and settle to a late time evolution for which $w_{\text{eff}} \approx -1$. As this limit is approached from above, none of the issues inherent with super-inflation or a violation of unitarity will be applicable

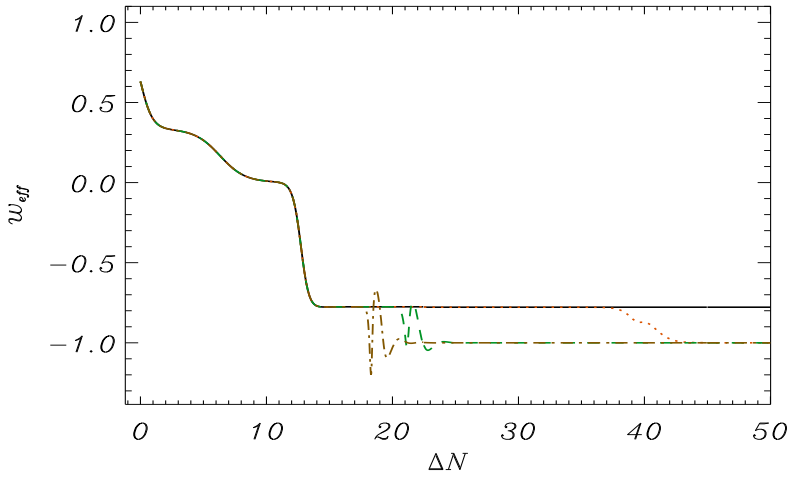

Figure 4.8: *Evolution of* $w_{\rm eff}$ *with* $\beta = \sqrt{2/3}$, $\gamma = 1$, $Q_d^2 = 10^{-5}$ *and* $Q_s^2 = 0.01$*;* $\alpha = 12$ *(dash-dot),* 8 *(dashes),* 3 *(dots),* $\sqrt{2/3}$ *(solid), with initial values* $x = \sqrt{6}\times10^{-4}$, $y = 5\times10^{-20}$, $u = 0.08$, $\Omega_r = 0.549$ *and* $\Omega_s = 0.45$.

to the late time cosmology.

As the parameter space for the initial conditions is very large we have presented solutions with initial conditions and parameters selected to give reasonable periods of radiation and dust-like matter domination as well as other physically favourable features. Although the quantitative behaviour is observed to change smoothly with changes in initial conditions and parameters, such changes do have some qualitative effects as limits of certain behaviour are encountered. A quantitative variation in the period of dust-like matter domination can be attributed to altering the initial value of y or $\Omega_{d,\rm ini}$; lower values of $y_{\rm ini}$ extend the period before scalar field domination begins. This is effectively a change in the initial potential and has a monotonic effect on the epoch at which scalar field domination begins. In a quantitative sense, it has no effect on the period of radiation domination until a $y_{\rm ini}$ is selected which is large enough that the scalar field contribution completely suppresses the dust-like matter domination period. The value of $\Omega_{d,\rm ini}$ is relevant to the epoch of matter-radiation equality, larger values result in an earlier epoch. For small values, no dust-like matter domination occurs and the solution is entirely dominated by the other four constituents considered. The limits at which all these effects occur are dependent on other parameters and hence

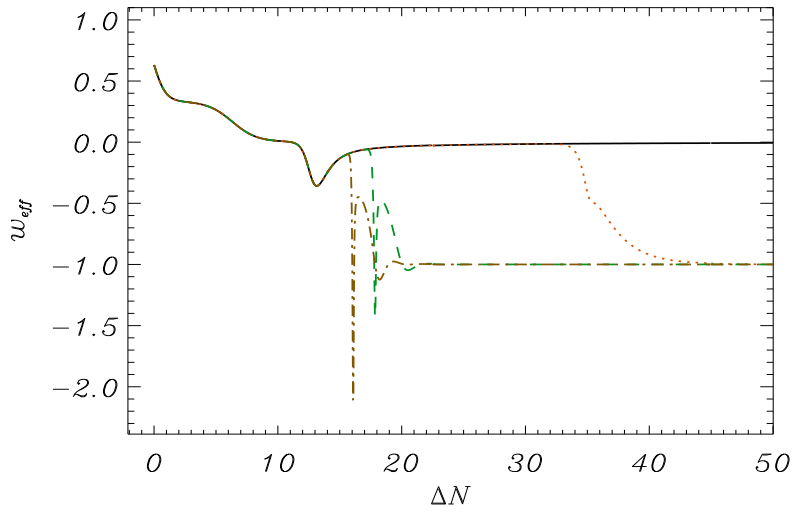

Figure 4.9: *Evolution of* $\mathrm{w_{eff}}$ *with* $\beta = \sqrt{3}$, $\gamma = 1$, $Q_d^2 = 10^{-5}$ *and* $Q_s^2 = 0.01$; $\alpha = 12$ *(dash-dot),* 8 *(dashes),* 3 *(dots),* $\sqrt{2/3}$ *(solid), with initial values* $x = \sqrt{6} \times 10^{-4}$, $y = 5 \times 10^{-20}$, $u = 0.08$, $\Omega_r = 0.549$ *and* $\Omega_s = 0.45$.

discussion of actual values instead of the general behaviour does not add further insight. The initial values of these parameters require a better understanding of the underlying fundamental theory and the implications in the early Universe to be constrained more tightly, and therefore add some predictability to the theory discussed here.

We note that the exponential terms for both the potential and the coupling have some noticeable effects on the evolution of the system. This may be seen to an extent in terms of β in figures 4.6–4.9. It does, however, appear that the ratio of these parameters also influences the expansion during dust-like matter domination, remaining relatively unchanged when this ratio is constant within realistic β and α parameter ranges. Phenomenological bounds on these values have been studied in Koivisto and Mota [159].

For $\alpha \sim \beta$ we do not observe a significant period of Gauss-Bonnet contribution and hence no crossing of the $w_{\mathrm{eff}} = -1$ limit. The closer the value of α is to this limit the later this period of significant Gauss-Bonnet density fraction occurs. As α increases there is a minimum epoch at which the Gauss-Bonnet contribution becomes significant. This epoch occurs after the scalar field becomes the dominant component in the energy

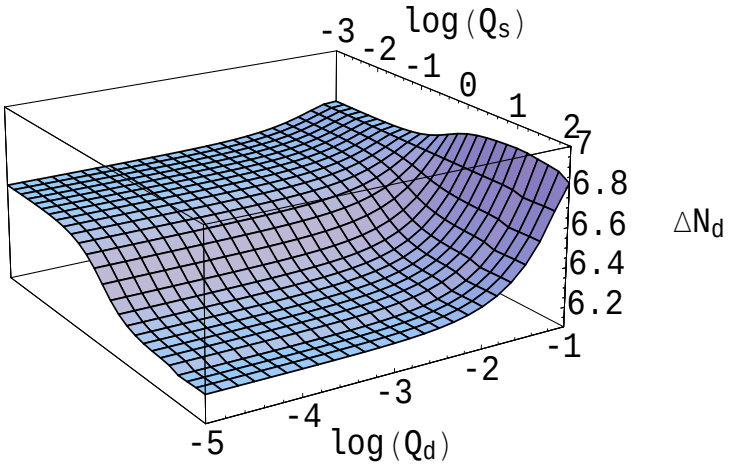

Figure 4.10: *The period of dust-like matter domination for varying Q_s and Q_d for $\gamma = 1$, $\alpha = 12$ and $\beta = \sqrt{2/3}$ with initial conditions $x = \sqrt{6} \times 10^{-5}$, $y = 5 \times 10^{-20}$, $u = 0.08$, $\Omega_r = 0.549$ and $\Omega_s = 0.45$.*

budget of our universe. Results for various values of α are shown in figures 4.8 and 4.9.

The consequences of matter coupling to the scalar field on the cosmology are of particular interest. The effect in the period of dust-like matter-domination is minimal in relation to both Q_d and Q_s and can be seen in figure 4.10, though we allowed the value $Q_s \gg Q_d$. As there is a lack of observational or theoretical motivation refuting the possibility of a high relativistic matter-scalar coupling, we consider a range that extends beyond $Q_s = 1$, whereas the dust-like-matter-scalar coupling must take values $Q_d^2 < 10^{-5}$ due to the current level of experimental verification in solar system tests of general relativity.

The solution undergoes a transition in qualitative behaviour when we extend through the limit $Q_{s,\mathrm{lim}} \sim 1$, where the exact onset and amplitude of its effects are dependent on the other parameter values taken. Hence our remarks again apply to the general behaviour observed rather than specific cases. Couplings greater than $Q_{s,\mathrm{lim}}$ cause a non-negligible reemergence of the stiff-matter contribution at the end of dust-like matter domination. The density fraction of the relativistic matter undergoes a damped oscillation, generally with a much shorter period than the oscillations observed in the non-negligible Gauss-Bonnet contribution. This causes corresponding oscillations in the effective equation of state parameter, while still generally showing the same overall

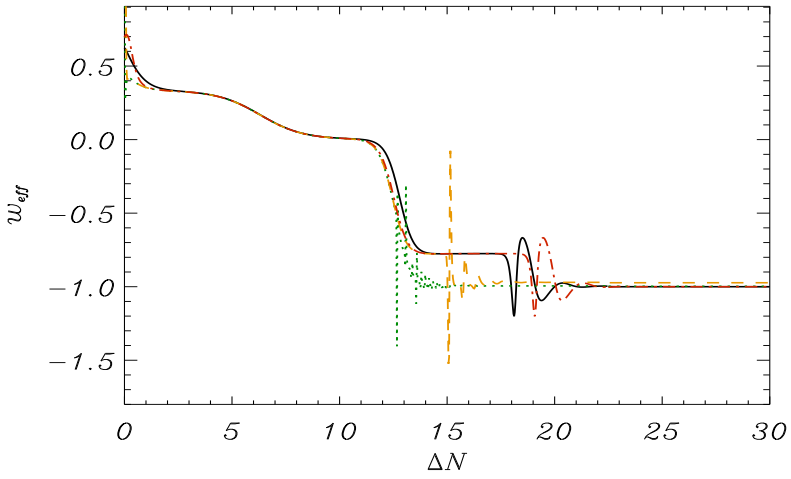

Figure 4.11: *Evolution of* $w_{\rm eff}$ *for different values of* Q_s*:* $Q_s^2 = 10^4$ *(dots)* 100 *(dashes),* 0 *(solid) and* 1 *(dash-dot) with fixed* $Q_d = \sqrt{10^{-5}}$ *and* $\gamma = 1$*,* $\alpha = 12$*,* $\beta = \sqrt{2/3}$*. The initial conditions are* $x = \sqrt{6} \times 10^{-4}$*,* $y = 5 \times 10^{-20}$*,* $u = 0.1$*,* $\Omega_r = 0.549$ *and* $\Omega_s = 0.45$*. The larger, more violent oscillations seen for* $Q_s > 1$ *are due to significant scalar-stiff-matter couplings, while the smooth oscillations for smaller couplings at some later stage are due to an appreciable contribution of the coupled Gauss-Bonnet term.*

trend as for lower Q_s values of the otherwise same solution, with the density fraction of the relativistic matter stabilising to a non-zero late time value. This cosmological behaviour does not appear to be physically valid, as no mechanism to generate this relativistic matter seems plausible and would hence lead us to suggest that the value of Q_s would have an upper-bound such that $Q_{s,\rm max} \sim Q_{s,\rm lim}$. The effects of Q_s and Q_d on the effective equation of state parameter, $w_{\rm eff}$, may be seen in figures 4.11 and 4.12. Note that in figure 4.12 we have considered Δw_{eff} rather than w_{eff} as the effects of varying Q_d are so minimal that no discernable variation can be seen otherwise. In these figures we have considered the same solutions as in figure 4.6. The magnitude of the effects are, however, the same throughout the parameter space.

4.5.4 A canonical potential

From section 4.3, we consider the potential

$$V(\varphi) = H^2(\Lambda_0 + \Lambda_1 e^{\beta\varphi}). \tag{4.65}$$

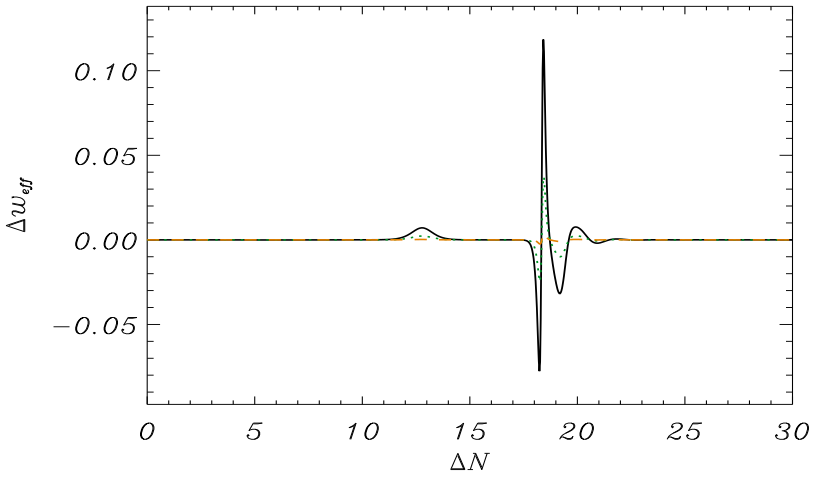

Figure 4.12: *Variation of* $w_{\rm eff}$ *for non-zero* Q_d *as compared to the* $Q_d = 0$ *case,* $\Delta w_{\rm eff} \equiv w_{\rm eff}(Q_d \neq 0) - w_{\rm eff}(Q_d = 0)$*;* $Q_d^2 = 10^{-5}$ *(solid),* 10^{-6} *(dots) and* 10^{-8} *(dashes) and* $Q_s = 0.1$*. Clearly, for higher values of the scalar dust-matter couplings,* $Q_d^2 > 10^{-5}$*, we find slightly larger variations in* $w_{\rm eff}$*.*

Imposing this ansatz along with the scalar-GB coupling given in equation (4.60), $f(\varphi) \propto e^{\alpha\varphi}$, allows us to find solutions that have reasonable agreement with concurrent observations while not crossing the $w_{\rm eff} = -1$ limit at any stage of the evolution. From figure (4.13) we can see that the cosmic evolution shows a smooth progression to $w_{\rm eff} = -1$, which may be physically more sensible. The amplitude of the Gauss-Bonnet density fraction at maximum is dependent on the values of slope α, for smaller α it never becomes relevant. The period of dust-like matter domination again shows a heavy dependence on the initial value of y or the potential $V(\varphi)$.

4.5.5 Double scalar case

Multiple scalar exponential potentials, which may arise in time-dependent compactifications of supergravity on symmetric or twisted product manifolds [165], exhibit *assisted inflation* [124] or *assisted quintessence* [166, 167] depending on the epoch of interest. This is of interest in string motivated scenarios, as in the low energy effective 4-dimensional theory one would expect multiple scalar fields, and the potentials which arise naturally from symmetry breaking are significantly steeper than those attributable

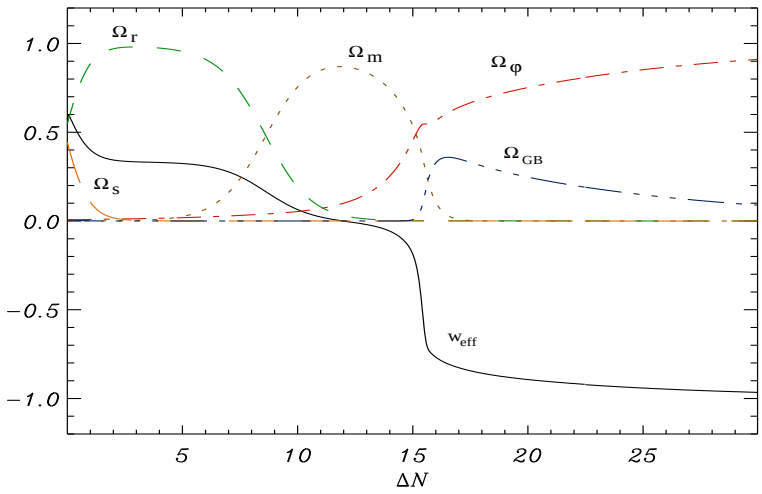

Figure 4.13: *Evolution of the fractional densities and* $w_{\rm eff}$ *(solid line) for the potential ansatz* $V(\varphi) = H^2(\Lambda_0 + \Lambda_1 e^{-\beta\varphi})$ *where* $\gamma = 1$, $\alpha = 9$, $\beta = \sqrt{2/3}$, $\Lambda_0 = 10^{-8}$, $Q_d^2 = 10^{-5}$ *and* $Q_s^2 = 0.01$ *with initial conditions* $x = \sqrt{6} \times 10^{-2}$, $y = 9 \times 10^{-3}$, $u = 0.1$, $\Omega_r = 0.549$ *(dashes) and* $\Omega_d = 10^{-4}$ *(dots).* Ω_s *is represented by long dashes,* Ω_φ *by dot-dash and* Ω_{GB} *by dot-dot-dot-dash.*

to an equation of state parameter $w_{\rm scalar} < -1/3$. It was shown by Liddle *et al.* [124] that for a double scalar exponential potential,

$$V(\varphi_1, \varphi_2) = v_1 \mathrm{e}^{-\beta_1 \varphi_1} + v_2 \mathrm{e}^{-\beta_2 \varphi_2}, \tag{4.66}$$

the dynamics match that of a single scalar theory with a slope, β_{eff}, where

$$\frac{1}{\beta_{eff}^2} = \frac{1}{\beta_1^2} + \frac{1}{\beta_2^2}\,. \tag{4.67}$$

To obtain an inflationary (or accelerating) universe in the case of a minimally coupled gravity-scalar field theory with an exponential potential, one requires $\beta_{eff} < \sqrt{2}$. In the potential dominated, minimally coupled model $w_{eff} = \beta_{eff}^2/3 - 1$.

Here we extend the results of [158] by considering two scalar fields coupled to matter and the Gauss-Bonnet correction to gravity. We show that the coupling to the Gauss-Bonnet term further *assists* quintessence, with accelerating late-time behaviour being observed for cases where $\beta_{eff} > \sqrt{2}$.

Model

We consider the matter and radiation contribution in addition to the curvature and scalar field terms, such that,

$$\mathcal{L} = \mathcal{L}_{grav} + \mathcal{L}_{scalar} + \mathcal{L}_m, \tag{4.68}$$

where

$$\mathcal{L}_{grav} = \sqrt{-g}\left(\frac{R}{2} - \frac{1}{8}f(\varphi,\sigma)\mathcal{R}^2_{GB}\right), \tag{4.69}$$

$$\mathcal{L}_{scalar} = \sqrt{-g}\left(-\frac{\gamma}{2}(\nabla\varphi)^2 - \frac{\xi}{2}(\nabla\sigma)^2 - V(\varphi,\sigma)\right) \tag{4.70}$$

$$\text{and} \quad \mathcal{L}_m = \sqrt{-g}\left[A_s^4(\varphi)\rho_s + A_d^4(\varphi)\rho_d + A_r^4(\varphi)\rho_r\right]. \tag{4.71}$$

The constants, γ and ξ, are assumed to be positive, ignoring on physical grounds the negative kinetic energy case. We set $\gamma = \xi = 1$ throughout this analysis without loss of generality due to the freedom to rescale the scalar field. We make the physical identification that one of the scalar fields, φ, is the dilaton while the other, σ, is a modulus field. This is not rigorous by any means but allows us to make some general simplifying assumptions regarding the physical behaviour.

We only consider a coupling between one scalar field, φ and the matter fields, $A(\varphi)$. As the field equations are only dependent on the derivative of the coupling, and the modulus field would generally have $|\dot{\sigma}| \ll 1$ during the post-inflation period, the coupling is likely neligible.

We take the standard 4-dimensional FLRW spacetime metric, as above, which, along with (4.68), gives the Friedmann constraint equation,

$$\begin{aligned}\frac{\dot{\varphi}^2}{6} + \frac{\dot{\sigma}^2}{6} + \frac{V(\varphi,\sigma)}{3} + \dot{\varphi}f_{,\varphi}H^3 + \dot{\sigma}f_{,\sigma}H^3 \\ + \frac{1}{3}\left[A_s^4(\varphi)\rho_s + A_d^4(\varphi)\rho_d + A_r^4(\varphi)\rho_r\right] = H^2,\end{aligned} \tag{4.72}$$

and the scalar equations of motion for φ and σ,

$$\ddot{\varphi} + 3H\dot{\varphi} + V_{,\varphi} + 3(1+\epsilon)f_{,\varphi}H^4 + 2Q_sA_s^4(\varphi)\rho_s - Q_dA_d^4(\varphi)\rho_d = 0, \tag{4.73}$$

$$\ddot{\sigma} + 3H\dot{\sigma} + V_{,\sigma} + 3(1+\epsilon)f_{,\sigma}H^4 = 0, \tag{4.74}$$

respectively, where

$$V_{,\sigma} \equiv \frac{\partial V}{\partial \sigma}, \quad \text{and} \quad f_{,\sigma} \equiv \frac{\partial f}{\partial \sigma}$$

In order to solve the system above, certain anstazes must be made. We only consider minimal coupling between the scalar fields. Hence the potential is separable into the linear sum of exponentials given by (4.66) where $\varphi_1 = \varphi$ and $\varphi_2 = \sigma$. While in the effective 4-dimensional theory the modulus field can be assumed to have a flat potential, we leave a more general form here. We also assume exponential couplings to both gravity and matter. Hence we get $Q = \text{const}$ and

$$f(\varphi, \sigma) = g(\varphi) + h(\sigma) = f_1 \mathrm{e}^{\alpha_1 \varphi} + f_2 \mathrm{e}^{\alpha_2 \sigma}. \tag{4.75}$$

Additionally we supplement (4.72) – (4.74) with the equation of motion for a barotropic perfect fluid, (4.54) – (4.56).

For the purposes of numerical integration it is convenient reparamterise to dimensionless variables, as we do in earlier sections. The field equations, (4.72) – (4.74), therefore can be written as the autonomous equations,

$$\begin{aligned}
-3 + \frac{1}{2}\, x_1^2(N) + \frac{1}{2}\, x_2^2(N) + y_1(N) + y_2(N) + 3u_1(N)x_1(N) & \\
+3u_2(N)x_2(N) + 3\left[\Omega_s(N) + \Omega_d(N) + \Omega_r(N)\right] &= 0, \quad (4.76) \\
x_1(N)\left\{x_1'(N) + [\epsilon(N) + 3]x_1(N)\right\} + y_1'(N) + 2y_1(N)\epsilon(N) & \\
+3u_1(N)x_1(N)\left[1 + \epsilon(N)\right] + 3x_1(N)\left[2Q_s\Omega_s - Q_d\Omega_d\right] &= 0, \quad (4.77) \\
x_2(N)\left\{x_2'(N) + [\epsilon(N) + 3]x_2(N)\right\} + y_2'(N) + 2y_2(N)\epsilon(N) & \\
+3u_2(N)x_2(N)\left[1 + \epsilon(N)\right] &= 0, \quad (4.78)
\end{aligned}$$

where

$$x_i = \frac{\dot{\Phi}_i}{H}\,, \quad y_i = \frac{V(\Phi_i)}{H^2}\,, \quad u_i = f_{,\Phi_i} H^2, \ \text{ with } \ i \in \{1, 2\}, \tag{4.79}$$

such that $\Phi_1 = \varphi$ and $\Phi_2 = \sigma$.

Numerical Solutions

The system described above has a lot of freedom. This is both convenient and problematic, while it allows fits to many scenarios, the predictive power is poor. We will look to constrain some of the freedom on physical and theoretical grounds.

In the conformal transformation from the string frame to the Einstein frame, intuitively one would expect $f(\varphi) \approx A(\varphi)$. We also note that the scalar fields must

adhere to the nucleosynthesis upper bound, $\Omega_\varphi + \Omega_\sigma < 0.2$, at temperatures around 1 MeV [168]. This has been further tightened by the observed abundances of primordial light elements to $\Omega_\varphi + \Omega_\sigma < 0.045$ [169].

As mentioned in the earlier sections, $Q_m^2 \lesssim 10^{-5}$. We have shown for the single scalar case that values of $Q_s \gtrsim 1$ cause the relativistic stiff matter contribution to become significant in the late-time evolution of the Universe and is therefore ruled unphysical.

We note that in the limit that the scalar-Gauss-Bonnet contribution and the matter and radiation fields are set to zero, we recover the expected results [167]. The limiting case between inflating solutions, $w_{eff} < -1/3$, and non-inflating solutions, $w_{eff} > -1/3$, corresponds to $\beta_{eff} = \sqrt{2}$.

The presence of the Gauss-Bonnet term allows inflating solutions when β_{eff} is greater than this limit. The degree to which the Gauss-Bonnet term *assists* the inflationary limit on β_{eff} is dependent on the value of α_1 and α_2. For values of $\alpha_1, \alpha_2 > 2$, a significant weakening of the condition is observed when $\beta_{eff} = \sqrt{2}$. Only one of α_1 or α_2 has to exceed this *bound*, α_{lim}. The behaviour is largely driven by the term with the largest coupling constant with very little effect due to the sub-dominant coupling term.

There is a definite change in qualitative behaviour when this bound, α_{lim}, is exceeded with the value of w_{eff} being pushed to $w_{eff} = -1 + \delta$, where $\delta \ll 1$. For cases where the dominant term has a value $\alpha < \alpha_{lim}$, very little effect is observed in addition to the regular assisted quintessence seen in the absence of the Gauss-Bonnet term. The value of α_{lim} is dependent on the value of β_{eff}, with α_{lim} increasing with increasing β_{eff}. This allows asymptotically inflating solutions in cases where $\beta_{eff} > \sqrt{2}$.

The inclusion of the background fields, matter and radiation, has the effect of driving the effective equation of state parameter toward w_b. It is therefore easy to construct situations where the Gauss-Bonnet contribution and background fields are competing effects on the effective equation of state parameter.

In figure 4.14 we show a general solution, involving contributions from all terms shown in (3.1). This solution shows a physically reasonable evolution. The period of radiation domination is $\Delta N = 6.3$, with matter domination lasting for $\Delta N = 8.2$. The

period since the onset of accelerating expansion ($w_{eff} = -1/3$) to the present epoch, defined as the epoch where $\Omega_d = 0.27$ [7] following the period of matter domination, is $\Delta N \simeq 0.60$, which is not unrealistic when presented in redshift, $z \simeq 0.45$ [14, 51]. The individual behaviour of the scalar fields is shown in figure 4.15.

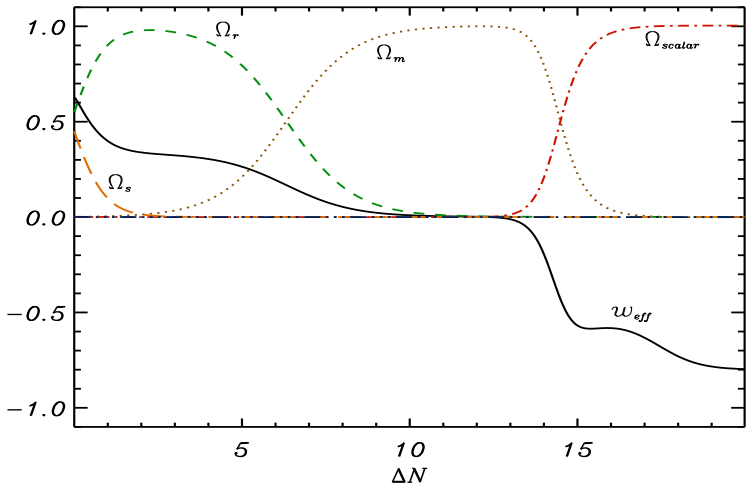

Figure 4.14: *Evolution of the fractional densities and* $w_{\rm eff}$ *(solid line) where* $\alpha_1 = 2.0$, $\alpha_2 = 2.0$, $\beta_1 = 1.2$, $\beta_2 = 1.0$, $Q_d^2 = 10^{-5}$ *and* $Q_s^2 = 0.01$ *with initial conditions* $x_1 = \sqrt{6}\times 10^{-6}$, $x_2 = \sqrt{6} \times 10^{-4}$, $y_1 = 5 \times 10^{-24}$, $y_2 = 5 \times 10^{-22}$, $u_1 = 0.08$, $u_2 = 0.08$, $\Omega_r = 0.549$ *(dashes) and* $\Omega_s = 0.45$ *(dots).* Ω_s *is shown as long dashes,* $\Omega_{scalar} = \Omega_\varphi + \Omega_\sigma$ *as dot-dash and* $\Omega_{GB} = \Omega_{GB,\varphi} + \Omega_{GB,\sigma}$ *as dot-dot-dot-dash although it never makes a significant contribution over the range of* N *displayed here.*

Due to the large number of degrees of freedom, evident in the parameterisation of the solution, we do not analyse the general behaviour in relation to every variable. We do, however, investigate the α dependence as this has interesting physical consequences. The evolution of w_{eff} is shown in figure 4.16 for various values of α where $\alpha_1 = \alpha_2 = \alpha$. The epoch at which $w_{eff} \to -1$ is dependent on the epoch of significant Gauss-Bonnet contribution. For large α, this contribution oscillates markedly causing the equation of state parameter to momentarily take values $w_{eff} < -1$ violating the dominant energy condition. These oscillations are likely not a realistic phenomena in the late–time evolution of the Universe and therefore, it would appear that α must take values near or less than unity.

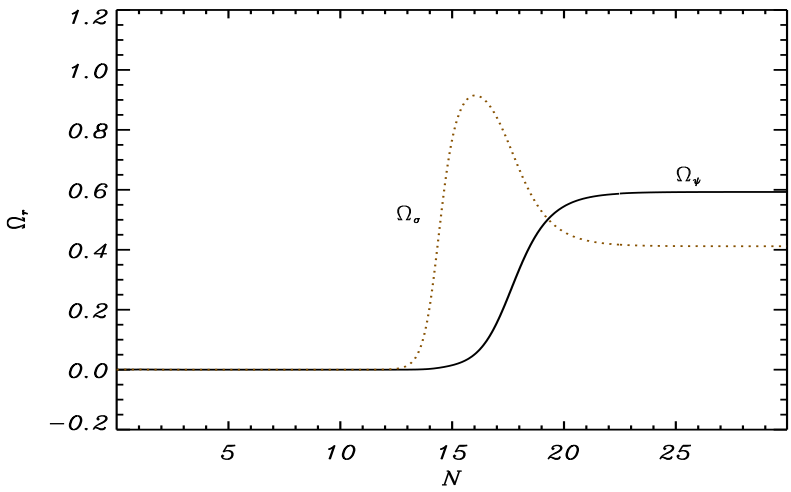

Figure 4.15: *Fractional densities of the scalar fields,* Ω_φ *(solid line) and* Ω_σ *(dotted line) where* $\alpha_1 = 2.0$, $\alpha_2 = 2.0$, $\beta_1 = 1.2$, $\beta_2 = 1.0$, $Q_d^2 = 10^{-5}$ *and* $Q_s^2 = 0.01$ *with initial conditions* $x_1 = \sqrt{6} \times 10^{-6}$, $x_2 = \sqrt{6} \times 10^{-4}$, $y_1 = 5 \times 10^{-24}$, $y_2 = 5 \times 10^{-22}$, $u_1 = 0.08$, $u_2 = 0.08$, $\Omega_r = 0.549$ *and* $\Omega_s = 0.45$.

The solutions presented have some intriguing features. However, the lack of predictive power is problematic. The number of free parameters in the theory would need to be reduced through recourse to an underlying fundamental theory to allow proper analysis of the validity of the theory. Another issue is the Gauss-Bonnet contribution, which, while offering a mechanism to induce acceleration, appears very unstable, particularly in the late-time universe. This likely indicates it is unphysical, at least with coupling constants, α, greater than unity.

We note that the solutions in section 4.5 are completely invariant under a constant shift in N. Therefore the choice of $N_0 = 0$ is arbitrary. We can equivalently set the present epoch to $N = 0$ ($a_0 = 1$), it is simply convenient numerically to present the results as shown.

4.6 Linear Stability Analysis

Here we consider a basic stability analysis to small homogeneous perturbations about a critical or fixed point. The earlier analysis of Nojiri *et al.* [132] would constitute

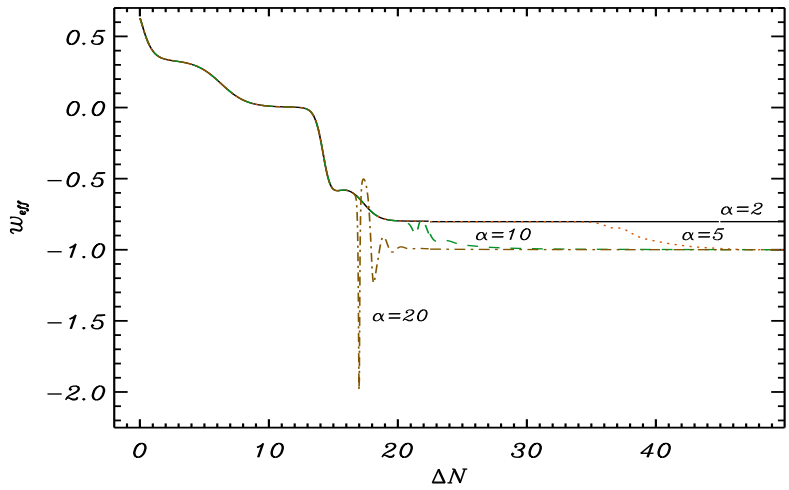

Figure 4.16: *The evolution of* $w_{\rm eff}$ *is shown for:* $\alpha = 2$ *(solid line),* $\alpha = 5$ *(dots),* $\alpha = 10$ *(dashes),* $\alpha = 20$ *(dot-dash), where* $\alpha = \alpha_1 = \alpha_2$*. The fixed parameters are* $\beta_1 = 1.2$*,* $\beta_2 = 1.0$*,* $Q_d^2 = 10^{-5}$ *and* $Q_s^2 = 0.01$ *with initial conditions* $x_1 = \sqrt{6} \times 10^{-6}$*,* $x_2 = \sqrt{6} \times 10^{-4}$*,* $y_1 = 5 \times 10^{-24}$*,* $y_2 = 5 \times 10^{-22}$*,* $u_1 = 0.08$*,* $u_2 = 0.08$*,* $\Omega_r = 0.549$ *and* $\Omega_s = 0.45$*.*

a special case of the treatment which follows. Consider the potential $V(\varphi)$ and the coupling $f(\varphi)$ as the simplest exponential functions of the field:

$$V(\varphi) = V_1 \, \mathrm{e}^{m\varphi/\varphi_0}, \quad f(\varphi) = f_1 \, \mathrm{e}^{n\varphi/\varphi_0}. \tag{4.80}$$

These choices may be motivated in the heterotic string theory as the first term of the perturbative string expansion [140]. One may solve the equations (4.5)–(4.7) by expressing $V(\varphi)$ and $f(\varphi)$ as in (4.80), with $n = -m = 2$, and dropping the effects of matter fields. The simplest way of solving field equations is to make a particular ansatz for the scale factor and scalar field, namely

$$a = a_0 \left(\tfrac{t}{t_0}\right)^h, \quad \varphi = \varphi_0 \ln \tfrac{t}{t_1} \quad (h > 0, \ t > 0), \tag{4.81}$$

$$a = a_0 \left(\tfrac{t_\infty - t}{t_0}\right)^h, \quad \varphi = \varphi_0 \ln \tfrac{t_\infty - t}{t_1} \quad (h < 0, \ t < 0 \text{ or } 0 < t < t_\infty). \tag{4.82}$$

The system of autonomous equations, in the absence of matter fields, from (4.5) – (4.7) using the substitutions in (4.9), is given by

$$\frac{dx}{dN} = \frac{\gamma^2 \varphi_0 x^3 - \gamma x(2ux^2 - 13ux\varphi_0 + 6\varphi_0) + 2(2y - 3ux) - 6u(\varphi_0 - 2xu\varphi_0 + x^2 u)}{\varphi_0(2\gamma - 2\gamma xu + 3u^2)}, \tag{4.83}$$

$$\frac{du}{dN} = \frac{2u\left(-\gamma^2x^2\varphi_0 + u(2y - 3(\varphi_0 - x)u) + 2\gamma(x - 2\varphi_0 u)\right)}{\varphi_0(2\gamma - 2\gamma xu + 3u^2)}\,. \tag{4.84}$$

For the following critical solution [158]

$$x = x_0 = \frac{\varphi_0}{h}\,, \qquad y = y_0 = \frac{V_1 t_1^2}{h^2}\,, \qquad u = u_0 = \frac{2f_1 h^2}{\varphi_0 t_1^2}\,, \tag{4.85}$$

the right hand sides of the above equations are trivially satisfied, implying that $x' = y' = z' = 0$.

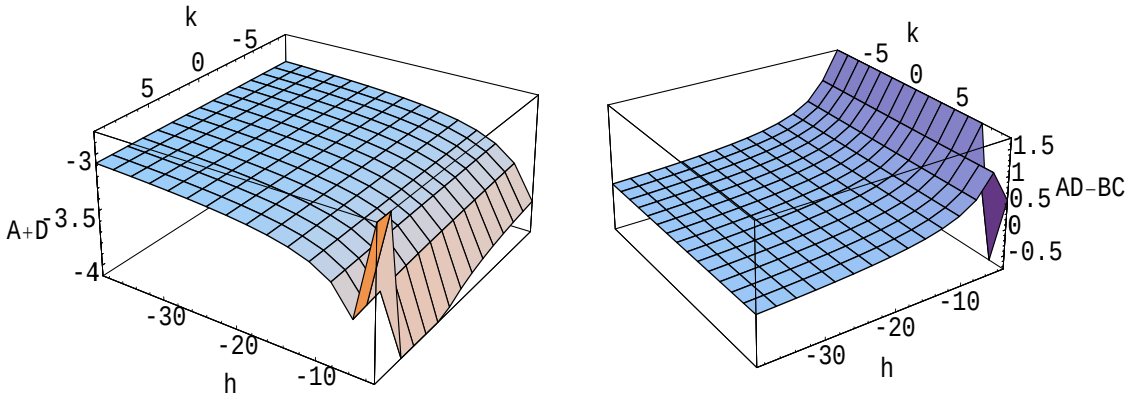

Figure 4.17: *Only for negative eigenvalues, satisfying the conditions $A + D < 0$ and $AD - BC > 0$ the linear perturbations become small and the system may be stable.*

We consider the following homogeneous perturbation around the critical solution (4.81) and (4.82):

$$x = x_0 + \delta x, \qquad u = u_0 + \delta u. \tag{4.86}$$

Since the functional form of the potential is already specified, the variation of y is encoded into the variation of φ. For stability of the solution, under a small perturbation about the critical or fixed-point solution, requires

$$A + D < 0, \qquad AD - BC > 0, \tag{4.87}$$

where A, B, C, D are the eigenvalues of a 2×2 matrix, as given by

$$\frac{d}{dN}\begin{pmatrix} \delta x \\ \delta z \end{pmatrix} = M \begin{pmatrix} \delta x \\ \delta z \end{pmatrix}, \qquad M = \begin{pmatrix} A & B \\ C & D \end{pmatrix}. \tag{4.88}$$

In the following, we define $V_1 t_1^2 \equiv k$. We find

$$A = -\frac{\tilde{A}}{hE}\,, \quad B = -\frac{\tilde{B}}{\gamma E}\,, \quad C = -\frac{\gamma\,\tilde{C}}{3h^2(3h^2 - 3h - 2k)E}\,, \quad D = -\frac{\tilde{D}}{hE} \tag{4.89}$$

where

$$\tilde{A} \equiv 18h^4(h-1)(9h^2-4h+1)+3k(1-24h)h^2+k^2(132h^3-22h^2-7h+1), \tag{4.90}$$

$$\tilde{B} \equiv 3(3h^2-3h-2k)\left(6h^2(3h^2-2h+1)-k(22h^2-13h+1)\right), \tag{4.91}$$

$$\tilde{C} \equiv \left(36h^5(3h^2-1)-2kh^2(72h^3+42h^2-12h(3h+2)+6)+2k^2(28h^2-12h+1)\right) \times(9h^3-3h^2-6hk+k), \tag{4.92}$$

$$\tilde{D} = 36h^4(3h-1)(h-1)^2+2k^2(24h^3-68h^2+17h-1)-4kh^2(36h^3-93h^2+51h-6). \tag{4.93}$$

$$E = 18h^4(5h^2-4h+1)+k^2(60h^2-16h+1)-6kh^2(25h^2+17h-2). \tag{4.94}$$

We find the result in Nojiri *et al.* [132] by taking $k=0$ [10]. In the case $\gamma>0$ and $h<0$, all eigenvalues are negative, except when $|h|$ is small, $|h|\lesssim 2$, or when the parameter k takes a large value, c.f., figure 4.17. In the case $\gamma<0$, two of the coeffiecents, B and C, take positive values, leading to a classical instability of the critical solution. Such a system is normally unstable also under inhomogeneous cosmological perturbations. In particular, for a large and positive potential, so that $k\gg 0$, only the $h>0$ solution can be stable.

4.7 Remarks on Ghost Conditions

Recently, a number of authors [151, 170][11] discussed constraints on the field-dependent Gauss-Bonnet couplings with a single scalar field, so as to avoid the short-scale instabilities or superluminal propagation of scalar and tensor modes [12]. These conditions

[10] The results here also correct errors/typos that appeared in the appendix of Nojiri *et al.* [132].

[11] The case studied by De Felice *et al.* [170] has only limited applications within our model, as the kinetic term for φ is dropped, and also a rather atypical coupling $f(\varphi)\propto\varphi^n$, with $n<0$, is considered.

[12] If the existence of a superluminal propagation is seen only as a transient effect, then the model is phenomenologically viable. However, a violation of causality or null energy condition should not be seen as an effect of higher curvature couplings, at least, for late time cosmology. Such corrections to Einstein's theory are normally suppressed as compared to the Ricci-scalar term, as well as the scalar potential, at late times. For a realistic cosmology the quantity $f(\varphi)H^2$ should be a monotonically decreasing function of the number of e-folds, N, since $f(\varphi)R^2_{GB}\propto f(\varphi)H^4$ and $V(\varphi)\propto H^2(\varphi)$.

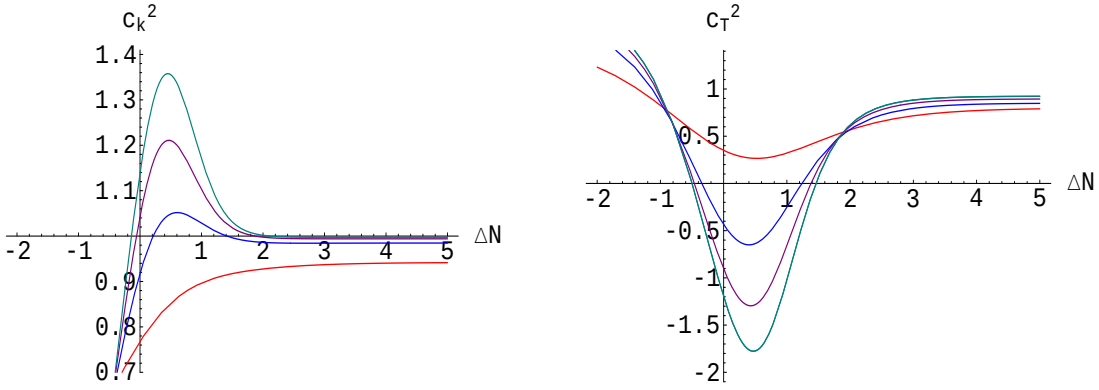

Figure 4.18: *The speeds of propagation for scalar and tensor modes, corresponding to the solution (4.21) with* $\sqrt{\gamma}\varphi_0 = 3, 4, 5$ *and* 6 *from top to bottom (bottom to top) for the left (right) panel.*

are

$$0 < c_{\mathcal{R}}^2 \leq 1, \quad 0 < c_T^2 \leq 1, \quad 1 - \mu > 0. \tag{4.95}$$

As long as $\mu < 1$ and $\mu'/\mu < \epsilon$, we also find $c_{\mathcal{R}}^2 < 1$ and $c_T^2 < 1$. The short-scale instabilities observed in Calcagni *et al.* [151] corresponding to the value $\mu \sim 1$, or equivalently $\nu' - 2\epsilon\nu \sim 1$, may not be physical as the condition $\mu \sim 1$ effectively invalidates the assumptions of linear perturbation theory [159, 152]. Furthermore, in the limit $|\mu| \to 1$, other higher order curvature corrections, like cubic terms in the Riemann tensor, may be relevant. Hence, the Gauss-Bonnet modification of Einstein's theory alone is possibly not sufficient for describing cosmology in the regime $\Omega_{GB} \to \Omega_{\rm total}$. For the consistency of the model under cosmological perturbations, the condition $|\mu| = |\Omega_{GB}| < 2/3$ must hold, in general [159, 163].

Let us first neglect the contribution of matter fields and consider the special solution given in Leith and Neupane [158],

$$x = \varphi_0 - \alpha\,\varphi_0 \tanh\alpha(N + N_1), \quad u = -\tfrac{\gamma x}{3}, \quad \epsilon = \tfrac{2\gamma x^2\varphi_0 - 2x(6+\gamma x^2)}{\varphi_0(6+\gamma x^2)}, \tag{4.96}$$

obtained with a simple exponential potential. From figure (4.18) we see that both $c_{\mathcal{R}}^2$ and c_T^2 temporarily exceed unity, because of which cosmological perturbations may exhibit a superluminal scalar or tensor mode. However, this behaviour can be significantly different in the presence of matter, especially, if φ is allowed to couple non-minimally to matter fields.

The propagation speeds normally depend on the spatial intrinsic curvature of the universe rather than on a specific realization of the background evolution during the stage of quantum generation of scalar and tensor modes (gravity waves). Thus a plausible explanation for the existence of super-luminal scalar or tensor modes ($c^2_{\mathcal{R}} > 1$ or $c^2_T > 1$) is that at the initial phase of inflation the spatial curvature K is non-negligible, while the interpretation of c^2_T (and $c^2_{\mathcal{R}}$) as the propagation speed is valid only for $K = 0$. Additionally, in the presence of matter, the above result for $c^2_{\mathcal{R}}$ does not quite hold since the scalar modes are naturally coupled to the matter sector. The result for c^2_T may be applicable as tensor modes are generally not coupled to matter fields.

From figures (4.19) and (4.20) we can see that, for ansätze such as (4.60), $c^2_{\mathcal{R}}$ and c^2_T may become negative, though temporarily, if one allows a larger slope for the scalar-GB coupling, namely $\alpha \gg \beta$. It is precisely this last case for which $c^2_{\mathcal{R}}$ and c^2_T may also take values larger than unity at subsequent stages, leading to superluminal propagation speeds for scalar and/or tensor modes. [For discussions on a similar theme see references [144, 171].] The case where $c^2_T > 1$ normally corresponds to the epoch where the contribution of the coupled Gauss-Bonnet term becomes significant. However, for smaller values of α and β, satisfying $\alpha \lesssim \beta$, both $c^2_{\mathcal{R}}$ and c^2_T never become negative and there do not arise any ghost-like states. However, depending upon the initial conditions the tensors modes may become superluminal, temporarily.

4.8 Discussion

We have analysed the cosmological solutions of systems which allow nontrivial couplings between the scalar field φ and the matter and gravitational fields. The cosmological viability of such a generalized theory of scalar-tensor gravity is fully investigated by placing minimal constraints on the model parameters and the scalar-matter couplings.

Some astrophysical and cosmological constraints applicable to a general scalar-tensor gravity models are discussed. Under the assumptions that the quantity $\varphi' = \dot{\varphi}/H$ and the time-derivative of the scalar-GB coupling decrease during inflation, where they are given by exponential functions of $N \equiv \ln[a(t)]$, namely $\dot{\varphi}/H \propto e^{\alpha_1 N}$ and $\dot{f}H \propto$

$e^{\alpha_2 N}$, the reconstructed scalar potential was shown to take the form $V(\varphi) = H^2(\varphi)(C_0 + C_1\,\varphi^2 + C_2\,e^{\alpha_2/\alpha_1})$. Such a potential, being proportional to the square of the Hubble parameter, would naturally relax its value as the Universe expands and might have useful implications for inflation in the early Universe. With the approximation $\varphi' \approx$ const, $V(\varphi)$ was shown to take the form $V(\varphi) = H^2(\varphi)\left(V_0 + V_1\,e^{\beta\varphi}\right)$, for which the effective equation of state approaches -1 without exhibiting any pathological features at late times.

In the case were no matter or radiation contribution is considered we show that, while not specifying the form of the potential, with an ansatz for the Gauss-Bonnet coupling it is possible to find inflating solutions. These can be separated into two special cases, $\Omega_{GB} =$ const and $u =$ const. Both show attractor behaviour, the first being dependent on the value of Ω_{GB} while the latter is the cosmological constant solution. Neither of these solutions appear to offer a natural exit from the inflationary period, although for some values of Ω_{GB} we have non-inflating solutions throughout. Addition of matter fields may help resolve such an issue.

We consider the theory in the presence of non-minimally coupled matter fields for a number of scenarios. When a constant Ω_{GB} is considered, the form of the potential does not need to be specified. This allows us to examine whether realistic late-time cosmologies exist without constraining the potential. Although we can find behaviour which includes periods of radiation, matter and scalar field domination, the periods of radiation and matter domination are too brief to be considered realistic.

Taking ansätze for both the form of the potential and Gauss-Bonnet coupling allows us to find more realistic models of the late-time behaviour. We consider a number of conditions on the current apparent structure of the Universe in order to examine the validity of the model. The agreement, while not perfect, for string theory motivated slopes of the potential, is encouraging. The effects of the scalar coupling to matter are also examined. The coupling to dust is found to be negligible when considered in the range $Q_d^2 < 10^{-5}$. We do, however, find that the coupling to stiff, relativistic matter, which is otherwise unconstrained, starts to cause what would generally be considered unphysical effects for $Q_s \gtrsim \mathcal{O}(1)$.

When considering the canonical potential in place of the exponential potential in

section 4.5.4 the behaviour is shown to have reasonable agreement with observation. It is also without, it appears, the problem presented in the exponential potential case, viz., having periods, during significance of the Gauss-Bonnet term in the late-time evolution, which force the solution momentarily to values where $w_{\text{eff}} < -1$. The issues relating to such cosmologies are presented in section 2.3.1.

The solutions above can also be generalised to a second scalar field. This is an obvious extension, as one would expect multiple scalar fields to be relevant on cosmological scales if string theory is the underlying theory. These solutions show further freedom and benefit from assisted quintessence allowing a greater range of values of the slope of the potential while still providing the mechanism for accelerating solutions.

The solutions above can be shown to be linearly stable under certain conditions. We also include a short discussion and analysis of the ghost conditions with respect to analysis of the scalar and tensor modes. Superluminal modes are shown to become relevant when a significant Gauss-Bonnet contribution exists. This constrains the slopes the coupling to the Gauss-Bonnet term take as no late-time evidence exists of such behaviour.

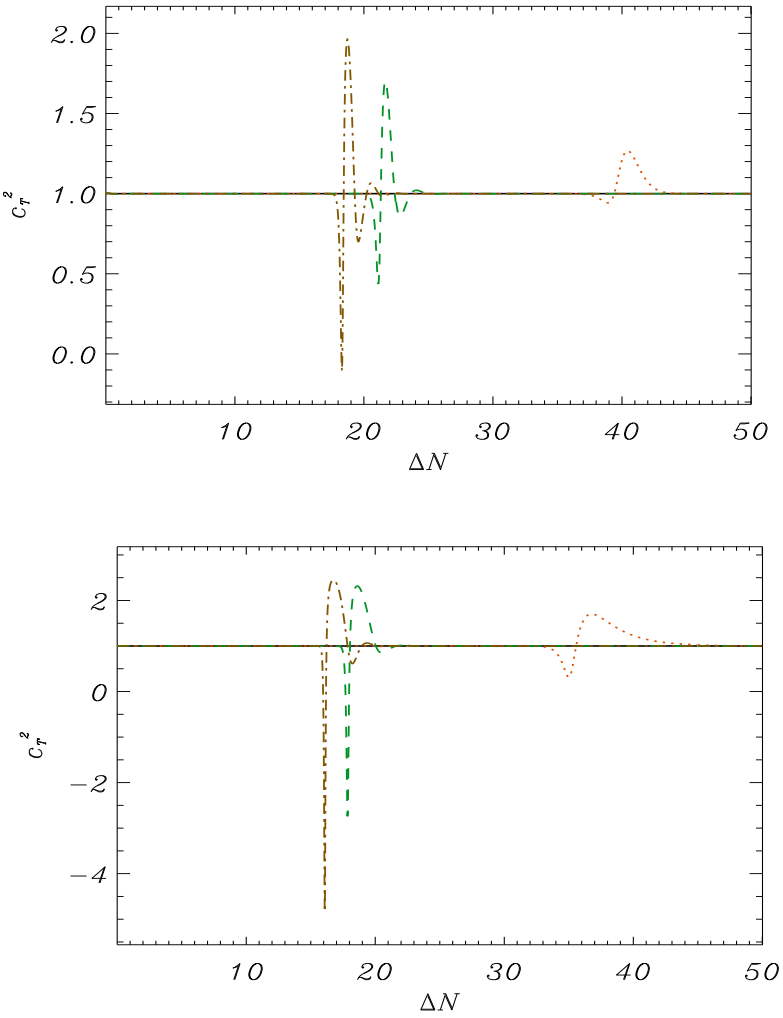

Figure 4.19: *The variation of* c_T^2 *with* ΔN*; (top panel)* $\beta = \sqrt{2/3}$ *and* $\alpha = 12\,(\text{dash}-\text{dot}),\ 8\,(\text{dashes}),\ 3\,(\text{dots}),\ \sqrt{2/3}\,(\text{solid})$*; (bottom panel)* $\beta = \sqrt{3}$ *and* $\alpha = 12\,(\text{dash}-\text{dot}),\ 8\,(\text{dashes}),\ 3\,(\text{dots}),\ \sqrt{2/3}\,(\text{solid})$*. Other parameters are chosen as* $\gamma = 1$*,* $Q_d^2 = 10^{-5}$ *and* $Q_s^2 = 0.01$*, with initial conditions* $x = \sqrt{6} \times 10^{-4}$*,* $y = 5 \times 10^{-20}$*,* $u = 0.08$*,* $\Omega_r = 0.549$ *and* $\Omega_s = 0.45$*.*

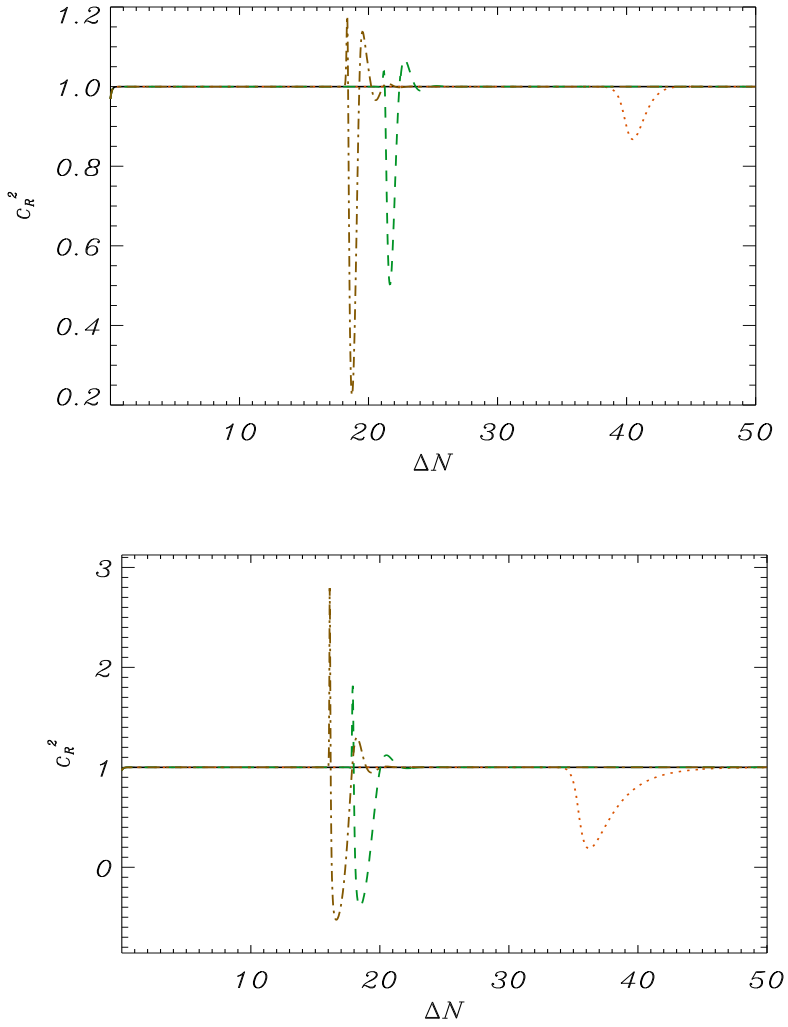

Figure 4.20: *The variation of* $c^2_{\mathcal{R}}$ *with* ΔN*; (top panel)* $\beta = \sqrt{2/3}$ *and* $\alpha = 12\,(\text{dash}-\text{dot}),\ 8\,(\text{dashes}),\ 3\,(\text{dots}),\ \sqrt{2/3}\,(\text{solid})$*; (bottom panel)* $\beta = \sqrt{3}$ *and* $\alpha = 12\,(\text{dash}-\text{dot}),\ 8\,(\text{dashes}),\ 3\,(\text{dots}),\ \sqrt{2/3}\,(\text{solid})$*, for* $\gamma = 1$*,* $Q_d^2 = 10^{-5}$ *and* $Q_s^2 = 0.01$ *with initial conditions* $x = \sqrt{6} \times 10^{-4}$*,* $y = 5 \times 10^{-20}$*,* $u = 0.08$*,* $\Omega_r = 0.549$ *and* $\Omega_s = 0.45$*.*

Chapter 5

Type Ia Supernovae analysis

5.1 Introduction

The Fractal Bubble (FB) model, presented in section 1.2.5, was recently put forward by Wiltshire [37]. This model sidesteps the conundrums outlined in section 4.1. Firstly, there is no cosmological constant, so the cosmological constant problem becomes "why is the cosmological constant exactly zero?". This question is not directly answered in Wiltshire's scheme. However, the other question of why apparent cosmic acceleration begins at the epoch when complex structures form is answered. Apparent cosmic acceleration is largely a consequence of clock rate variance between bound systems and the volume average. Since positive gravitational energy is largely associated with the negative spatial curvature of voids, the gradient becomes large at the epoch when complex structures form and voids begin to dominate. Apparent cosmic acceleration begins at a redshift of $z \simeq 0.9$.

To check the model's physicial validity, comparison to a number of cosmological observations is required. The obvious analysis to be carry out initially is a statistical test on the type Ia Supernovae (SneIa) observations [51]. This gives a quantitative measure of the fit of the model to the observed late-time evolution of the Universe. It is of particular interest in testing the well–known observation of apparent cosmological acceleration in the new paradigm. In the context of the Fractal Bubble model, this is interpreted as an apparent effect due to differences in quasi-local gravitational energy

gradients. We analyse this model both without the back–reaction, in a earlier, more naive form of the model, and then also in the case where the full Buchert equations, (1.32), with back–reaction, are considered. We also fit the spatially flat ΛCDM model without initial priors on H_0. The two models are then compared using Bayesian statistics [172].

The fit of the model to two other observations is also examined, the baryon acoustic oscillation scale (BAO) and the angular scale of the sound horizon at last scattering. These observations have already been discussed in section 1.3. The tests of the fit to these three observations are independent methods of verification of the model.

A number of concerns have arisen in the analysis of SneIa in relation to FLRW cosmologies. The Riess07 SneIa data at redshifts less than 0.023 has been excluded in recent analyses [51] due to the so called "Hubble bubble" [39, 40, 41]. This data was included in the Riess04 gold data set [15]. As indicated in section 1.2.5, the Fractal Bubble model may give a natural resolution to the apparently anomalous variance in the Hubble constant in this region, due to the inhomogeneous void and wall structure on scales less than the scale of apparent homogeneity. We can therefore justify excluding the Hubble bubble data on physical grounds. In the ΛCDM model, there is no clear theoretical rationale for this; it is merely observed empirically that a significant difference in the inferred Hubble constant occurs at the Hubble bubble scale [40].

Another quantity which directly effects the BAO and angular scale tests is the baryon–to–photon ratio, $\eta_{B\gamma}$. The observed abundances of the light elements, deuterium, helium-3, helium-4 and lithium, put strong constraints on the value of the baryon-to-photon ratio with the current understanding of Big Bang nucleosynthesis (BBN). Previously these have been compared solely within the FLRW paradigm. Regardless of model assumptions, there appears to be an intrinsic tension in the data between lithium and deuterium abundance measurements [173].

Prior to the the detailed measurements of the Doppler peaks in the CMBR, the values quoted for $\eta_{B\gamma}$ tended to be somewhat lower than the WMAP best–fit value. For example, Olive, Steigman and Walker [174] quoted two possible ranges at the 95% confidence level: $\eta_{B\gamma} = 1.2\text{–}2.8 \times 10^{-10}$ or $\eta_{B\gamma} = 4.2\text{–}6.3 \times 10^{-10}$, depending on

whether one accepted higher or lower values of the primordial D/H abundance. At a similar time, Tytler *et al.* [175], accepting the lower D/H abundances, quoted a range $\eta_{B\gamma} = 4.6\text{–}5.6 \times 10^{-10}$ at the 95% confidence level. The WMAP parameter estimates moved the best–fit range of the baryon to photon ratio to $\eta_{B\gamma} = 6.1^{+0.3}_{-0.2} \times 10^{-10}$ [6, 7] at the very edge [174], or beyond [175], the earlier 95% confidence limits. This is not concordant with lithium abundance and pushed agreement with helium-4 abundances to the previous 2σ confidence limit.

In Wiltshire's approach [37], the baryon fraction inferred from the baryon–to–photon ratio changes since the value of $\eta_{B\gamma}$ predicted by standard analysis is the volume–average quantity. Volume–averaged values of the bare baryon density parameter, $\bar{\Omega}_{B0}$, consistent with a lower $\eta_{B\gamma}$ at the volume–average, give a higher conventional dressed Ω_{B0} as measured by wall observers. We use the range of Tytler *et al.* [175], which sets the baryon-photon ratio in the range $\eta_{B\gamma} = 4.6\text{–}5.6\times10^{-10}$ to 95% confidence level.

There are a number of other observational anomalies that may be resolved by further analysis of the Fractal Bubble model, they are not of direct relevance here but are outlined by Wiltshire [37].

5.2 Analysis

5.2.1 ΛCDM model

In order to present a comparison to our own results we calculate the fit of the ΛCDM model to the Riess07 data set. First we require definitions of the observed quantities. We use the standard definition of the redshift z,

$$1 + z \equiv \frac{\lambda_{\rm observed}}{\lambda_{\rm emitted}} \ , \tag{5.1}$$

and distance modulus, μ,

$$\mu \equiv m - M = 5\log_{10}(d_{_L}) + 25\,. \tag{5.2}$$

where m is the apparent magnitude and M is the absolute magnitude, and d_L is the luminosity distance in units of Mpc. For the flat ΛCDM model it is given by

$$d_L = \frac{c(1+z)}{H_0} \int_0^z \frac{dz'}{\sqrt{(1+z')^2(1+\Omega_{m0}z') - (z')^2(2+z')\Omega_{\Lambda 0}}}\,, \tag{5.3}$$

where $\Omega_{\Lambda 0}$ is the fractional energy denisity of the cosmological constant with $\Omega_{\Lambda 0} = 1 - \Omega_{m0}$ in the approximation that $\Omega_{radiation} \ll 1$. We also define $\Delta\mu = m_{\rm model} - m_{\rm empty}$, where $m_{\rm empty}$ is the apparent magnitude for the $\Omega_m = 0$, $\Lambda = 0$ universe with the same Hubble constant. The $\Omega_m = 0$, $\Lambda = 0$ universe is known as the Milne Universe.

We find a best-fit of $\chi^2 = 158.75$ for $H_0 = 62.59$ km/sec/Mpc and $\Omega_m = 0.342$ for the 182 data points of the Riess07 "gold data set". The confidence levels for 1σ, 2σ and 3σ are shown in figure 5.1.

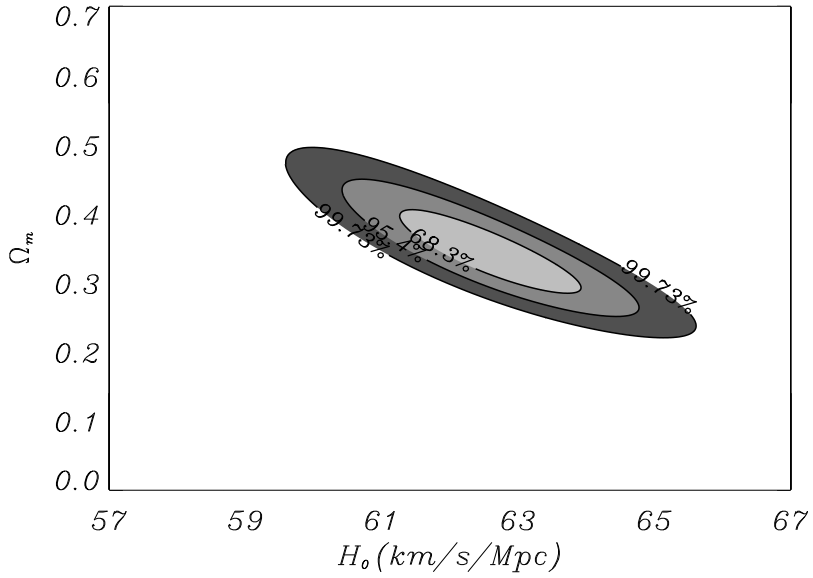

Figure 5.1: *1σ, 2σ and 3σ confidence limits (oval contours) for fits of luminosity distances of type Ia supernovae (SneIa) in the Riess07 gold data set [51] for the ΛCDM model*

These values are not those quoted by Riess *et al.* [51] as they have made prior assumptions of the value of H_0, generally treating it as a *nuisance parameter* and not explicitly stating the value. Different values appear to be used for different tests. It appears that since 2005 Riess *et al.* favour values of the Hubble constant near the WMAP value, $H_0 = 70.4^{+1.5}_{-1.6}$ km sec^{-1}. Mpc^{-1}. In particular, in reference [176] Riess *et al.* chose a different Cepheid calibration, which involves a systematic subtraction

of 0.32 mag from all the distance moduli in their data set. This re-calibration has been disputed by the Hubble Key team of Sandage *et al.* [177], although more recently support has come from van Leeuwen *et al.* [178]. Sandage *et al.* [177] determine a value of the Hubble parameter, $H_0 = 62.3 \pm 1.3$ (random) ± 5.0 (systematic), which differs from the values which best-fit the WMAP data within the FLRW model, given in section 1.1, to 14%. Sandage *et al.* attempt to make as model–independent an estimate as possible. We find good agreement with the Sandage *et al.* value here.

From the perspective of the Fractal Bubble model of Wiltshire [37], we should expect an intrinsic variance in the Hubble parameter below the scale of apparent homogeneity, and on average larger values of H_0 within the Hubble bubble. Thus the above disputes between astronomers would appear perhaps to partly involve questions of the scale of averaging, as well as systematic issues relating to calibration of Cepheids. We will adopt the Cepheid calibration of Sandage *et al.* on account of the fact it is a natural choice theoretically in the Fractal Bubble model.

A recent paper by Li and Schwarz [179], which considers back–reaction in Buchert's scheme, gives observational evidence consistent with Wiltshire's proposal [37]. In particular the average Hubble parameter has a maximum at the scale of the dominant void fraction, $30h^{-1}\text{Mpc} \simeq 45\text{Mpc}$, measured by Hoyle and Vogeley [19], which then decreases until the scale of homogeneity is reached. Fig. 5.2 from [179] shows this graphically.

5.2.2 Fractal Bubble model with no back–reaction

Two years prior to releasing the details of the present Fractal Bubble model [37], Wiltshire first introduced a crude approximation [36] in which the wall regions were assumed to evolve in a Einstein–de Sitter fashion, and the volume–average geometry as an open FLRW model. In this approximation, one is able to compare clock rates using the same assumptions discussed in section 1.2.5. However, as there is no back–reaction term it turns out that wall observers see no apparent acceleration.

While the approximation of [36] is merely a toy model, it is interesting to compare it to data. One can then understand to what extent back–reaction effects contribute,

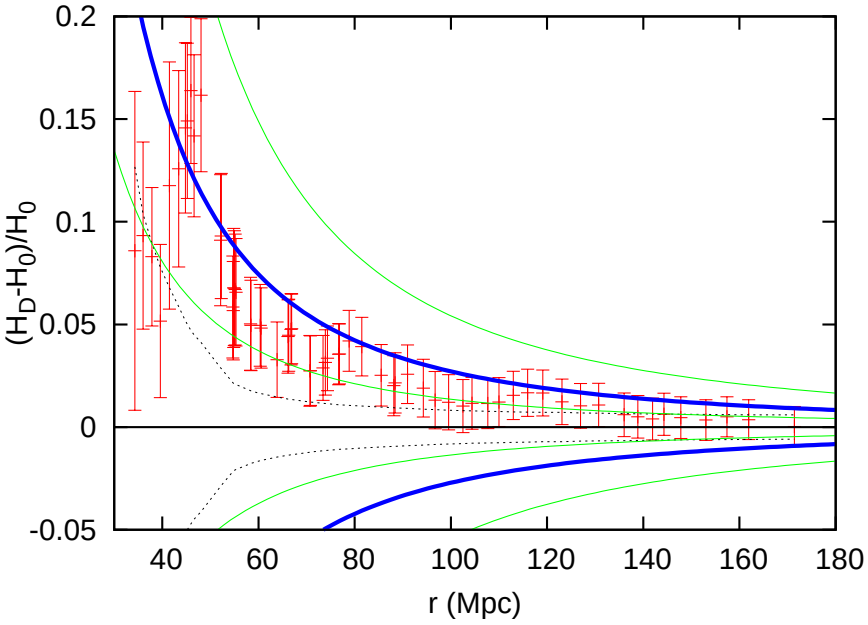

Figure 5.2: *The scale dependence of the normalized difference between the averaged Hubble rate H_D and its "global" value H_0. Data is from Freedman* et al. *[180]. Although Freedman et al. use a calibration of $H_0 = 72$ km/s/Mpc, since the fractional Hubble variance is shown the plot would be identical if Sandage et al.'s value for H_0 was adopted. The dashed lines are the expected statistical noise for a perfectly homogeneous and isotropic model. The solid lines show the expected values between which data should be randomly scattered assuming Buchert averaging and no clock rate variance.*

and to what extent clock–rate variance contributes to the observable quantities.

We consider the case of no back–reaction, i.e, $Q = 0$ in (1.21) – (1.23), against the Riess07 gold data set, originally presented in Carter *et al.* [181] for the Riess04 gold data set. Such a case, therefore, only takes into account of the differences in identification of the various cosmological parameters of interest which arise from clock rate variance and the subsequent dressing of parameters.

Within the no back–reaction approximation of [36], the observed quantities can be found in closed form. The luminosity distance for the cosmological model is [36]

$$d_{_L} = \frac{c(1+z)(2+\widetilde{\Omega}_0^2)}{H_0\widetilde{\Omega}_0(2+\widetilde{\Omega}_0)}\left[2\cosh\eta - \frac{2-\widetilde{\Omega}_0}{\sqrt{1-\widetilde{\Omega}_0}}\sinh\eta\right], \tag{5.4}$$

where H_0 is the currently measured global average value of the Hubble constant, $\widetilde{\Omega}_0$ is the equivalent of the bare density parameter, simply the density parameter of the

open FLRW universe. It is related to the current dressed matter density parameter, Ω_m, according to

$$\widetilde{\Omega}_0 = \frac{6}{\sqrt{\Omega_m}} \sin\left[\frac{\pi}{6} - \frac{1}{3}\cos^{-1}\sqrt{\Omega_m}\right] - 2\,, \tag{5.5}$$

and η is given by

$$\cosh\eta = -\frac{1}{2} + \frac{(1-\widetilde{\Omega}_0)(2+\widetilde{\Omega}_0) + \sqrt{\widetilde{\Omega}_0 z[9\widetilde{\Omega}_0 z - 2\widetilde{\Omega}_0^2 + 16\widetilde{\Omega}_0 + 4] + (\widetilde{\Omega}_0^2+2)^2}}{2\widetilde{\Omega}_0(z+1)}\,. \tag{5.6}$$

We find this gives a statistically favourable fit, for the 182 data points of the Riess07 "gold data set" we find a best-fit $\chi^2 = 172.58$ at $H_0 = 60.28$ km/sec/Mpc and $\Omega_m = 0.407$. This represents a best-fit (χ^2/degrees of freedom) < 1. The confidence levels for 1σ, 2σ and 3σ are shown in figure 5.3.

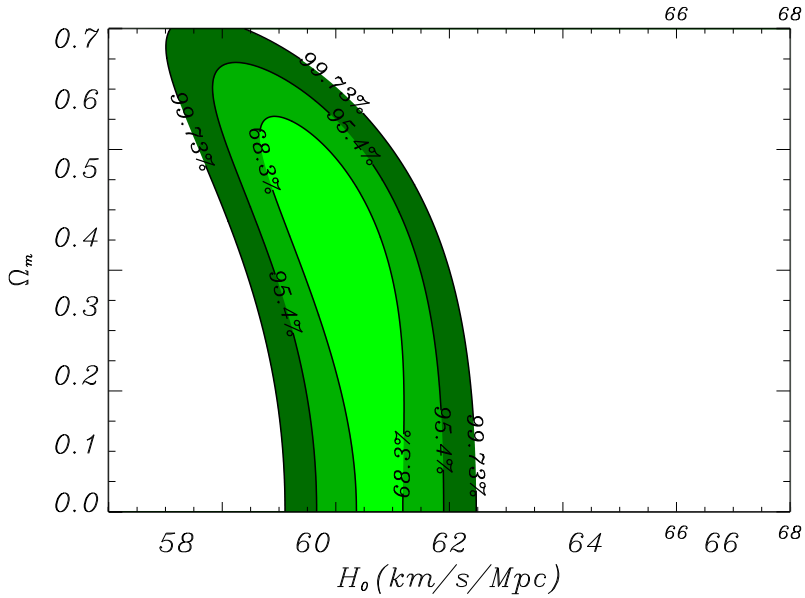

Figure 5.3: *1σ, 2σ and 3σ confidence limits (oval contours) for fits of luminosity distances of type Ia supernovae (SneIa) in the Riess07 gold data set [51] for the FB model.*

5.2.3 Fractal Bubble model with back–reaction

We now consider the full theory of Wiltshire [37]. As already mentioned, the back–reaction term can give apparent acceleration. This would be expected to allow a better fit than the no back–reaction case as the observational data seems to support some

acceleration, apparent or otherwise. The situation is somewhat more complex and hence, so are the definitions of the cosmological parameters. We use the exact solution given by Wiltshire [38],

$$(1-f_{\rm v})^{1/3}\,\bar{a} = {f_{\rm wi}}^{1/3} a_{\rm w} = \bar{a}_0\left[(1-\epsilon_i)\,\bar{\Omega}_{M0}\right]^{1/3}\left(\tfrac{3}{2}\bar{H}_0 t\right)^{2/3}, \tag{5.7}$$

$$\sqrt{u(u+C_\epsilon)} - C_\epsilon \ln\left(\sqrt{\left|\frac{u}{C_\epsilon}\right|} + \sqrt{\left|1+\frac{u}{C_\epsilon}\right|}\right) = \frac{\bar{\Omega}_{k0}^{1/2}}{{f_{\rm v0}}^{1/6}}\bar{H}_0\,(t+t_\epsilon)\,, \tag{5.8}$$

where $u \equiv {f_{\rm v}}^{1/3}\bar{a}/\bar{a}_0 = {f_{\rm vi}}^{1/3} a_{\rm v}/\bar{a}_0$, $C_\epsilon \equiv \epsilon_i \bar{\Omega}_{M0} {f_{\rm v0}}^{1/3}/\bar{\Omega}_{k0}$, $f_{\rm wi} = 1 - f_{\rm vi}$, and ϵ_i is a small integration constant appearing in the integral constraint

$$\Omega_{M{\rm w}} \equiv \frac{(1-\epsilon_i)\,\bar{\gamma}^2\bar{\Omega}_M}{1-f_{\rm v}} = 1, \tag{5.9}$$

which relates the bare matter density parameter, $\bar{\Omega}_M(t)$, to the void fraction, $f_{\rm v}(t)$, and mean lapse function, $\bar{\gamma}(t)$, at all times. The value of ϵ_i,

$$\epsilon_i = 1 - \frac{1-f_{\rm vi}}{\bar{\gamma}_i^2\,\bar{\Omega}_i}. \tag{5.10}$$

is determined by initial values of the void fraction, $f_{\rm vi}$, bare matter density, $\bar{\Omega}_i$, and mean lapse function $\bar{\gamma}_i$, at the time of last scattering. These are such that $f_{\rm vi} \ll 1$, $1-\bar{\Omega}_i \ll 1$ and $\bar{\gamma}_i - 1 \ll 1$. The parameters $\bar{\Omega}_{k0}$ and t_ϵ are related to the other parameters by the relations

$$\sqrt{(1-\epsilon_i)\bar{\Omega}_{M0}(1-f_{\rm v0})} + \sqrt{(\bar{\Omega}_{k0}+\bar{\Omega}_{M0}\epsilon_i)f_{\rm v0}} = 1\,. \tag{5.11}$$

and

$$\frac{\bar{\Omega}_{k0}^{3/2}}{{f_{\rm v0}}^{1/2}}\bar{H}_0(\tau_0+t_\epsilon) = \sqrt{\bar{\Omega}_{k0}(\bar{\Omega}_{k0}+\bar{\Omega}_{M0}\epsilon_i)} - \bar{\Omega}_{M0}\epsilon_i \ln\left[\sqrt{\left|\frac{\bar{\Omega}_{k0}}{\bar{\Omega}_{M0}\epsilon_i}\right|} + \sqrt{\left|1+\frac{\bar{\Omega}_{k0}}{\bar{\Omega}_{M0}\epsilon_i}\right|}\right], \tag{5.12}$$

where the age of the universe in volume–average time is

$$t_0 = \frac{2}{3\bar{H}_0}\sqrt{\frac{1-f_{\rm v0}}{(1-\epsilon_i)\bar{\Omega}_{M0}}}\,,$$

on account of (5.7).

The expansion age in terms of wall time, τ, relevant to observers in bound systems, is given by performing the integral $\tau = \int_0^t {\rm d}t'\bar{\gamma}(t')$, where the mean lapse function is given by

$$\bar{\gamma} = 1 - f_{\rm v} + f_{\rm v} h_r^{-1}. \tag{5.13}$$

Here $f_{\rm v}(t)$ is defined implicitly by (5.7) and (5.8) and

$$h_r(t) \equiv \frac{H_{\rm w}}{H_{\rm v}} = \sqrt{\frac{(1-\epsilon_i)\bar{\Omega}_{M0}{f_{\rm v0}}^{1/3} f_{\rm v}}{\left(\bar{\Omega}_{k0}u + \bar{\Omega}_{M0}{f_{\rm v0}}^{1/3}\epsilon_i\right)(1-f_{\rm v})}}\,. \tag{5.14}$$

Observers in bound systems measure a cosmological redshift, z, given by

$$z+1 = \frac{\bar{a}_0\bar{\gamma}}{\bar{a}\bar{\gamma}_0} \tag{5.15}$$

and a luminosity distance

$$d_{_L} = \frac{\bar{a}_0}{\bar{\gamma}_0}(1+z)r_{\rm w}, \tag{5.16}$$

where

$$r_{\rm w} = \bar{\gamma}\,(1-f_{\rm v})^{1/3}\int_t^{t_0}\frac{{\rm d}t'}{\bar{\gamma}(t')(1-f_{\rm v}(t'))^{1/3}\bar{a}(t')}\,, \tag{5.17}$$

One can define a conventional angular diameter distance $D_{_A} = d_{_L}/(1+z)^2$.

Of the four independent parameters $\{\bar{H}_0, \epsilon_i, \bar{\Omega}_{M0}, f_{\rm v0}\}$, two can be eliminated through the choice of physically realistic priors at the surface of the last scattering, which for bound system observers occurs at a redshift $z_i \simeq 1100$. In particular we choose $1 - h_{ri} \ll 1$ so that the initial velocity dispersion of underdense void perturbations is small relative the dominant "wall" regions which average to critical density. We also require that $f_{\rm vi} \ll 1$ to the extent that the overall density contrast of our present past horizon volume $\mathcal{H}$ at that epoch is

$$\left(\frac{\delta\rho}{\rho}\right)_{\mathcal{H}\rm i} = f_{vi}\left(\frac{\delta\rho}{\rho}\right)_{\rm vi} \sim -10^{-6}\,\text{to}\,-10^{-5},$$

once a realistic value for the underdense density contrast of the void regions is specified, based on expectations from the variance in cold dark matter density perturbations consistent with the CMB at last scattering. At last scattering both photons and baryons have perturbations of order $\delta\rho/\rho \sim 10^{-5}$. However, cold dark matter perturbations which are largely responsible for the temperature fluctuations at last scattering, via the dominant Sachs–Wolfe effect, can have $\delta\rho/\rho \sim 10^{-3}$ typically. In practice, the existence of a tracker solution, found in reference [38], means that the properties of cosmological solutions are insensitive to variations of h_{ri} and $f_{\rm vi}$ within the range of physically realistic priors. Our plots in figures 5.4 and 5.5 use $h_{ri} = 0.99999$ and $f_{\rm vi} = 10^{-4}$.

Once we specify h_{ri} and $f_{\rm vi}$, then by (5.13), $\bar{\gamma}_i = 1 - f_{\rm vi} + f_{\rm vi} h_{ri}^{-1}$, while Ω_i is fixed in terms of ϵ_i by (5.10). The integral constraint (5.9), combined with (5.15) gives

$$1 - f_{\rm v0} = \frac{(1-\epsilon_i)\bar{\Omega}_{M0}\bar{\gamma}_i^2 {f_{\rm vi}}^{2/3}\bar{\Omega}_{k0}^2}{(1+z_i)^2 {f_{\rm v0}}^{2/3} A_i^2} \tag{5.18}$$

where $z_i \simeq 1100$, and

$$A_i \equiv \frac{{f_{\rm vi}}^{1/3}\bar{\Omega}_{k0}\bar{a}_i}{{f_{\rm v0}}^{1/3}\bar{a}_0} = \bar{\Omega}_{M0}\left[\frac{f_{\rm vi}(1-\epsilon_i)}{(1-f_{\rm vi})h_{ri}^2} - \epsilon_i\right],$$

where we have used (5.14) to express $\bar{a}_0/\bar{a}_i$ in terms of h_{ri} and other parameters in the last step. We evaluate both (5.7) and (5.8) at the present epoch τ_0 and at the time of last scattering, t_i, and compare them at each epoch to eliminate τ_0 and t_i. We then further eliminate t_ϵ from the two resulting expressions to also obtain

$$\begin{aligned}
&\sqrt{A_i(A_i + \bar{\Omega}_{M0}\epsilon_i)} - \bar{\Omega}_{M0}\epsilon_i \ln\left(\sqrt{\frac{A_i}{\bar{\Omega}_{M0}|\epsilon_i|}} + \sqrt{\left|1 + \frac{A_i}{\bar{\Omega}_{M0}\epsilon_i}\right|}\right) - \frac{2}{3}\sqrt{\frac{(1-f_{\rm vi})A_i^3}{f_{\rm v0}(1-\epsilon_i)f_{\rm vi}\bar{\Omega}_{M0}}} \\
&= \sqrt{\bar{\Omega}_{k0}(\bar{\Omega}_{k0} + \bar{\Omega}_{M0}\epsilon_i)} - \bar{\Omega}_{M0}\epsilon_i \ln\left(\sqrt{\frac{\bar{\Omega}_{k0}}{\bar{\Omega}_{M0}|\epsilon_i|}} + \sqrt{\left|1 + \frac{\bar{\Omega}_{k0}}{\bar{\Omega}_{M0}\epsilon_i}\right|}\right) - \frac{2}{3}\sqrt{\frac{(1-f_{\rm v0})\bar{\Omega}_{k0}^3}{f_{\rm v0}(1-\epsilon_i)f_{\rm vi}\bar{\Omega}_{M0}}}
\end{aligned} \tag{5.19}$$

For fixed z_i, $f_{\rm vi}$ and h_{ri} then combination of (5.11), (5.18) and (5.19) determines two of the remaining parameters $\{\bar{H}_0, \epsilon_i, \bar{\Omega}_{M0}, f_{\rm v0}\}$. It makes most sense to take these to be the bare Hubble constant $\bar{H}_0$ and the present epoch void fraction $f_{\rm v0}$. However, the dressed Hubble constant and conventional dressed density parameter are those which compare most directly to parameters we are familiar with, and are therefore used in figures 5.4 and 5.5. On account of the existence of the tracker solution,

$$H_0 \simeq \frac{4{f_{\rm v0}}^2 + f_{\rm v0} + 4)\bar{H}_0}{2(2 + f_{\rm v0})}$$

and

$$\Omega_{M0} = \bar{\gamma}_0^3\bar{\Omega}_{M0} \simeq \tfrac{1}{2}(1 - f_{\rm v0})(2 + f_{\rm v0}).$$

From [37] we also have the proper distance to the comoving scale of the sound horizon,

$$\bar{D}_s = \frac{\bar{a}(t)}{\bar{a}_0}\frac{c}{\sqrt{3}\,\bar{H}_0}\int_0^{\bar{x}_{\rm dec}} \frac{{\rm d}\bar{x}}{\sqrt{(1 + 0.75\,\bar{\Omega}_{B0}\bar{x}/\bar{\Omega}_{\gamma 0})(\bar{\Omega}_{M0}\bar{x} + \bar{\Omega}_{R0})}}\,, \tag{5.20}$$

where $\bar{x} = \bar{a}/\bar{a}_0$, so that $\bar{x}_{\rm dec} = \bar{\gamma}_0^{-1}(1+z_{\rm dec})^{-1}$, with $z_{\rm dec}$ being the redshift of decoupling. The fractional densities $\bar{\Omega}_B$, $\bar{\Omega}_\gamma$ and $\bar{\Omega}_R$ are the bare parameters for baryons, photons and radiation respectively. At the present epoch observation indicates $\bar{\Omega}_{R0}, \bar{\Omega}_{\gamma 0} \ll 1$.

From (5.16) and (5.17) we have the angular diameter of the sound horizon at decoupling

$$d_{A\,\rm dec} = \frac{\bar{a}_0 r_{w\ dec}}{\bar{\gamma}_0(1+z_{\rm dec})} = \bar{a}_{\rm dec} r_{w\ dec}. \tag{5.21}$$

This, along with (5.20), allows us to calculate the observed angular scale, $\delta_s = \bar{D}_s/d_{A\,\rm dec}$. Evolving (5.21) forward to the present epoch gives the expected value of the BAO scale.

For the Riess07 "gold data set" [51] of SneIa we find that for 182 data points and two degrees of freedom the best–fit $\chi^2 = 162.7$, i.e., a χ^2 of approximately 0.9 per degree of freedom, which is a good fit. While a marginally lower $\chi^2 = 158.7$ is obtained for the best–fit flat ΛCDM model the difference is not significant. Indeed, on statistical grounds a χ^2 of about 1.0 per degree of freedom is to be expected. We have followed the procedures adopted by Riess *et al.* [51] as closely as possible, and conclude that the FB model fits the Riess07 data to a degree which is statistically indistinguishable from the spatially flat ΛCDM model.

This is supported by a Bayesian model comparison of the FB model against a flat ΛCDM model with flat priors $55 \leq H_0 \leq 75\,\mathrm{km\ sec^{-1}\,Mpc^{-1}}$ and $0.01 \leq \Omega_{M0} \leq 0.5$. This gives a Bayes factor of 1.3 in favour of the FB model, a margin which is "not worth more than a bare mention" [172] or "inconclusive" [182].

In Fig. 1 we display the residual difference $\Delta\mu = \mu_{\rm FB} - \mu_{\rm empty}$, in the standard distance modulus, $\mu = 5\log_{10}(d_L)+25$, of the best–fit FB model from that of a coasting Milne universe of the same Hubble constant, $H_0 = 61.7\,\mathrm{km\ sec^{-1}\,Mpc^{-1}}$, and compare the theoretical curve with binned data from the Riess07 gold data set. Apparent acceleration occurs for positive residuals in the range, $z \lesssim 0.9$. It should be noted that the exact range of redshifts corresponding to apparent acceleration also depend on the value of the Hubble constant of the Milne universe distance modulus used to compute the residual: for example, if the value of $H_0 = 60.7\,\mathrm{km\ sec^{-1}\,Mpc^{-1}}$ (2σ lower bound) is assumed, then the first data bin residual is entirely negative, whereas if the value $H_0 = 62.8\,\mathrm{km\ sec^{-1}\,Mpc^{-1}}$ (2σ upper bound) is assumed, then the same first data bin

residual straddles the $\Delta\mu = 0$ axis. To take this into account, in figure 5.4 we show the Riess07 "gold data set" binned and displayed for the two 2σ values including errors, $H_0 = 60.7\,\mathrm{km\ sec^{-1}\,Mpc^{-1}}$ and $H_0 = 62.8\,\mathrm{km\ sec^{-1}\,Mpc^{-1}}$, as whiskers and coloured bars where it overlaps the best–fit values. The black box indicates the binned data with errors for the best–fit value, $H_0 = 61.7\,\mathrm{km\ sec^{-1}\,Mpc^{-1}}$. The blue bars indicate an overlap between the lower 2σ limit, $H_0 = 60.7\,\mathrm{km\ sec^{-1}\,Mpc^{-1}}$ (green) and the upper 2σ limit, $H_0 = 62.8\,\mathrm{km\ sec^{-1}\,Mpc^{-1}}$ (red).

A general feature of the FB model is that the magnitude of the gradient of the theoretical residual of Fig. 1 versus redshift is less than that for comparable ΛCDM models. This reflects the fact that the distance modulus approaches that of a Milne universe at late times, regardless of the observer, and "acceleration" is an apparent effect which relates to clock–rate variance between bubble walls and the volume–average in voids. A volume–average observer in fact detects no apparent acceleration, and determines a volume–average deceleration parameter for which $\bar{q} \to 0^+$ at late times. For a wall observer the effective dressed deceleration parameter obeys $q \to 0^-$ at late times.

It is worth noting the effect of the back–reaction. For the best–fit value, one can see from figure 5.4 that the back–reaction causes apparent acceleration for observers in bound systems. While this does not occur when back–reaction is ignored the effects appear relatively minor regarding the statistical fit of χ^2. The case including back–reaction, however, appears more physically relevant and does show a slightly better fit to the data. The observational data supporting acceleration is also fairly strong, indicating a model with cosmic acceleration, apparent or real, has more physical relevance.

Statistical confidence limits for the SneIa data are displayed as the oval contours in the centre of Fig. 2, in the (H_0, Ω_{M0}) parameter space. The dressed density parameter is used here, since it is the one whose numerical value is likely to be closest to that of a FLRW model, and is thus most familiar. Since the tracker solution approximation [38] is very reliable at late epochs, Ω_{M0} is related to the present void volume fraction by $\Omega_{M0} \simeq \frac{1}{2}(1-f_{\mathrm{v}0})(2+f_{\mathrm{v}0})$, and to the bare density parameter by $\Omega_{M0} = \frac{1}{8}(2+f_{\mathrm{v}0})^3\Omega_{M0}$.

In Fig. 2 we also overplot parameter ranges for which two independent cosmological tests have been applied. The first test is the effective angular diameter of the sound

horizon, which very closely correlates with the angular scale of the first Doppler peak in the CMB anisotropy spectrum. It is often stated that the angular position of the first peak is a measure of the spatial curvature of the universe. However, this deduction relies on the assumption that the spatial curvature is the same everywhere, appropriate for the FLRW models. In the present model there are spatial curvature gradients, and the calculation must be revisited from first principles. Volume–average negative spatial curvature, which is actually consistent with other tests on the CMB that involve geodesic mixing [183, 184], can nonetheless be consistent with our local observation of the angular scale of the first peak [37].

Ideally we should recompute the spectrum of Doppler peaks for the FB model. However, this requires considerable effort, as the standard numerical codes have been written solely for FLRW models, and every step has to be carefully reconsidered. This task is left for future work. The test that we apply here is to ask whether parameters exist for which the effective angular diameter scale of the sound horizon matches the angular scale of the sound horizon, $\delta = 0.01$ rad, of the ΛCDM model, as determined by WMAP [6]. Since there is no change to the physics of recombination, but just an overall change to the *calibration* of cosmological parameters, this is entirely reasonable.

In Fig. 2 we plot parameter ranges which match the $\delta = 0.01$ rad sound horizon scale to within 2%, 4% and 6%. These limits have been arrived at assuming a *volume–average* baryon–to–photon ratio in the range $\eta_{B\gamma} = 4.6\text{–}5.6 \times 10^{-10}$ adopted by Tytler *et al.* [175] prior to the release of WMAP1. The 2% contour would roughly correspond to the 2σ limit if the WMAP uncertainties for the ΛCDM model are maintained. This is reasonable as the physics at recombination is identical for the two models. This can only be confirmed by detailed computation of the Doppler peaks, therefore the additional levels have been chosen cautiously. With this range it is possible to achieve concordance with lithium abundances, while also better fitting helium abundances. In the FB calibration, on account of the difference between the bare and dressed density parameters, a bare value of $\bar{\Omega}_B \simeq 0.03$ nonetheless corresponds to a dressed value $\Omega_B \simeq 0.08$, and an overall ratio of baryonic matter to non–baryonic dark matter of about 1:3, which is larger than in the ΛCDM model. This would indicate sufficient baryon drag to accommodate the ratio of the first two peak heights which has proved

problematic for the ΛCDM model. While this suggestion can only be confirmed by the detailed recomputation of the Doppler peaks in the FB model, on the basis of well–established underlying physics, we expect concordance is highly likely.

The final set of contours plotted in Fig. 2 relate to the independent test of the effective comoving scale of the baryon acoustic oscillation (BAO), as detected in galaxy clustering statistics [1]. Similarly to the case of the angular scale of the sound horizon, given that we do not have the resources to analyse the galaxy clustering data directly, we begin here with a simple but effective check. In particular, since the dressed geometry (1.35) does provide an effective almost–FLRW metric adapted to our clocks and rods in spatially flat regions, the effective comoving scale in this dressed geometry should match the corresponding scale of $104h^{-1}$Mpc seen in galaxy clustering [1]. We therefore plot parameter values which match this scale to within 2%, 4% or 6%.

The best–fit cosmological parameters, using SneIa only, are $H_0 = 61.7^{+1.2}_{-1.1}\,\mathrm{km\ sec^{-1}\,Mpc^{-1}}$ and $f_{\mathrm{v}0} = 0.76^{+0.12}_{-0.09}$, with 1σ uncertainties. The values of the mean lapse function, bare density parameter, conventional dressed density parameter, mass ratio of non–baryonic dark matter to baryonic matter, bare Hubble parameter, effective dressed deceleration parameter and age of the universe measured in a galaxy are respectively: $\bar{\gamma}_0 = 1.381^{+0.061}_{-0.046}$; $\bar{\Omega}_{M0} = 0.125^{+0.060}_{-0.069}$; $\Omega_{M0} = 0.33^{+0.11}_{-0.16}$; $(\bar{\Omega}_{M0} - \bar{\Omega}_{B0})/\bar{\Omega}_{B0} = 3.1^{+2.5}_{-2.4}$; $\bar{H}_0 = 48.2^{+2.0}_{-2.4}\,\mathrm{km\ sec^{-1}\,Mpc^{-1}}$; $q = -0.0428^{+0.0120}_{-0.0002}$; $\tau_0 = 14.7^{+0.7}_{-0.5}$ Gyr. Statistical uncertainties from the sound horizon and BAO tests cannot yet be given, but should significantly reduce the bounds on $f_{\mathrm{v}0}$, Ω_{M0} etc.

One striking feature of Fig. 2 is that even if the SneIa contours are disregarded, then the parameters which fit the two independent tests relating to the sound horizon and the BAO scale agree with each other to the accuracy shown for values of the Hubble constant which include the value of Sandage *et al.* However, they do *not* agree for the values of H_0 greater than $70\,\mathrm{km\ sec^{-1}\,Mpc^{-1}}$ which best–fit the WMAP data [6, 7] with the FLRW model.

The value of the Hubble constant quoted by Sandage *et al.* [177] has been controversial, given the 14% difference from values which best–fit the WMAP data with the ΛCDM model [6, 7]. However, the WMAP analysis only constitutes a direct measurement of CMB temperature anisotropies; the determination of cosmological

parameters involves model assumptions. We have removed the assumptions of the FLRW model, in an attempt to model the universe in terms of the distribution of galaxies that we actually observe, with an alternative proposal to averaging consistent with general relativity. Applied to the angular diameter of the sound horizon and the BAO scale this leads to different cosmological parameters: ones that concord with our SneIa analysis, and also the independent measurement of Sandage *et al.* [177].

5.3 Discussion

Both cases of the Fractal Bubble model analysed here fit the SneIa data very well. While the ΛCDM model has a slightly lower best–fit χ^2 value to the SneIa, the Bayesian analysis shows that the fit to Riess06 gold data set is indistinguishable statistically between the two models.

Our value of the Hubble constant corroborates the value of Sandage *et al.* This is a significant result given that it had been widely thought that values of the Hubble constant derived from the WMAP date did not accord with Sandage's value. However, our results show that the very same scales for the angular scale of the sound horizon and the baryon oscillation, which are key to the WMAP analysis, lead to different results once the model dependent assumptions of the FLRW model are removed. Naturally a detailed analysis of the Doppler peaks in the Fractal Bubble model still needs to be performed.

A systematic present epoch variation of 38% in clock rates between bound systems and the volume average is found for the Fractal Bubble model with back–reaction best–fit to the SneIa. This seems a large value, given our familiarity of large gravitational time dilation effects occurring only for extreme density contrasts, such as with black holes. However, in cosmology we are dealing with a circumstance in which intuition based on static Newtonian potentials may fail, because spacetime itself is dynamical and the definition of gravitational energy is extremely subtle. The normalization of clock rates in bound systems relative to expanding regions can accumulate significant differences, given that almost the entire age of the universe has been available for this to occur.

The Fractal Bubble model with back–reaction gives a best–fit void fraction of $f_{v0} = 0.76^{+0.06}_{-0.05}$. The observed universe at the present epoch displays an inhomogeneous structure on scales of less than 100–300 Mpc [1, 2]. Some 40–50% of the volume [19] of the universe at the present epoch is in voids of order $30h^{-1}$Mpc in diameter, h being the dimensionless Hubble parameter, $H_0 = 100h\,\mathrm{km\ sec^{-1}\,Mpc^{-1}}$. If larger [185] and smaller [186] voids are taken into account, the present universe can be said to be "void–dominated". The exact fraction, of order 70–90% perhaps, depends on how voids are defined. This is in good agreement with the value of f_{v0} found for the best–fit values[1].

The combination of best–fit cosmological parameters that arises is particularly interesting. The present void volume fraction, f_{v0}, is identical to the value claimed for the dark–energy density fraction, $\Omega_{\Lambda 0}$, in the ΛCDM model with WMAP [7]. If the FB model is closer to the correct description of the actual universe, then in trying to fit a FLRW model, we appear to be led to parameters in which the cosmological constant is mimicking the effect of voids as far as the WMAP normalization to FLRW models is concerned. This it does imperfectly, since for a flat ΛCDM model $\Omega_{M0} = 1 - \Omega_{\Lambda 0}$, with the result that the best–fit value of Ω_{M0} normalized to the CMB does not match the best–fit value of Ω_{M0} for SneIa with the FLRW model, nor for other tests which directly probe Ω_{M0}. In particular, it has been recently noted that the values of the normalization of the primordial spectrum $\sigma_8 \sim 0.76$ and matter content $\Omega_{M0} \sim 0.24$ implied by WMAP3 are barely compatible with the abundances of massive clusters determined from X–ray measurements [187]. For the FB model, by contrast, the best–fit dressed density parameter, $\Omega_{M0} = 0.33^{+0.06}_{-0.08}$, does match the range preferred in direct estimations of the conventional matter density parameter.

The age of the FB universe for observers in galaxies is one billion years more than the concordance ΛCDM model. The expansion age at large redshifts is increased by a greater relative fraction, allowing somewhat more time for structure formation, as would be consistent with the observations of old structures at large redshifts [188, 189]. Naturally much work remains to be done. The first tasks include the detailed computation of the CMB Doppler peaks; the calculation of the integrated Sachs–Wolfe

[1] In the Fractal Bubble model the void fraction is technically the fraction of the volume that is not inside finite infinity regions; which may be somewhat difficult to measure independently.

effect; and detailed tests to check whether the suggested resolution [37] of the ellipticity anomaly [183, 184] agrees quantitatively with what is observed.

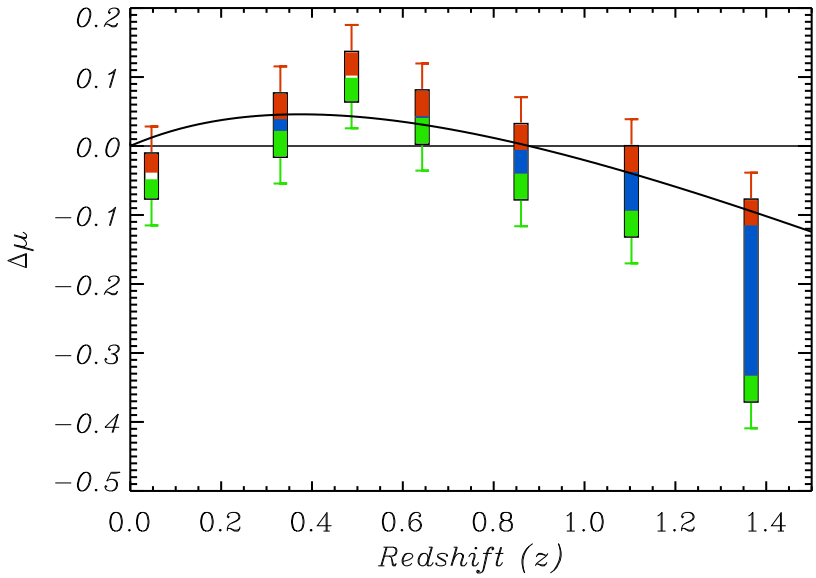

Figure 5.4: *The difference in the distance modulus, $\mu = 5\log_{10}(d_L) + 25$, with d_L in units Mpc, of the FB model with $H_0 = 61.7\,km\ sec^{-1}\,Mpc^{-1}$, $\Omega_{M0} = 0.326$ from that of an empty coasting Milne universe, with the same value of the Hubble constant. The Riess07 "gold data" [51] set of 182 SneIa is binned using the criterion $n_i\Delta z_i = 5.8$, where n is the number of data points, and Δz_i the width, of the ith bin. The first bin boundary is set at $z = 0.023$ as "Hubble bubble" points with $z \leq 0.023$ are excluded in Riess07 data set. Our bins are very slightly different to those used in Fig. 6 of Riess* et al. *[51]: in particular, with our choice the single outlier point at $z = 1.755$, falls in its own bin. This point which falls below the theoretical curve is not shown here, but is included in the χ^2 analysis. We use the original distance moduli of the Riess07 Gold data set reported at http://braeburn.pha.jhu.edu/∼ariess/R06/sn_sample, without the suggested systematic subtraction [176] of 0.32 mag, as we follow the Cepheid calibration of Sandage* et al. *[177]. The boxes show the standard statistical errors for the binned data using the reported uncertainties[51], which already accounts for luminosity corrections in the MLCS2K2 reduction [40]. The whiskers indicate how the residuals move relative to the horizontal axis for the 2σ limits on H_0 with $\Omega_{M0} = 0.326$ fixed: red corresponds to $H_0 = 62.8\,km\ sec^{-1}\,Mpc^{-1}$ and green to $H_0 = 60.7\,km\ sec^{-1}\,Mpc^{-1}$. The overlap in these two regions has been coloured blue.*

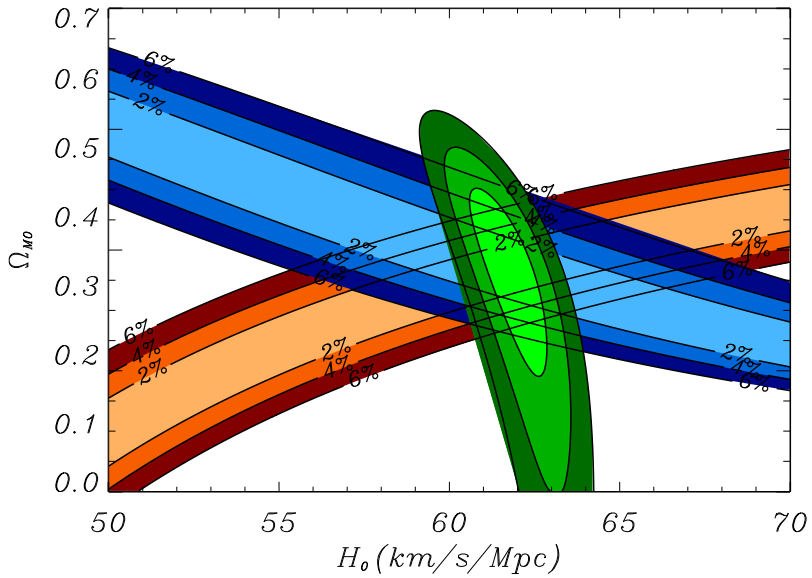

Figure 5.5: *1σ, 2σ and 3σ confidence limits (oval contours) for fits of luminosity distances of type Ia supernovae (SneIa) in the Riess07 gold data set [51] are compared to parameters within the* (Ω_m,H_0) *plane which fit the angular scale of the sound horizon* $\delta = 0.01$ *rad deduced for WMAP [6, 7], to within 2%, 4% and 6% (contours running top–left to bottom–right); and also to parameters which fit the effective comoving baryon acoustic oscillation (BAO) scale of* $104h^{-1}$*Mpc observed in galaxy clustering statistics [1], to within 2%, 4% and 6% (contours running bottom–left to middle–right).*

References

[1] Eisenstein, D.J. *et al.*, *"Detection of the baryon acoustic peak in the large-scale correlation function of SDSS luminous red galaxies"*, Astrophys. J. **633**, 560 (2005) [arXiv:astro-ph/0501171].

[2] M. Tegmark *et al.*, *"Cosmological Constraints from the SDSS Luminous Red Galaxies,"* Phys. Rev. D **74**, 123507 (2006) [arXiv:astro-ph/0608632];
W. J. Percival *et al.*, *"Measuring the matter density using baryon oscillations in the SDSS,"* Astrophys. J. **657**, 51 (2007) [arXiv:astro-ph/0608635]; *"The shape of the SDSS DR5 galaxy power spectrum,"* Astrophys. J. **657**, 645 (2007) [arXiv:astro-ph/0608636].

[3] S. Weinberg, *Gravitation and Cosmology: Principles and Applications of the General Theroy of Relativity*, John Wiley & Sons (1972).

[4] S. M. Carroll, *"Spacetime and Geometry: An Introduction to general relativity"*, San Francisco: Benjamin Cummings, 2003.

[5] http://lambda.gsfc.nasa.gov/product/map/current/params/lcdm_wmap.cfm

[6] C. L. Bennett *et al.* [WMAP Collaboration], *"First Year Wilkinson Microwave Anisotropy Probe (WMAP) Observations: Preliminary Maps and Basic Results,"* Astrophys. J. Suppl. **148**, 1 (2003) [arXiv:astro-ph/0302207].

[7] D. N. Spergel *et al.*, *"Wilkinson Microwave Anisotropy Probe (WMAP) three year results: Implications for cosmology,"* Astrophys. J. Suppl. **170**, 288 (2007) [astro-ph/0603449].

[8] S. Cole *et al.* [The 2dFGRS Collaboration], *"The 2dF Galaxy Redshift Survey: Power-spectrum analysis of the final dataset and cosmological implications,"* Mon. Not. Roy. Astron. Soc. **362**, 505 (2005) [arXiv:astro-ph/0501174].

[9] T. E. Montroy *et al.*, *"A Measurement of the CMB Spectrum from the 2003 Flight of BOOMERANG,"* Astrophys. J. **647**, 813 (2006) [arXiv:astro-ph/0507514].

[10] C. l. Kuo *et al.* [ACBAR collaboration], *"High Resolution Observations of the CMB Power Spectrum with ACBAR,"* Astrophys. J. **600**, 32 (2004) [arXiv:astro-ph/0212289].

[11] A. C. S. Readhead *et al.*, *"Extended Mosaic Observations with the Cosmic Background Imager,"* Astrophys. J. **609**, 498 (2004) [arXiv:astro-ph/0402359].

[12] C. Dickinson *et al.*, *"High sensitivity measurements of the CMB power spectrum with the extended Very Small Array,"* Mon. Not. Roy. Astron. Soc. **353**, 732 (2004) [arXiv:astro-ph/0402498].

[13] M. Tegmark *et al.* [SDSS Collaboration], *"The 3D power spectrum of galaxies from the SDSS,"* Astrophys. J. **606**, 702 (2004) [arXiv:astro-ph/0310725].

[14] P. Astier *et al.* [The SNLS Collaboration], *"The Supernova Legacy Survey: Measurement of Ω_M, $\Omega_L A$ and w from the First Year Data Set,"* Astron. Astrophys. **447**, 31 (2006) [arXiv:astro-ph/0510447].

[15] A. G. Riess *et al.* [Supernova Search Team Collaboration], *"Type Ia Supernova Discoveries at z¿1 From the Hubble Space Telescope: Evidence for Past Deceleration and Constraints on Dark Energy Evolution,"* Astrophys. J. **607**, 665 (2004) [arXiv:astro-ph/0402512].

[16] http://lambda.gsfc.nasa.gov/product/map/current/params/lcdm_all.cfm

[17] Andrzej Krasiński, *"Inhomogeneous Cosmological Models",* Cambridge University Press (1997).

[18] H. J. Rood, *"Voids,"* Ann. Rev. Astron. Astrophys. **26**, 245 (1988).
S. G. Patiri, J. Betancort-Rijo, F. Prada, A. Klypin and S. Gottlober, *"Statistics*

of Voids in the 2dF Galaxy Redshift Survey," Mon. Not. Roy. Astron. Soc. **369**, 335 (2006) [arXiv:astro-ph/0506668].

[19] F. Hoyle and M. S. Vogeley, *"Voids in the Point Source Catalogue Survey and the Updated Zwicky Catalog"*, Astrophys. J. **566** (2002) 641 [arXiv:astro-ph/0109357]; *"Voids in the 2dF Galaxy Redshift Survey,"* Astrophys. J. **607**, 751 (2004) [arXiv:astro-ph/0312533].

[20] J. M. Bardeen, *"Gauge Invariant Cosmological Perturbations,"* Phys. Rev. D **22**, 1882 (1980).

[21] T. Padmanabhan, *"Structure formation in the universe,"* Cambridge University Press (1993).

[22] P. J. E. Peebles, *"Principles of physical cosmology,"* Princeton University Press (1993).

[23] G. Lemaitre, *"The expanding universe,"* Gen. Rel. Grav. **29**, 641 (1997) [Annales Soc. Sci. Brux. Ser. I Sci. Math. Astron. Phys. A **53**, 51 (1933)].
R. C. Tolman, *"Effect of imhomogeneity on cosmological models,"* Proc. Nat. Acad. Sci. **20**, 169 (1934).
H. Bondi, *"Spherically symmetrical models in general relativity,"* Mon. Not. Roy. Astron. Soc. **107**, 410 (1947).

[24] S. Räsänen, *"Backreaction in the Lemaitre-Tolman-Bondi model,"* JCAP **0411**, 010 (2004) [arXiv:gr-qc/0408097].
K. Bolejko, *"Supernovae Ia observations in the Lemaître-Tolman model"* [arXiv:astro-ph/0512103].
R. Mansouri, *"Structured FRW universe leads to acceleration: A non-perturbative approach,"* arXiv:astro-ph/0512605.
R. A. Vanderveld, É. É. Flanagan and I. Wasserman, *"Mimicking Dark Energy with Lemaître-Tolman-Bondi Models: Weak Central Singularities and Critical Points,"* Phys. Rev. D. **74**, 023506 (2006), [arXiv:astro-ph/0602476].

[25] D. Garfinkle, *"Inhomogeneous spacetimes as a dark energy model"*, arXiv:gr-qc/0605088.

[26] P. Szekeres, *"A Class Of Inhomogeneous Cosmological Models,"* Commun. Math. Phys. **41**, 55 (1975).

[27] D. A. Szafron, *"Inhomogeneous cosmologies: New exact solutions and their evolution",* J. Math. Phys. **18**, 1973 (1977).

[28] G. C. McVittie *"The mass-particle in an expanding universe,"* Mon. Not. Roy. Ast. Soc. **93**, 325 (1933)

[29] V. Faraoni and A. Jacques, *"Cosmological expansion and local physics,"* arXiv:0707.1350 [gr-qc].

[30] A. Einstein and E. G. Straus, *"The influence of the expansion of space on the gravitation fields surrounding the individual stars,"* Rev. Mod. Phys. **17**, 120 (1945); *"Corrections and Additional Remarks to our Paper: The Influence of the Expansion of Space on the Gravitation Fields Surrounding the Individual Stars,"* Rev. Mod. Phys. **18**, 148 (1946).

[31] M. H. Partovi and B. Mashhoon, *"Toward Verification Of Large Scale Homogeneity In Cosmology"*, Astrophys. J. **276**, 4 (1984).

L. J. Goicoechea and J. M. Martin-Mirones, *"Magnitude-redshift test: cosmological inhomogeneity effects"*, Astron. & Astrophys. **186**, 22 (1987).

N. Humphreys, R. Maartens and D. Matravers, *"Anisotropic Observations in Universes with Nonlinear Inhomogeneity"*, Astrophys. J. **477**, 47 (1997), [arXiv:astro-ph/9602033].

S. Räsänen, *"Backreaction of linear perturbations and dark energy,"* arXiv:astro-ph/0407317.

S. Räsänen, *"Backreaction and spatial curvature in a dust universe,"* Class. Quant. Grav. **23**, 1823 (2006) [arXiv:astro-ph/0504005].

H. Alnes, M. Amarzguioui and Ø. Grøn, *"An inhomogeneous alternative to dark energy?"*, Phys. Rev. D. **73**, 083519 (2006), [arXiv:astro-ph/0512006].

P. S. Apostolopoulos, N. Brouzakis, N. Tetradis and N. Tzavara, *"Cosmological Acceleration and Gravitational Collapse,"* JCAP **0606**, 009 (2006), [arXiv:astro-ph/0603234].

H. Alnes and M. Amarzguioui, *"CMB anisotropies seen by an off-center observer in a spherically symmetric inhomogeneous universe,"* arXiv:astro-ph/0607334.
S. Räsänen, *"Accelerated expansion from structure formation,"* JCAP **0611**, 003 (2006) [arXiv:astro-ph/0607626].

[32] G. F. R. Ellis and T. Buchert, *"The universe seen at different scales,"* Phys. Lett. A **347**, 38 (2005) [arXiv:gr-qc/0506106].

[33] M-N. Célérier, *"Do we really see a cosmological constant in the supernovae data?"*, Astron. & Astrophys. **353**, 63 (1999), [arXiv:astro-ph/9907206].
H. Iguchi, T. Nakamura and K-i. Nakao, *"Is Dark Energy the Only Solution to the Apparent Acceleration of the Present Universe?"*, Prog. Theor. Phys. **108**, 809 (2002), [arXiv:astro-ph/0112419].
S. Räsänen, *"Dark energy from backreaction,"* JCAP **0402**, 003 (2004) [arXiv:astro-ph/0311257].
K. Enqvist and T. Mattsson, *"The effect of inhomogeneous expansion on the supernova observations,"* arXiv:astro-ph/0609120.

[34] R. M. Zalaletdinov, *"Averaging out the Einstein equations and macroscopic space-time geometry,"* Gen. Rel. Grav. **24**, 1015 (1992).
A. A. Coley, N. Pelavas and R. M. Zalaletdinov, *"Cosmological solutions in macroscopic gravity,"* Phys. Rev. Lett. **95**, 151102 (2005) [arXiv:gr-qc/0504115].

[35] T. Buchert, *"On average properties of inhomogeneous fluids in general relativity. I: Dust cosmologies,"* Gen. Rel. Grav. **32**, 105 (2000) [arXiv:gr-qc/9906015].

[36] D. L. Wiltshire, *"Viable inhomogeneous model universe without dark energy from primordial inflation,"* arXiv:gr-qc/0503099.

[37] D. L. Wiltshire, *"Cosmic clocks, cosmic variance and cosmic averages,"* New J. Phys., in press [arXiv:gr-qc/0702082].

[38] D. L. Wiltshire, *"Exact solution to the averaging problem in cosmology,"*, in preparation.

[39] Tomita, K. A local void and the accelerating universe. Mon. Not. R. Astr. Soc. **326**, 287 (2001).

[40] Jha, S., Riess, A.G. & Kirshner, R.P., *"Improved distances to type Ia supernovae with Multicolor Light Curve Shapes: MLCS2k2,"* Astrophys. J. **659**, 122 (2007) [arXiv:astro-ph/0612666].

[41] Conley, A., Carlberg, R.G., Guy, J., Howell, D.A., Jha, S., Riess, A.G. & Sullivan, M., *"Is there evidence for a Hubble bubble? The nature of SN Ia colors and dust in external galaxies,"* arXiv:astro-ph/0705.0367.

[42] B. E. Schaefer, *"Gamma-Ray Burst Hubble Diagram to z=4.5,"* Astrophys. J. **583**, L67 (2003) [arXiv:astro-ph/0212445];
Z. G. Dai, E. W. Liang and D. Xu, *"Constraining Ω_M and Dark Energy with Gamma-Ray Bursts,"* Astrophys. J. **612**, L101 (2004) [arXiv:astro-ph/0407497];
G. Ghirlanda, G. Ghisellini, D. Lazzati and C. Firmani, *"Gamma Ray Bursts: new rulers to measure the Universe,"* Astrophys. J. **613**, L13 (2004) [arXiv:astro-ph/0408350];
D. Q. Lamb *et al.*, *"A Gamma-Ray Burst Mission to Investigate the Properties of Dark Energy,"* arXiv:astro-ph/0507362.

[43] W. Hillebrandt and J. C. Niemeyer, *"Type Ia Supernova Explosion Models,"* Ann. Rev. Astron. Astrophys. **38**, 191 (2000) [arXiv:astro-ph/0006305].
P. A. Mazzali, F. K. Ropke, S. Benetti and W. Hillebrandt, *"A Common Explosion Mechanism for Type Ia Supernovae,"* Science **315**, 825 (2007) [arXiv:astro-ph/0702351].

[44] B. P. Schmidt *et al.* [Supernova Search Team Collaboration], *"The High-Z Supernova Search: Measuring Cosmic Deceleration and Global Cur vature of the Universe Using Type Ia Supernovae,"* Astrophys. J. **507**, 46 (1998) [arXiv:astro-ph/9805200].

[45] M. M. Phillips, *"The absolute magnitudes of Type IA supernovae,"* Astrophys. J. **413**, L105 (1993).

[46] A. G. Riess, W. H. Press and R. P. Kirshner, *"Using SN-Ia light curve shapes to measure the Hubble constant,"* Astrophys. J. **438**, L17 (1995) [arXiv:astro-ph/9410054]; *"A Precise Distance Indicator: Type Ia Supernova Multicolor Light Curve Shapes,"* Astrophys. J. **473**, 88 (1996) [arXiv:astro-ph/9604143].
M. Hamuy, M. M. Phillips, J. Maza, N. B. Suntzeff, R. A. Schommer and R. Aviles, *"A Hubble diagram of distant type IA supernovae,"* Astron. J. **109**, 1669 (1995); *"The Absolute Luminosities of the Calan/Tololo Type Ia Supernovae,"* Astron. J. **112**, 2391 (1996) [arXiv:astro-ph/9609059].;
S. Perlmutter *et al.* [Supernova Cosmology Project Collaboration], *"Measurements of the Cosmological Parameters Ω and Λ from the First 7 Supernovae at z ¿= 0.35,"* Astrophys. J. **483**, 565 (1997) [arXiv:astro-ph/9608192].

[47] A. G. Riess *et al.* [Supernova Search Team Collaboration], *"Observational Evidence from Supernovae for an Accelerating Universe and a Cosmological Constant,"* Astron. J. **116**, 1009 (1998) [arXiv:astro-ph/9805201].

[48] S. Perlmutter *et al.* [Supernova Cosmology Project Collaboration], *"Measurements of Omega and Lambda from 42 High-Redshift Supernovae,"* Astrophys. J. **517**, 565 (1999) [arXiv:astro-ph/9812133].

[49] J. L. Tonry *et al.* [Supernova Search Team Collaboration], *"Cosmological Results from High-z Supernovae,"* Astrophys. J. **594**, 1 (2003) [arXiv:astro-ph/0305008].
R. A. Knop *et al.* [Supernova Cosmology Project Collaboration], *"New Constraints on Ω_M, Ω_Λ, and w from an Independent Set of Eleven High-Redshift Supernovae Observed with HST,"* Astrophys. J. **598**, 102 (2003) [arXiv:astro-ph/0309368].
B. J. Barris *et al.*, *"23 High Redshift Supernovae from the IfA Deep Survey: Doubling the SN Sample at z¿0.7,"* Astrophys. J. **602**, 571 (2004) [arXiv:astro-ph/0310843].

[50] A. J. Conley *et al.* [Supernova Cosmology Project Collaboration], *"Measurement of Ω_m, Ω_Λ from a blind analysis of Type Ia supernovae with CMAGIC: Using color information to verify the acceleration of the Universe,"* Astrophys. J. **644**, 1 (2006) [arXiv:astro-ph/0602411].

[51] A. G. Riess *et al.*, *"New Hubble Space Telescope Discoveries of Type Ia Supernovae at $z > 1$: Narrowing Constraints on the Early Behavior of Dark Energy,"* Astrophys. J. **659**, 98 (2007) [arXiv:astro-ph/0611572].

[52] C. Cattoen and M. Visser, *"Cosmography: Extracting the Hubble series from the supernova data,"* arXiv:gr-qc/0703122.

[53] A. A. Penzias and R. W. Wilson, *"A Measurement of excess antenna temperature at 4080-Mc/s,"* Astrophys. J. **142**, 419 (1965).

[54] A. McKellar, Publs. Dominion AStrophys. Observatory (Victoria, B. C.), **7**, 251 (1941).

[55] G. Gamow, *"The Origin of Elements and the Separation of Galaxies"*, Physical Review **74**, 505 (1948).
G. Gamow, *"The evolution of the universe"*, Nature **162**, 680 (1948).
R. A. Alpher, H. Bethe and G. Gamow, *"The origin of chemical elements,"* Phys. Rev. **73**, 803 (1948).
R. A. Alpher and R. Herman, *"On the Relative Abundance of the Elements"*, Physical Review **74**, 1577 (1948).
A. G. Doroshkevich and I. D. Novikov, *"Mean Density of Radiation in the Metagalaxy and Certain Problems in Relativistic Cosmolog"* Sov. Phys. Doklady **9**, 111 (1964).
R. H. Dicke, P. J. E. Peebles, P. G. Roll and D. T. Wilkinson, *"Cosmic Black-Body Radiation"*, Astrophysical Journal **142**, 414 (1965).

[56] P. E. Freeman, C. R. Genovese, C. J. Miller, R. C. Nichol and L. Wasserman, *"Examining the Effect of the Map-Making Algorithm on Observed Power Asymmetry in WMAP Data,"* Astrophys. J. **638**, 1 (2006) [arXiv:astro-ph/0510406].

[57] K. Land and J. Magueijo, *"The axis of evil,"* Phys. Rev. Lett. **95**, 071301 (2005) [arXiv:astro-ph/0502237]; *"The Axis of Evil revisited,"* Mon. Not. Roy. Astron. Soc. **378**, 153 (2007) [arXiv:astro-ph/0611518].

[58] Alex B. Nielsen, *"Horizons, Entropy and Information"*, Ph.D Thesis, University of Canterbury (2007)

[59] S. W. Hawking and G. F. R. Ellis, *"The Large Scale Structure of Space-time,"* Cambridge Univesity Press (1973).

[60] J. M. Bardeen, B. Carter and S. W. Hawking, *"The Four laws of black hole mechanics,"* Commun. Math. Phys. **31**, 161 (1973).

[61] K. Schwarzschild, *"Über das Gravitationsfeld eines Massenpunktes nach der Einsteinschen Theorie",* Sitzungsber. Preuss. Akad. Wiss., Phys. Math. Kl., **1** 1916.

[62] R. Arnowitt, S. Deser, C. Misner *"Coordinate Invariance and Energy Expressions in General Relativity,"* Phys. Rev. **122**, 997-1006 (1961); *"Gravitation: an introduction to current research",* Louis Witten ed. (Wiley 1962), chapter 7, 227, [arxiv: gr-qc/0405109]

[63] Bendicit M. N. Carter, *"Higher Dimensional Gravity, Black Holes and Brane Worlds",* Ph.D Thesis, University of Canterbury (2006)

[64] http://www.theory.caltech.edu/people/preskill/new_naked_bet.html

[65] M. Simpson and R. Penrose, *"Internal instability in a Reissner-Nordstrom black hole,"* Int. J. Theor. Phys. **7**, 183 (1973).

[66] R. Maartens, *"Brane-world gravity,"* Living Rev. Rel. **7**, 7 (2004) [arXiv:gr-qc/0312059].

[67] T. Kaluza, Sitzungsber. Preuss. Akad. Wiss., 966-972 (1921).

[68] O. Klein, Z. Phys. (1926) **31** 895-906; Nature **118**, 516 (1926).

[69] N. Hitchin, *"Generalized Calabi-Yau manifolds,"* Quart. J. Math. Oxford Ser. **54**, 281 (2003) [arXiv:math/0209099].

[70] Michio Kaku, *"Quantum Field Theory: A Modern Introduction,"* Oxford University Press (1993).

[71] A. Salam and J. A. Strathdee, *"On Kaluza-Klein Theory,"* Annals Phys. **141**, 316 (1982).

[72] E. W. Kolb and R. Slansky, *"Dimensional Reduction In The Early Universe: Where Have The Massive Particles Gone?,"* Phys. Lett. B **135**, 378 (1984).

[73] G. W. Gibbons and P. J. Ruback, *"Classical Gravitons And Their Stability In Higher Dimensions,"* Phys. Lett. B **171**, 390 (1986).

[74] C. J. Isham, A. Salam and J. A. Strathdee, *"Broken chiral and conformal symmetry in an effective-lagrangian formalism,"* Phys. Rev. D **2**, 685 (1970).

[75] R. D. Peccei, *"QCD, strong CP and axions,"* J. Korean Phys. Soc. **29**, S199 (1996) [arXiv:hep-ph/9606475].

[76] R. D. Peccei and H. R. Quinn, *"Constraints Imposed By CP Conservation In The Presence Of Instantons,"* Phys. Rev. D **16**, 1791 (1977).
R. D. Peccei and H. R. Quinn, *"CP Conservation In The Presence Of Instantons,"* Phys. Rev. Lett. **38**, 1440 (1977).

[77] S. J. Asztalos *et al.*, *"An improved RF cavity search for halo axions,"* Phys. Rev. D **69**, 011101 (2004) [arXiv:astro-ph/0310042].

[78] A. D. Linde, *"A New Inflationary Universe Scenario: A Possible Solution Of The Horizon, Flatness, Homogeneity, Isotropy And Primordial Monopole Problems,"* Phys. Lett. B **108**, 389 (1982).
A. D. Linde, *"Coleman-Weinberg Theory And A New Inflationary Universe Scenario,"* Phys. Lett. B **114**, 431 (1982).
A. D. Linde, *"Temperature Dependence Of Coupling Constants And The Phase Transition In The Coleman-Weinberg Theory,"* Phys. Lett. B **116**, 340 (1982).
A. Albrecht and P. J. Steinhardt, *"Cosmology For Grand Unified Theories With Radiatively Induced Symmetry Breaking,"* Phys. Rev. Lett. **48**, 1220 (1982).

[79] A. D. Linde, *"Inflationary cosmology,"* Phys. Rept. **333**, 575 (2000).

[80] C. Wetterich, *"Cosmology and the Fate of Dilatation Symmetry,"* Nucl. Phys. B **302**, 668 (1988).

[81] B. Ratra and P. J. E. Peebles, *"Cosmological Consequences of a Rolling Homogeneous Scalar Field,"* Phys. Rev. D **37**, 3406 (1988).

P. J. E. Peebles and B. Ratra, *"Cosmology with a Time Variable Cosmological Constant,"* Astrophys. J. **325**, L17 (1988).

[82] R. R. Caldwell, R. Dave and P. J. Steinhardt, *"Cosmological Imprint of an Energy Component with General Equation-of-State,"* Phys. Rev. Lett. **80**, 1582 (1998) [arXiv:astro-ph/9708069].

[83] R. R. Caldwell, *"A Phantom Menace?,"* Phys. Lett. B **545**, 23 (2002) [arXiv:astro-ph/9908168];

[84] S. M. Carroll, M. Hoffman and M. Trodden, *"Can the dark energy equation-of-state parameter w be less than -1?,"* Phys. Rev. D **68**, 023509 (2003) [arXiv:astro-ph/0301273].

[85] F. Hoyle and J. V. Narlikar, Proc. Roy. Soc. Lond. **A273**, 1 (1963); Proc. Roy. Soc. Lond. **278**, 465 (1964); Proc. Roy. Soc. Lond. **282**, 178 (1964).

[86] R. M. Wald, *"General Relativity,"* University of Chicago Press (1984)

[87] G. W. Gibbons, *"Phantom matter and the cosmological constant,"* arXiv:hep-th/0302199.

[88] G. M. Hossain, *"On energy conditions and stability in effective loop quantum cosmology,"* Class. Quant. Grav. **22**, 2653 (2005) [arXiv:gr-qc/0503065].

[89] P. S. Corasaniti, M. Kunz, D. Parkinson, E. J. Copeland and B. A. Bassett, *"The foundations of observing dark energy dynamics with the Wilkinson Microwave Anisotropy Probe,"* Phys. Rev. D **70**, 083006 (2004) [arXiv:astro-ph/0406608].

[90] I. Antoniadis, C. Bachas, J. R. Ellis and D. V. Nanopoulos, *"An Expanding Universe in String Theory,"* Nucl. Phys. B **328**, 117 (1989).
G. Veneziano, *"Scale Factor Duality For Classical And Quantum Strings,"* Phys. Lett. B **265**, 287 (1991).
E. J. Copeland, A. Lahiri and D. Wands, *"Low-energy effective string cosmology,"* Phys. Rev. D **50**, 4868 (1994) [arXiv:hep-th/9406216].
R. Easther, K. i. Maeda and D. Wands, *"Tree-level String Cosmology,"* Phys. Rev. D **53**, 4247 (1996) [arXiv:hep-th/9509074].

R. Easther and K. i. Maeda, *"One-Loop Superstring Cosmology and the Non-Singular Universe,"* Phys. Rev. D **54**, 7252 (1996) [arXiv:hep-th/9605173].

[91] E. S. Fradkin and A. A. Tseytlin, *"Effective Field Theory From Quantized Strings,"* Phys. Lett. B **158**, 316 (1985).
C. G. . Callan, E. J. Martinec, M. J. Perry and D. Friedan, *"Strings In Background Fields,"* Nucl. Phys. B **262**, 593 (1985).

[92] N. Arkani-Hamed, S. Dimopoulos and G. R. Dvali, *"The hierarchy problem and new dimensions at a millimeter,"* Phys. Lett. B **429**, 263 (1998) [arXiv:hep-ph/9803315];
L. Randall and R. Sundrum, *"A large mass hierarchy from a small extra dimension,"* Phys. Rev. Lett. **83**, 3370 (1999) [arXiv:hep-ph/9905221];
L. Randall and R. Sundrum, *"An alternative to compactification,"* Phys. Rev. Lett. **83**, 4690 (1999) [arXiv:hep-th/9906064].

[93] H. Leutwyler, Arch. Sci. **13**, 549 (1960).

[94] J. D. Bekenstein, *"Nonexistence of baryon number for static black holes,"* Phys. Rev. D **5**, 1239 (1972); *"Nonexistence of baryon number for black holes. ii,"* Phys. Rev. D **5**, 2403 (1972).

[95] J. E. Chase, Comm. Math. Phys. **19**, 276 (1970); J. D. Bekenstein, *"Exact Solutions Of Einstein Conformal Scalar Equations,"* Annals Phys. **82**, 535 (1974); *"Black Holes With Scalar Charge,"* Annals Phys. **91**, 75 (1975).

[96] G. W. Gibbons and K. i. Maeda, *"Black Holes And Membranes In Higher Dimensional Theories With Dilaton Fields",* Nucl. Phys. B **298**, 741 (1988).

[97] P. C. W. Davies, *"Thermodynamics Of Black Holes,"* Proc. Roy. Soc. Lond. A **353**, 499 (1977).

[98] F. S. Accetta and M. Gleiser, *"Thermodynamics Of Higher Dimensional Black Holes,"* Annals Phys. **176**, 278 (1987).

[99] N. H. Barth and S. M. Christensen, *"Quantizing Fourth Order Gravity Theories. 1. The Functional Integral,"* Phys. Rev. D **28**, 1876 (1983).

[100] D. Lovelock, *"The Einstein tensor and its generalizations,"* J. Math. Phys. **12**, 498 (1971).

[101] B. Zwiebach, *"Curvature Squared Terms And String Theories,"* Phys. Lett. B **156**, 315 (1985).

[102] P. Jordan, *"The present state of Dirac's cosmological hypothesis,"* Z. Phys. **157**, 112 (1959).

[103] C. Brans and R. H. Dicke, *"Mach's principle and a relativistic theory of gravitation,"* Phys. Rev. **124**, 925 (1961).
R. H. Dicke, *"Mach's principle and invariance under transformation of units,"* Phys. Rev. **125**, 2163 (1962).

[104] D. Sudarsky and T. Zannias, *"Spherical black holes cannot support scalar hair,"* Phys. Rev. D **58**, 087502 (1998) [arXiv:gr-qc/9712083].

[105] S. R. Coleman, J. Preskill and F. Wilczek, *"Growing hair on black holes,"* Phys. Rev. Lett. **67**, 1975 (1991); *"Quantum hair on black holes,"* Nucl. Phys. B **378**, 175 (1992) [arXiv:hep-th/9201059]; A. D. Shapere, S. Trivedi and F. Wilczek, *"Dual dilaton dyons,"* Mod. Phys. Lett. A **6**, 2677 (1991).

[106] S. Mignemi and D. L. Wiltshire, *"Stability of multiscalar black holes,"* Phys. Rev. D **70**, 124012 (2004) [arXiv:hep-th/0408215].

[107] S. Mignemi and N. R. Stewart, *"Charged black holes in effective string theory,"* Phys. Rev. D **47**, 5259 (1993) [arXiv:hep-th/9212146].

[108] C. M. Chen, D. V. Gal'tsov and D. G. Orlov, *"Extremal black holes in $D = 4$ Gauss-Bonnet gravity,"* Phys. Rev. D **75**, 084030 (2007) [arXiv:hep-th/0701004].

[109] O. Bechmann and O. Lechtenfeld, *"Exact black hole solution with selfinteracting scalar field,"* Class. Quant. Grav. **12**, 1473 (1995) [arXiv:gr-qc/9502011].

[110] H. Dennhardt and O. Lechtenfeld, *"Scalar deformations of Schwarzschild holes and their stability,"* Int. J. Mod. Phys. A **13**, 741 (1998) [arXiv:gr-qc/9612062].

[111] K. A. Bronnikov and G. N. Shikin, *"Spherically symmetric scalar vacuum: No-go theorems, black holes and solitons,"* Grav. Cosmol. **8**, 107 (2002) [arXiv:gr-qc/0109027].

[112] U. Nucamendi and M. Salgado, *"Scalar hairy black holes and solitons in asymptotically flat spacetimes,"* Phys. Rev. D **68**, 044026 (2003) [arXiv:gr-qc/0301062].

[113] M. Heusler, S. Droz and N. Straumann, *"Linear stability of Einstein Skyrme black holes,"* Phys. Lett. B **285**, 21 (1992).

[114] P. Dobiasch and D. Maison, *"Stationary, Spherically Symmetric Solutions Of Jordan's Unified Theory Of Gravity And Electromagnetism,"* Gen. Rel. Grav. **14**, 231 (1982).

[115] G. W. Gibbons and D. L. Wiltshire, *"Black Holes In Kaluza-Klein Theory,"* Annals Phys. **167**, 201 (1986) [Erratum-ibid. **176**, 393 (1987)].

[116] D. Garfinkle, G. T. Horowitz and A. Strominger, *"Charged black holes in string theory,"* Phys. Rev. D **43**, 3140 (1991) [Erratum-ibid. D **45**, 3888 (1992)].

[117] S. Mignemi, *"Primary scalar hair in dilatonic theories with modulus fields,"* Phys. Rev. D **62**, 024014 (2000) [arXiv:gr-qc/9910041].

[118] M. Cadoni and S. Mignemi, *"Dilatonic Black Holes In Theories With Moduli Fields,"* Phys. Rev. D **48**, 5536 (1993) [arXiv:hep-th/9305107].

[119] E. Witten, *"Dimensional Reduction Of Superstring Models,"* Phys. Lett. B **155**, 151 (1985).

[120] L. E. Ibanez and H. P. Nilles, *"Low-Energy Remnants Of Superstring Anomaly Cancellation Terms,"* Phys. Lett. B **169**, 354 (1986).

[121] V. S. Kaplunovsky, *"One Loop Threshold Effects in String Unification,"* Nucl. Phys. B **307**, 145 (1988) [Erratum-ibid. B **382**, 436 (1992)] [arXiv:hep-th/9205068];

L. J. Dixon, V. Kaplunovsky and J. Louis, *"Moduli dependence of string loop corrections to gauge coupling constants,"* Nucl. Phys. B **355**, 649 (1991).

[122] A. B. Nielsen and M. Visser, *"Production and decay of evolving horizons,"* Class. Quant. Grav. **23**, 4637 (2006) [arXiv:gr-qc/0510083].

[123] M. R. Douglas and S. Kachru, *"Flux compactification,"* Rev. Mod. Phys. **79**, 733 (2007) [arXiv:hep-th/0610102].

[124] A. R. Liddle, A. Mazumdar and F. E. Schunck, *"Assisted inflation,"* Phys. Rev. D **58**, 061301 (1998) [arXiv:astro-ph/9804177].

[125] A. B. Nielsen, *in preparation.*

[126] D. N. Spergel *et al.* [WMAP Collaboration], *"First Year Wilkinson Microwave Anisotropy Probe (WMAP) Observations: Determination of Cosmological Parameters,"* Astrophys. J. Suppl. **148**, 175 (2003).

[127] T. Padmanabhan, *"Cosmological constant: The weight of the vacuum,"* Phys. Rept. **380**, 235 (2003) [arXiv:hep-th/0212290];
E. J. Copeland, M. Sami and S. Tsujikawa, *"Dynamics of dark energy,"* Int. J. Mod. Phys. D **15** (2006) 1753 [arXiv:hep-th/0603057];
V. Sahni and A. Starobinsky, *"Reconstructing dark energy,"* arXiv:astro-ph/0610026.

[128] C. Wetterich, *"Cosmology and the fate of dilatation symmetry,"* Nucl. Phys. B **302**, 668 (1988);
P. G. Ferreira and M. Joyce, *"Structure formation with a self-tuning scalar field,"* Phys. Rev. Lett. **79**, 4740 (1997) [arXiv:astro-ph/9707286];
I. Zlatev, L. M. Wang and P. J. Steinhardt, *"Quintessence, Cosmic Coincidence, and the Cosmological Constant,"* Phys. Rev. Lett. **82**, 896 (1999) [arXiv:astro-ph/9807002].

[129] L. Amendola, *"Coupled quintessence,"* Phys. Rev. D **62**, 043511 (2000) [arXiv:astro-ph/9908023].

[130] C. Armendariz-Picon, T. Damour and V. F. Mukhanov, *"k-inflation,"* Phys. Lett. B **458**, 209 (1999) [arXiv:hep-th/9904075];

F. Piazza and S. Tsujikawa, *"Dilatonic ghost condensate as dark energy,"* JCAP **0407**, 004 (2004) [arXiv:hep-th/0405054].

[131] B. Boisseau, G. Esposito-Farese, D. Polarski and A. A. Starobinsky, *"Reconstruction of a scalar-tensor theory of gravity in an accelerating universe,"* Phys. Rev. Lett. **85**, 2236 (2000) [arXiv:gr-qc/0001066];
E. Elizalde, S. Nojiri and S. D. Odintsov, *"Late time cosmology in (phantom) scalar-tensor theory: Dark energy and the cosmic speed-up,"* Phys. Rev. D **70**, 043539 (2004) [arXiv:hep-th/0405034].
R. Gannouji, D. Polarski, A. Ranquet and A. A. Starobinsky, *"Scalar-tensor models of normal and phantom dark energy,"* astro-ph/0606287.

[132] S. Nojiri, S. D. Odintsov and M. Sasaki, *"Gauss-Bonnet dark energy,"* Phys. Rev. D **71**, 123509 (2005) [arXiv:hep-th/0504052].

[133] M. Sami, A. Toporensky, P. V. Tretjakov and S. Tsujikawa, *"The fate of (phantom) dark energy universe with string curvature corrections,"* Phys. Lett. B **619**, 193 (2005) [arXiv:hep-th/0504154];
G. Calcagni, S. Tsujikawa and M. Sami, *"Dark energy and cosmological solutions in second-order string gravity,"* Class. Quant. Grav. **22**, 3977 (2005) [arXiv:hep-th/0505193].

[134] P. J. Steinhardt and N. Turok, *"A cyclic model of the universe,"* arXiv:hep-th/0111030; *"Cosmic evolution in a cyclic universe,"* Phys. Rev. D **65**, 126003 (2002) [arXiv:hep-th/0111098].

[135] I. P. Neupane and B. M. N. Carter, *"Dynamical Relaxation of Dark Energy: A Solution to Early Inflation, Late time Acceleration and the Cosmological Constant Problem,"* Phys. Lett. B **638**, 94 (2006) [arXiv:hep-th/0510109];
I. P. Neupane and B. M. N. Carter, *"Towards inflation and dark energy cosmologies from modified Gauss-Bonnet theory,"* JCAP **0606**, 004 (2006) [arXiv:hep-th/0512262].

[136] I. P. Neupane, *"On compatibility of string effective action with an accelerating universe,"* Class. Quant. Grav. **23**, 7493 (2006) [arXiv:hep-th/0602097];

I. P. Neupane, *"Towards inflation and accelerating cosmologies in string-generated gravity models,"* arXiv:hep-th/0605265.

[137] P. Creminelli, M. A. Luty, A. Nicolis and L. Senatore, *"Starting the universe: Stable violation of the null energy condition and non-standard cosmologies,"* arXiv:hep-th/0606090;
N. Arkani-Hamed, H. C. Cheng, M. A. Luty and S. Mukohyama, *"Ghost condensation and a consistent infrared modification of gravity,"* JHEP **0405**, 074 (2004) [arXiv:hep-th/0312099].

[138] I. Y. Aref'eva and I. V. Volovich, *"On the null energy condition and cosmology,"* hep-th/0612098.

[139] S. Capozziello, S. Carloni and A. Troisi, *"Quintessence without scalar fields,"* astro-ph/0303041;
S. M. Carroll, V. Duvvuri, M. Trodden and M. S. Turner, Phys. Rev. D **70**, 043528 (2004) [arXiv:astro-ph/0306438];
S. Nojiri and S. D. Odintsov, *"Modified gravity with ln R terms and cosmic acceleration,"* Gen. Rel. Grav. **36**, 1765 (2004) [arXiv:hep-th/0308176].

[140] I. Antoniadis, J. Rizos and K. Tamvakis, *"Singularity - free cosmological solutions of the superstring effective action,"* Nucl. Phys. B **415**, 497 (1994) [arXiv:hep-th/9305025].

[141] D. J. Gross and J. H. Sloan, *"The quartic effective action for the heterotic string,"* Nucl. Phys. B **291**, 41 (1987);
I. Antoniadis, E. Gava and K. S. Narain, *"Moduli Corrections To Gauge And Gravitational Couplings In Four-Dimensional Superstrings,"* Nucl. Phys. B **383**, 93 (1992) [arXiv:hep-th/9204030].

[142] R. Easther and K. i. Maeda, *"One-Loop Superstring Cosmology and the Non-Singular Universe,"* Phys. Rev. D **54**, 7252 (1996) [arXiv:hep-th/9605173];
P. Kanti, J. Rizos and K. Tamvakis, *"Singularity-free cosmological solutions in quadratic gravity,"* Phys. Rev. D **59**, 083512 (1999) [arXiv:gr-qc/9806085];

S. Kawai, M. a. Sakagami and J. Soda, *"Instability of 1-loop superstring cosmology,"* Phys. Lett. B **437**, 284 (1998) [arXiv:gr-qc/9802033];
S. Tsujikawa, R. Brandenberger and F. Finelli, *"On the construction of nonsingular pre-big-bang and ekpyrotic cosmologies and the resulting density perturbations,"* Phys. Rev. D **66**, 083513 (2002) [arXiv:hep-th/0207228].

[143] P.J. Steinhardt and N.Turok, *"A cyclic model of the Universe,"* Science 296 (2002) 1436-39.

[144] S. Tsujikawa and M. Sami, *"String-inspired cosmology: Late time transition from scaling matter era to dark energy universe caused by a Gauss-Bonnet coupling,"* JCAP **0701** (2007) 006 [arXiv:hep-th/0608178].

[145] A. Coc, K. A. Olive, J. P. Uzan and E. Vangioni, *"Big bang nucleosynthesis constraints on scalar-tensor theories of gravity,"* Phys. Rev. D **73**, 083525 (2006) [arXiv:astro-ph/0601299].

[146] T. Damour, F. Piazza and G. Veneziano, *"Violations of the equivalence principle in a dilaton-runaway scenario,"* Phys. Rev. D **66**, 046007 (2002) [arXiv:hep-th/0205111].

[147] T. Damour, G. W. Gibbons and C. Gundlach, *"Dark Matter, Time Varying G, And A Dilaton Field,"* Phys. Rev. Lett. **64**, 123 (1990).

[148] J. Martin, C. Schimd and J. P. Uzan, *"Testing for $w < -1$ in the solar system,"* Phys. Rev. Lett. **96**, 061303 (2006) [arXiv:astro-ph/0510208].

[149] J. Khoury and A. Weltman, *"Chameleon fields: Awaiting surprises for tests of gravity in space,"* Phys. Rev. Lett. **93**, 171104 (2004) [arXiv:astro-ph/0309300].

[150] D. F. Mota and D. J. Shaw, *"Evading equivalence principle violations, astrophysical and cosmological constraints in scalar field theories with a strong coupling to matter,"* Phys. Rev. D **75**, 063501 (2007) [arXiv:hep-ph/0608078].

[151] G. Calcagni, B. de Carlos and A. De Felice, *"Ghost conditions for Gauss-Bonnet cosmologies,"* Nucl. Phys. B **752**, 404 (2006) [arXiv:hep-th/0604201].

[152] J. c. Hwang and H. Noh, *"Cosmological perturbations in generalized gravity theories,"* Phys. Rev. D **54**, 1460 (1996);
C. Cartier, J. c. Hwang and E. J. Copeland, *"Evolution of cosmological perturbations in non-singular string cosmologies,"* Phys. Rev. D **64**, 103504 (2001) [arXiv:astro-ph/0106197];
J. c. Hwang and H. Noh, *"Classical evolution and quantum generation in generalized gravity theories including string corrections and tachyon: Unified analyses,"* Phys. Rev. D **71**, 063536 (2005) [arXiv:gr-qc/0412126].

[153] I. P. Neupane, *"Accelerating cosmologies from exponential potentials,"* Class. Quant. Grav. **21**, 4383 (2004) [arXiv:hep-th/0311071];
I. P. Neupane, *"Cosmic acceleration and M theory cosmology,"* Mod. Phys. Lett. A **19**, 1093 (2004) [arXiv:hep-th/0402021];
I. P. Neupane and D. L. Wiltshire, *"Cosmic acceleration from M theory on twisted spaces,"* Phys. Rev. D **72**, 083509 (2005) [arXiv:hep-th/0504135]; I.P. Neupane, hep-th/0609086.

[154] S. Nojiri, S. D. Odintsov and M. Sami, *"Dark energy cosmology from higher-order, string-inspired gravity and its reconstruction,"* arXiv:hep-th/0605039.
G. Cognola, E. Elizalde, S. Nojiri, S. Odintsov and S. Zerbini, *"String-inspired Gauss-Bonnet gravity reconstructed from the universe expansion history and yielding the transition from matter dominance to dark energy,"* arXiv:hep-th/0611198.

[155] E. D. Stewart and D. H. Lyth, *"A More accurate analytic calculation of the spectrum of cosmological perturbations produced during inflation,"* Phys. Lett. B **302**, 171 (1993) [arXiv:gr-qc/9302019];
E. J. Copeland, E. W. Kolb, A. R. Liddle and J. E. Lidsey, *"Reconstructing the inflaton potential: Perturbative reconstruction to second order,"* Phys. Rev. D **49**, 1840 (1994) [arXiv:astro-ph/9308044].

[156] H. Peiris and R. Easther, *"Recovering the Inflationary Potential and Primordial Power Spectrum With a Slow Roll Prior: Methodology and Application to WMAP 3 Year Data,"* JCAP **0607**, 002 (2006) [arXiv:astro-ph/0603587].

[157] Z. K. Guo, N. Ohta and S. Tsujikawa, *"Realizing scale-invariant density perturbations in low-energy effective string theory,"* Phys. Rev. D **75** (2007) 023520 [arXiv:hep-th/0610336].

[158] B. M. Leith and I. P. Neupane, *"Gauss-Bonnet cosmologies: crossing the phantom divide and the transition from matter dominance to dark energy,"* JCAP **0705**, 019 (2007) [arXiv:hep-th/0702002].

[159] T. Koivisto and D. F. Mota, *"Cosmology and Astrophysical Constraints of Gauss-Bonnet Dark Energy,"*, Phys. Lett. B **644** (2007) 104 [arXiv:astro-ph/0606078]; *ibid*, *"Gauss-Bonnet quintessence: Background evolution, large scale structure and cosmological constraints,"* (to appear in Phys. Rev. D) [arXiv:hep-th/0609155].

[160] G. N. Felder, L. Kofman and A. D. Linde, *"Instant preheating,"* Phys. Rev. D **59**, 123523 (1999) [arXiv:hep-ph/9812289].

[161] Y. Wang and M. Tegmark, *"New dark energy constraints from supernovae, microwave background and galaxy clustering,"* Phys. Rev. Lett. **92**, 241302 (2004) [arXiv:astro-ph/0403292].

[162] U. Alam, V. Sahni and A. A. Starobinsky, *"Exploring the Properties of Dark Energy Using Type Ia Supernovae and Other Datasets,"* arXiv:astro-ph/0612381.

[163] L. Amendola, C. Charmousis and S. C. Davis, *"Constraints on Gauss-Bonner gravity in dark energy cosmologies,"* JCAP **0612** (2006) 020 [arXiv:hep-th/0506137].

[164] S. M. Carroll, M. Hoffman and M. Trodden, *"Can the dark energy equation of state parameter w be less than −1?,"* Phys. Rev. D **68**, 023509 (2003) [astro-ph/0301273];

P. Singh, M. Sami and N. Dadhich, *"Cosmological dynamics of phantom field,"* Phys. Rev. D **68**, 023522 (2003) [arXiv:hep-th/0305110];

U. Alam, V. Sahni and A. A. Starobinsky, *"The case for dynamical dark energy revisited,"* JCAP **0406**, 008 (2004) [arXiv:astro-ph/0403687];

W. Hu, *"Crossing the phantom divide: Dark energy internal degrees of freedom,"*

Phys. Rev. D **71**, 047301 (2005) [arXiv:astro-ph/0410680];

S. Nojiri, S. D. Odintsov and S. Tsujikawa, *"Properties of singularities in (phantom) dark energy universe,"* Phys. Rev. D **71**, 063004 (2005) [arXiv:hep-th/0501025];

H. K. Jassal, J. S. Bagla and T. Padmanabhan, *"Observational constraints on low redshift evolution of dark energy: How consistent are different observations?,"* Phys. Rev. D **72**, 103503 (2005) [arXiv:astro-ph/0506748];

L. Perivolaropoulos, *"Crossing the phantom divide barrier with scalar tensor theories,"* JCAP **0510**, 001 (2005) [arXiv:astro-ph/0504582];

M. z. Li, B. Feng and X. m. Zhang, *"A single scalar field model of dark energy with equation of state crossing -1,"* JCAP **0512**, 002 (2005) [arXiv:hep-ph/0503268];

I. Y. Aref'eva, A. S. Koshelev and S. Y. Vernov, *"Crossing of the $w = -1$ barrier by D3-brane dark energy model,"* Phys. Rev. D **72**, 064017 (2005) [arXiv:astro-ph/0507067];

P. S. Apostolopoulos and N. Tetradis, *"Late acceleration and w = -1 crossing in induced gravity,"* Phys. Rev. D **74**, 064021 (2006) [arXiv:hep-th/0604014];

Z. G. Huang, H. Q. Lu and W. Fang, *"Dilaton coupled quintessence model in the omega-omega' plane,"* arXiv:hep-th/0610018;

H. Wei and R. G. Cai, *"A note on crossing the phantom divide in hybrid dark energy model,"* Phys. Lett. B **634**, 9 (2006) [arXiv:astro-ph/0512018]; *"Interacting vector-like dark energy, the first and second cosmological coincidence problems,"* Phys. Rev. D **73**, 083002 (2006) [arXiv:astro-ph/0603052];

Z. G. Huang, H. Q. Lu and W. Fang, *"Coupled quintessence and phantom based on dilaton,"* Class. Quant. Grav. **23**, 6215 (2006) [arXiv:hep-th/0604160];

[165] C. M. Chen, P. M. Ho, I. P. Neupane and J. E. Wang, *"A note on acceleration from product space compactification,"* JHEP **0307**, 017 (2003) [arXiv:hep-th/0304177]; C. M. Chen, P. M. Ho, I. P. Neupane, N. Ohta and J. E. Wang, *"Hyperbolic space cosmologies,"* JHEP **0310**, 058 (2003) [arXiv:hep-th/0306291].
I. P. Neupane and D. L. Wiltshire, *"Cosmic acceleration from M theory on twisted spaces,"* Phys. Rev. D **72**, 083509 (2005) [arXiv:hep-th/0504135].

[166] A. A. Coley and R. J. van den Hoogen, *"The dynamics of multi-scalar field*

cosmological models and assisted inflation," Phys. Rev. D **62**, 023517 (2000) [arXiv:gr-qc/9911075].

[167] S. A. Kim, A. R. Liddle and S. Tsujikawa, *"Dynamics of assisted quintessence,"* Phys. Rev. D **72**, 043506 (2005) [arXiv:astro-ph/0506076].

[168] P. J. Kernan and S. Sarkar, *"No Crisis for Big Bang Nucleosynthesis,"* Phys. Rev. D **54**, 3681 (1996) [arXiv:astro-ph/9603045]; M. Birkel and S. Sarkar, *"Nucleosynthesis bounds on a time-varying cosmological 'constant',"* Astropart. Phys. **6**, 197 (1997) [arXiv:astro-ph/9605055].

[169] R. Bean, S. H. Hansen and A. Melchiorri, *"Early universe constraints on dark energy,"* Phys. Rev. D **64**, 103508 (2001) [arXiv:astro-ph/0104162].

[170] A. De Felice, M. Hindmarsh and M. Trodden, *"Ghosts, instabilities, and superluminal propagation in modified gravity models,"* JCAP **0608**, 005 (2006) [arXiv:astro-ph/0604154].

[171] C. Bonvin, C. Caprini and R. Durrer, *"A no-go theorem for k-essence dark energy,"* Phys. Rev. Lett. **97**, 081303 (2006) [arXiv:astro-ph/0606584].

[172] R. E. Kass and A. E. Raftery, *"Bayes Factors"*, J. Am. Statist. Assoc. **90**, 430 (1995)

[173] G. Steigman, *"Primordial nucleosynthesis: Successes and challenges"*, Int. J. Mod. Phys. **E 15**, 1 (2006) [arXiv:astro-ph/0511534].

[174] K.A. Olive, G. Steigman and T.P. Walker, *"Primordial nucleosynthesis: Theory and observations"*, Phys. Rept. **333**, 389 (2000) [arXiv:astro-ph/9905320].

[175] Tytler, D., O'Meara, J.M., Suzuki, N. & Lubin, D., *"Review of big bang nucleosynthesis and primordial abundances"*, Phys. Scripta **T85**, 12 (2000) [arXiv:astro-ph/0001318].

[176] Riess, A.G. *et al.* *"Cepheid calibrations from the Hubble Space Telescope of the luminosity of two recent type Ia supernovae and a re-determination of the Hubble constant"*, Astrophys. J. **627**, 579 (2005) [arXiv:astro-ph/0503159].

[177] Sandage, A., Tammann, G.A., Saha, A., Reindl, B., Macchetto, F.D. & Panagia, N., *"The Hubble constant: A summary of the HST program for the luminosity Calibration of type Ia supernovae by means of Cepheids,"* Astrophys. J. **653**, 843 (2006) [arXiv:astro-ph/0603647].

[178] F. van Leeuwen, M. W. Feast, P. A. Whitelock and C. D. Laney, Mon. Not. Roy. Astron. Soc. **379**, 723 (2007) [arXiv:0705.1592 [astro-ph]].

[179] N. Li and D. J. Schwarz, *"Signatures of cosmological backreaction,"* arXiv:0710.5073 [astro-ph].

[180] W.L. Freedman *et al.*, *"Final Results from the Hubble Space Telescope Key Project to Measure the Hubble Constant,"* Astrophys. J. **553**, 47 (2001) [arXiv:astro-ph/0012376].

[181] B. M. N. Carter, B. M. Leith, S. C. C. Ng, A. B. Nielsen and D. L. Wiltshire, *"Exact model universe fits type IA supernovae data with no cosmic acceleration,"* arXiv:astro-ph/0504192.

[182] R. Trotta, *"Applications of Bayesian model selection to cosmological parameters"*, Mon. Not. R. Astron. Soc. **378**, 72 (2007).

[183] Gurzadyan, V.G. *et al. "Elliptic CMB Sky"*, Mod. Phys. Lett. **A 20**, 813 (2005), [arXiv:astro-ph/0503103].

[184] Gurzadyan, V.G., Bianco, C.L., Kashin, A.L., Kuloghlian, H. & Yegorian, G., *"Ellipticity in cosmic microwave background as a tracer of large-scale universe"*, Phys. Lett. **A 363**, 121 (2007) [arXiv:astro-ph/0607160].

[185] Rudnick, L., Brown, S. & Williams, L.R., *"Extragalactic radio sources and the WMAP cold spot,"* arXiv:astro-ph/0704.0908.

[186] Tikhonov, A.V. & Karachentsev, I.D., *"Minivoids in the local volume,"* Astrophys. J. **653**, 969 (2006) [astro-ph/0609109].

[187] Yepes, G., Sevilla, R., Gottloeber S. & Silk, J., *"Is WMAP3 normalization compatible with the X-ray cluster abundance?"*, arXiv:astro-ph/0707.3230.

[188] Glazebrook, K. *et al.* *"A high abundance of massive galaxies 3.6 billion years after the Big Bang"*, *Nature* **430**, 181 (2004).

[189] Cimatti, A. *et al.* *"Old galaxies in the young universe"*, *Nature* **430**, 184 (2004).